



Technisch-Naturwissenschaftliche
Fakultät

Biocatalytic and Bio-electrocatalytic Reduction of CO₂ using Enzymes and Microorganisms

DISSERTATION

zur Erlangung des akademischen Grades

Doktorin der Technischen Wissenschaften

im Doktoratsstudium der

Technischen Wissenschaften

Eingereicht von:

Dipl. Ing. Stefanie Schlager

Angefertigt am:

Institut für Physikalische Chemie

Beurteilung:

o. Univ. Prof. Mag. Dr. DDr. h.c. Niyazi Serdar Sariciftci

Ass. Prof. Dipl. Ing. Dr. Clemens Schwarzinger

Mitwirkung:

Ass. Prof. Mag. Dr. Helmut Neugebauer

Linz, November 2015

Acknowledgement

“A goal is a dream with a deadline.”

Napoleon Hill

I am thankful for finally having reached the deadline of my dream after several years. Looking back makes me overall pleased and overwhelmed, especially in respect of the people accompanying in that period of my life.

Above all, this would never have been possible without the great support of my parents:

Dear Mum and Dad, thank you for your steady encouragement; for promoting but never forcing me into a direction; for letting me make my own choices, for being there whenever things went wrong or right; for conveying me your proud. Overall, I want to thank you for every personal and of course also financial support, enabling to make my way.

Liebe Mama, lieber Papa! Danke für eure stetige Unterstützung, dafür, dass ihr mich angetrieben habt jedoch nie versucht habt mich in eine Richtung zu drängen, dass ihr mich stets selbst entscheiden lasst, dafür, dass ihr immer da seid egal ob die Dinge gut oder weniger gut laufen, dafür, dass ihr mir zeigt wie stolz ihr seid. Ich danke euch für alles, vor allem für eure persönliche und natürlich auch finanzielle Unterstützung, die mir ermöglicht hat meinen Weg zu gehen.

Further I want to thank my family and my friends for always being there and to back me up all time. An extraordinary thank you goes to my girls: Marion Müller, Carola Wachholder, Romana Linninger, Nadine Tillner, Melanie Weichselbaumer, Martina Appl, Verena Eder, Martina Mair, Martina Hagauer, Martina Fuchs, Claudia Wögerbauer, Ulli Witzmann, Ute Kraushaar, Andrea Söllradl, Michaela Niedermayr, Andrea and Lisa Kinast, Nicole Korner and Alexandra Mayrhofer - thank you for your friendship, for lovely distraction when necessary, for laughing and crying together and for your support in the last months and years. Manfred Neudorfer and Florian Haas, thank you for being there my whole life. A big thank you goes to all of my friends spending the last years with me and for being such an important part of my life.

A very special thank you goes to my professor, supervisor and mentor Prof. Sariciftci. Six years ago he encouraged me to work at his institute and further doing my diploma thesis under his supervision. Offering the opportunity further to continue my research in this topic within a PhD thesis, his strong belief in what I am capable of to reach and his amazing support as a boss but also as a mentor made it possible to find my passion and profession. I am pleased to have learned from the best. Thank you for always impelling me, introducing me to science and for supporting me to find my “Berufung”.

Last but not least I also want to thank my colleagues of the whole LIOS team and of LIOS partners that have gone along with me all the years: Anita Fuchsbauer and Marianne Haberbauer for your amazing help during my time as PhD and for getting me into this topic. Dogukan Apaydin, Herwig Heilbrunner, Christoph Ulbricht, Sandra and Christina Enengl, Engelbert Portenkirchner, Stepan Demchyshyn, Marie Jakesova for sharing the office, lots of funny but also fruitful discussions. Gerda Kalab, Gabi Hinterberger, Birgit Paulik, Nadja Aichinger, Sara Gusner, Sabine Naßl for being such good friends at work and off of work. Helmut Neugebauer for your critical, important and helpful inputs and for teaching me a scientific view. And all others for friendship, great collaboration and for making me part of such a great team: Philipp Stadler, Petra Neumair, Markus Scharber, Matthew White, Eric Glowacki, Patrick Denk, Jacek Gasiorowski, Liviu Dumitru, Marek Havlicek, Halime Coskun, Cigdem Yumusak, Zeynep Bozkurt, Dominik Farka, Thomas Bielz, Daniel Egbe, Adam Getachew, Samuel Inack Ngi, Patchanita Thamyongkit, Sekai Lana Tombe, Vivian Suru John, Ayaka Toba, Jun Matsui, Akito Masuhara, Ken-Ichi Nakayama, Elisa Tordin, Kurt Aricanli, Gundula Voss, Andre Kwapil, Meltem Akcay, Elif Arici, Sameh Boudiba, Gottfried Aufischer, Lukas Bernhauser, Mateusz Bednorz, Valery Bliznyuk, Oleksandra Korovyanko, Oleksandr Boiko, Nicoleta Dobre, Jean-Benoit Giguere, Mihai Irimia-Vladu, Alessandra Operamolla, Kerstin Oppelt just to mention some.

Thank you!

Abstract

Atmospheric greenhouse gas content, particularly content of carbon dioxide (CO₂), is one of the most discussed topics nowadays in science and throughout society. Rising demand on fuels and increasing atmospheric CO₂ content initiate the idea of reducing the greenhouse gas on the one hand and regarding CO₂ as chemical feedstock for fuels and chemicals on the other hand.

In this work the biocatalytic and bio-electrocatalytic reduction of CO₂ is presented. Microorganisms and dehydrogenase enzymes are used as catalysts. One approach shows the application of methanogenic microorganisms, grown on a carbon felt electrode, for microbial electrolysis cells (MEC), converting CO₂ to methane by electron uptake. Such microorganisms are known for their ability to convert CO₂ together with H₂ selectively to methane. However up to now, H₂ had to be added artificially. This is not practical for sustainable processes in industrial scale due to the necessity of production, storage and transport of the required H₂ to the microbial reactors for CO₂ conversion. Here the direct electron uptake of the microorganisms from an electrode without adding H₂ artificially is shown for the reduction of CO₂ to methane.

In a second approach dehydrogenase enzymes are investigated for being addressed electrochemically. Dehydrogenase enzymes are known from natural processes, where co-enzymes like Nicotinamide adenine dinucleotide (NADH) deliver electrons and protons for the reduction of CO₂ to hydrocarbons. Nevertheless, such co-enzymes are oxidized during such reactions and need to be steadily supplied or regenerated. This limits the technical use of enzymes for CO₂ reduction to small scale experiments, due to high costs for the supply of co-enzymes and the regeneration of such. In this work the substitution of the co-enzyme NADH for the reduction of CO₂ using dehydrogenase enzymes is presented. Modification of a carbon felt electrode with an alginate-silicate hybrid gel containing dehydrogenase enzymes enables direct electron injection from the electrode into the enzymes and makes the necessity of NADH redundant. This approach is shown for addressing single dehydrogenase enzymes for the conversion of CO₂ to formate and for the conversion of butyraldehyde to

butanol as well as for addressing three dehydrogenase enzymes at the same time for the reduction of CO₂ to methanol.

Both approaches depict direct electron injection into biocatalytic systems. This substitutes the addition of hydrogen and electron equivalents. Further, such electrochemical methods can possibly be driven by renewable energy sources like solar or wind, which are lacking in transport and storage options. Combining biocatalytic reduction of the greenhouse gas CO₂ with e.g. solar or wind driven electrochemical systems, offers the possibility of renewable energy storage in fuels and valuable chemicals.

Kurzfassung

Der Gehalt an Treibhausgasen in der Atmosphäre, vor allem der Gehalt an Kohlendioxid (CO_2) gilt als eines der meist diskutierten Themen in Wissenschaft und Gesellschaft. Die steigende Nachfrage nach Treibstoffen und der gleichzeitige Anstieg an CO_2 in der Atmosphäre geben Anlass zur Reduktion von CO_2 einerseits und Betrachtung des CO_2 als chemischen Rohstoff für Treibstoffe und Chemikalien andererseits.

In dieser Arbeit werden die biokatalytische und die bio-elektrokatalytische Reduktion von CO_2 gezeigt. Als Katalysatoren dienen Mikroorganismen und Dehydrogenase Enzyme. Ein Ansatz behandelt die Verwendung von methanogenen Mikroorganismen, welche auf Graphitfilz aufgewachsen werden. Dabei wird CO_2 durch Elektronenaufnahme der Mikroorganismen zu Methan konvertiert. Diese Mikroorganismen sind für deren Fähigkeit bekannt, CO_2 zusammen mit H_2 selektiv zu Methan umzuwandeln. Dennoch war bisher die gezielte Zugabe von H_2 notwendig. Dies ist für nachhaltige Prozesse im industriellen Bereich ungeeignet, da es zuvor einer Produktion, Lagerung und eines Transports des H_2 zu den mikrobiellen Reaktoren für die Reduktion von CO_2 bedarf. In diesem Ansatz wird die direkte Elektronenaufnahme der Mikroorganismen von einer Elektrode gezeigt, wodurch die Reduktion von CO_2 zu Methan ohne Zugabe von H_2 ermöglicht wird.

In einem zweiten Ansatz werden Dehydrogenase Enzyme für die elektrochemische Adressierung untersucht. Dehydrogenasen sind von natürlichen Prozessen bekannt, in denen Co-Enzyme wie Nikotinamid Adenin Dinukleotid (NADH) Elektronen und Protonen für die Reduktion von CO_2 zu Kohlenwasserstoffen liefern. Solche Co-Enzyme werden während dieser Prozesse jedoch oxidiert und müssen entweder stets nachgeliefert oder regeneriert werden. Diese Anwendung ist daher auf Experimente in kleinen Größenordnungen eingeschränkt, da die Zufuhr von Co-Enzymen sowie auch deren Regeneration große Kostenfaktoren darstellen. In dieser Arbeit wird die Substitution des Co-Enzyms NADH für die Reduktion von CO_2 mit Dehydrogenase Enzymen vorgestellt. Durch die Modifizierung von Graphitfilz-Elektroden mit einem Alginat-Silicat Hybrid Gel, in welchem die Enzyme vorgelegt

werden, wird der direkte Elektronentransfer von der Elektrode zu den Enzymen ermöglicht. Dadurch wird die Verwendung von NADH überflüssig. Dieser Ansatz zeigt die Adressierung von einzelnen Enzymen für die Konvertierung von CO₂ zu Formiat und für die Umwandlung von Butyraldehyd zu Butanol sowie die Adressierung von drei Dehydrogenasen zugleich für die Reduktion von CO₂ zu Methanol.

Beide Ansätze beschreiben die direkte Elektronenzufuhr in biokatalytische Systeme. Dadurch wird die Zugabe von Wasserstoff bzw. Elektronen-Äquivalenten substituiert. Weiters können zukünftig solche elektrochemischen Methoden durch erneuerbare Energiequellen (Sonne, Wind,...), welche weder effizient transportiert noch gespeichert werden können, angetrieben werden. Die Kombination von biokatalytischer Reduktion von CO₂ mit, von erneuerbaren Energien betriebener Elektrochemie, stellt eine Möglichkeit zur Speicherung von erneuerbaren Energien in Form von Treibstoffen und hochwertigen Chemikalien dar.

Contents

1.	Introduction.....	1
1.1.	Background.....	1
1.2.	CO ₂ as Chemical Feedstock	6
1.3.	Microorganisms as Catalysts	9
1.4.	Dehydrogenase Enzymes as Catalysts.....	14
2.	Experimental	19
2.1.	Microbial Electrolysis for CO ₂ Reduction.....	19
2.1.1.	Setup.....	19
2.1.2.	Growing of Methanogenic Microorganisms.....	23
2.1.3.	Microbial Electrolysis.....	24
2.1.4.	Preparation of Catalyst Covered Anode	25
2.1.5.	SEM-EDX Analysis	26
2.1.6.	Anodic Oxygen Evolution with Nocera Catalyst	26
2.1.7.	Analysis of Methane	27
2.1.8.	Determination of Efficiency.....	27
2.2.	Enzyme Catalyzed Reduction Reactions.....	29
2.2.1.	Immobilization of Enzymes	29
2.2.2.	Reduction Reaction Using NADH.....	32
2.2.3.	Enzymatic Electrochemical Reduction Reaction	34
2.2.4.	Analysis of Products	37
2.2.5.	Calculation of Efficiency	39
2.3.	Microscopic Characterization of Carbon Felt	40
3.	Results and Discussion	41
3.1.	Microbial Electrolysis for CO ₂ Reduction.....	41
3.1.1.	MEC 1-Microbial Electrolysis at Lower Potential	41
3.1.2.	MEC2-Microbial Electrolysis at Higher Potential.....	52
3.1.3.	Anodic Oxygen Evolution with Nocera Catalyst	57
3.2.	Enzyme Catalyzed Reduction Reactions.....	65
3.2.1.	Formate Dehydrogenase for CO ₂ Reduction to Formate	65
3.2.2.	Enzymatic Electrochemical CO ₂ Reduction to Formate Using F _{ate} DH.....	67
3.2.3.	Dehydrogenase Enzymes for CO ₂ Reduction to CH ₃ OH	71

3.2.4.	Enzymatic Electrochemical CO ₂ Reduction to CH ₃ OH Using Dehydrogenase Enzymes	75
3.2.5.	Alcohol Dehydrogenase for Butyraldehyde Reduction to Butanol	88
3.2.6.	Enzymatic Electrochemical Reduction of Butyraldehyde Using ADH.....	89
3.3.	Microscopic Characterization of Carbon Felt	96
4.	Summary and Conclusion	99
5.	Appendix.....	101
	Symbols and Abbreviations	101
	List of Figures.....	103
	List of Tables.....	109
	List of Equations	111
	Bibliography.....	113

1. Introduction

1.1. Background

“Thus if the quantity of carbonic acid increases in geometric progression, the augmentation of the temperature will increase nearly in arithmetic progression.”

Svante Arrhenius

As one of the first scientists Svante Arrhenius quantified in 1896 in his work “On the influence of Carbonic Acid in the Air upon the Temperature of the Ground.” the impact of atmospheric carbon dioxide (CO₂) on the greenhouse effect. According to his calculations Arrhenius stated already back then the correlation of CO₂ content in the atmosphere and increase of Earth’s temperature.^[1]

Nowadays this correlation is regarded as matter of fact. Atmospheric CO₂ content, climate change and global warming are the most intensively discussed topics not only in science but also society. As a result for the combustion of fossil fuels by industry, transportation and residential purposes the Earth's atmosphere is changing. The combustion of hydrocarbon fuels increases atmospheric CO₂ content and photosynthesis in plants is no longer able to regulate accordingly.

Records of atmospheric CO₂ content in correlation with temperature have been initiated by the group of Keeling in the 1950’s.^[2] In the first period of records, up to the 70’s, atmospheric CO₂ concentration increased by around 10 ppm. Over the most recent decade that value is three times higher as depicted in the Keeling curve (Figure 1). In addition progressive industrialization will increase CO₂ emissions further and even faster. To date CO₂ content in the atmosphere has reached approximately 400 ppm, a peak value that has never been that high.^[3]

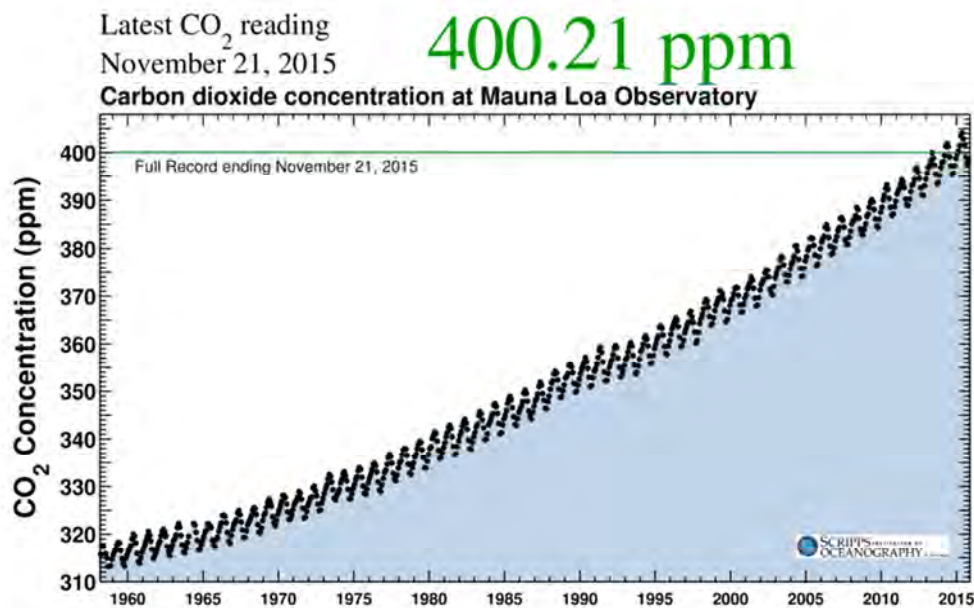


Figure 1 Records of the atmospheric CO₂ content at Mauna Loa from 1958 by the Scripps Institution of Oceanography show a steady increase. Fluctuating behavior of the curve indicates the variation of the CO₂ content within a year depending on the time of year and season respectively.^[3]

In further investigations ice core inclusions have been examined and delivered correlation of atmospheric CO₂ content and atmospheric temperature dated back to 800 000 years ago. Figure 2 displays the content of atmospheric CO₂ obtained from those ice core investigations. More recent values from 1958 were delivered from records at Mauna Loa by Keeling et al.^[2, 3] In Figure 3 further the parallel behavior of temperature and CO₂, utilizing results from ice core investigations as well, is depicted. Temperature and CO₂ are both following the same fluctuations within a range of about 100 ppm. However, as obvious, nowadays values of atmospheric CO₂ have never reached that extent and a strong impact on global temperature is therefore obvious.

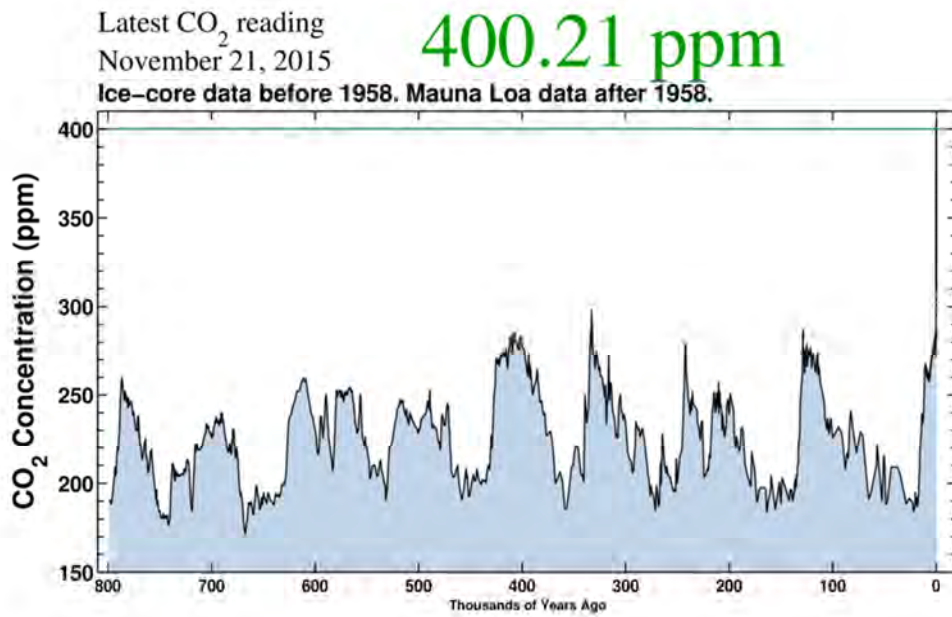


Figure 2 Record of the development of CO₂ concentration in the atmosphere dated back to 800 000 years from present, recorded from ice core data. From 1958 data are obtained from records from Mauna Loa observatory.^[3]

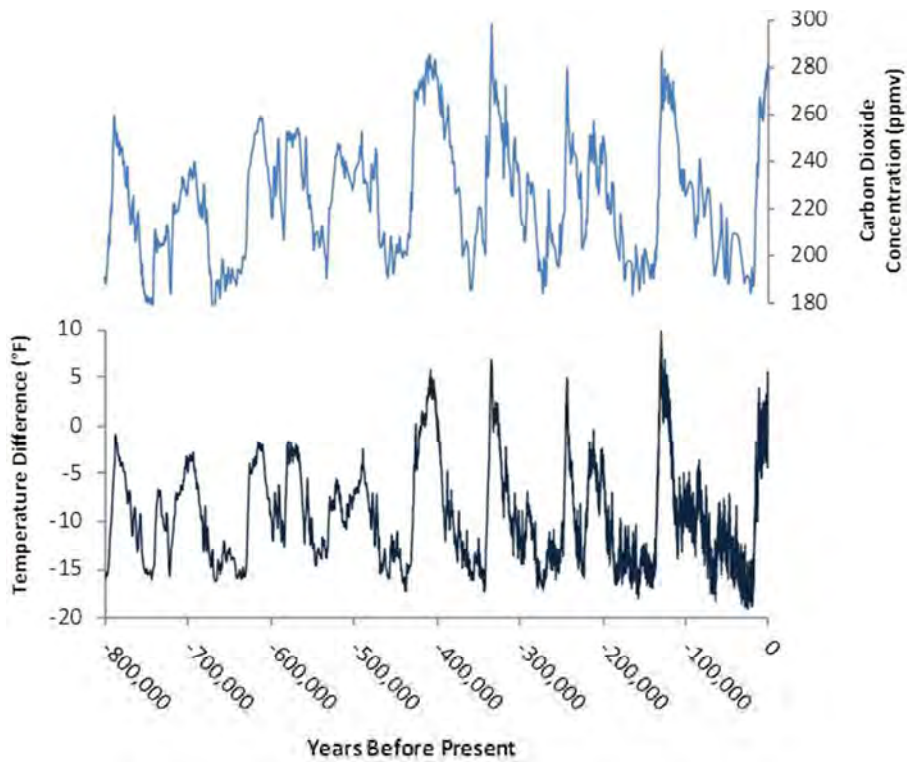


Figure 3 Correlation of atmospheric CO₂ content and earth's temperature back to 800k years before present from records of ice core measurements.^[4]

Those observations are alarming concerning the rapid change of the atmosphere, especially with regard to future development.

The main source for high CO₂ emission is the combustion of fossil fuels. Basically, to handle global warming, greenhouse effect and depletion in fossil fuels, there are two issues targeted at the same time. First of all decrease of atmospheric greenhouse gas content and emissions, particularly of CO₂, are intended. Further substitution of fossil fuels by, for instance, renewable energy sources is targeted. However, this is still one of the biggest challenges since energy sources like wind and solar lack in storage and transportation possibilities. Time of generation of such energies mostly is not aligned with the time and place when and where energies are required (Figure 4). That means that those energies possibly should be stored as a chemical or fuel to enable sufficient use.

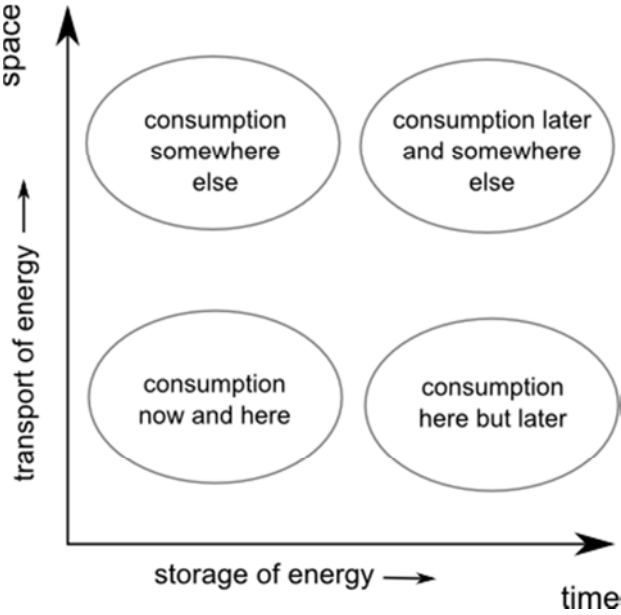


Figure 4 Correlation of time and space according to utilization and transport for renewable energies.

According to the reduction of atmospheric CO₂ there are mainly two approaches discussed in literature, dealing with this issue. Techniques are distinguished between capturing and storing CO₂ in deep rocks and ocean, the so called Carbon Capture and Sequestration

approach (CCS), and regarding CO₂ as chemical feedstock within the Carbon Capture and Utilization approach (CCU).

Large-scale carbon capture and storage can be done by storing the CO₂ in underground cavities as shown in Figure 5.

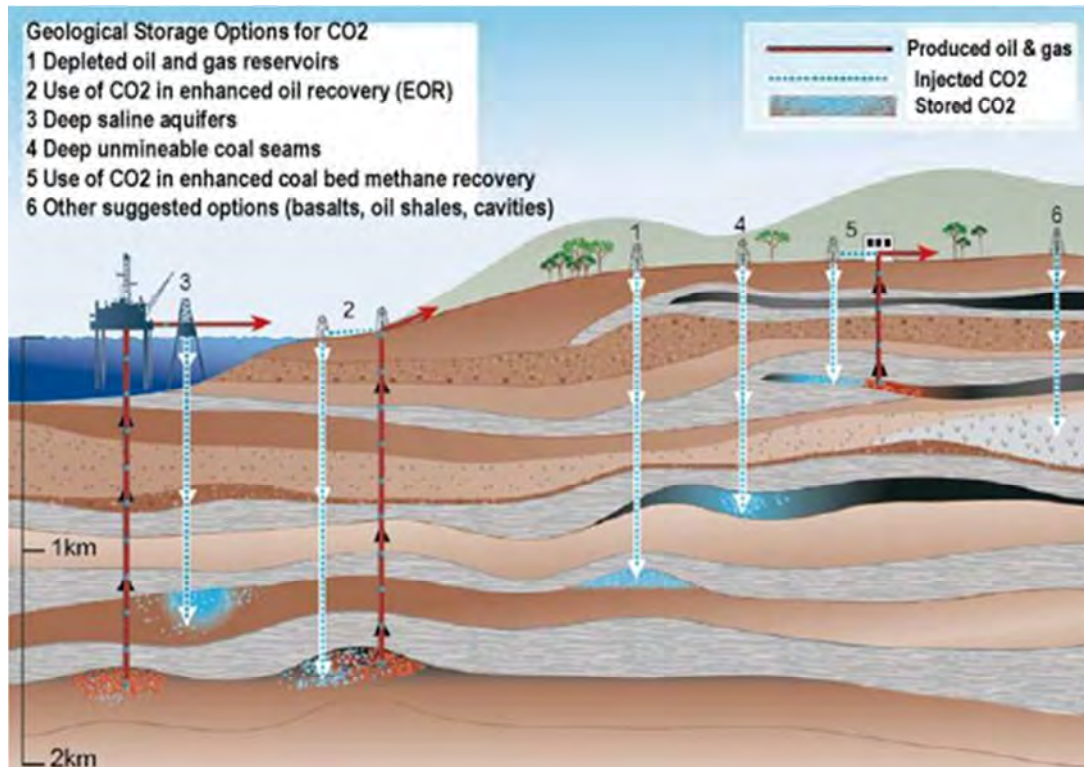
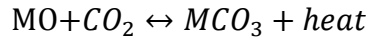


Figure 5 Possible storage options for CO₂ in underground storage options like under ocean and in deep rocks.^[5]

However possible storage options for CO₂ are limited. Further this poses the risk of eruption of such gas filled cavities and therefore involves great danger of explosions as it is known from natural gas chamber eruption like at Lake Nyos, causing many dead in 1986. Additionally, for storing the gas in cavities it requires high energy input for pumping the gas into the deep, making this process neither environmentally, nor economically practical. As a further approach of CCS mineral carbonation has to be mentioned. In this technique natural weathering processes are mimicked by generating a metal-carbonate from the reaction of CO₂ with metal oxides (Equation 1).^[6]



Equation 1 Reaction for the mineralization of CO₂.^[6]

Even though the latter CCS method of mineralization is more favorable due to trapping of CO₂ within a compound in comparison to storage in geological cavities, both approaches are not advantageous since they simply store carbon dioxide but do not use it as such.

In contrast to the idea of CCS, CCU focuses on the utilization of CO₂ by conversion to valuable chemicals or artificial fuels. This work demonstrates an approach following carbon dioxide utilization. CCU and according techniques will be discussed in the following chapters.

1.2. CO₂ as Chemical Feedstock

Recycling of CO₂ to useful fuels and/or to technologically relevant organic molecules offers great potential to decrease atmospheric greenhouse gases and to provide sustainable carbon cycles.^[6, 7, 8, 9, 10] Carbon dioxide is regarded as a source for several materials. Figure 6 shows a variation of possible options for reaction routes to chemically utilize and convert CO₂ into different carbohydrates.^[11]

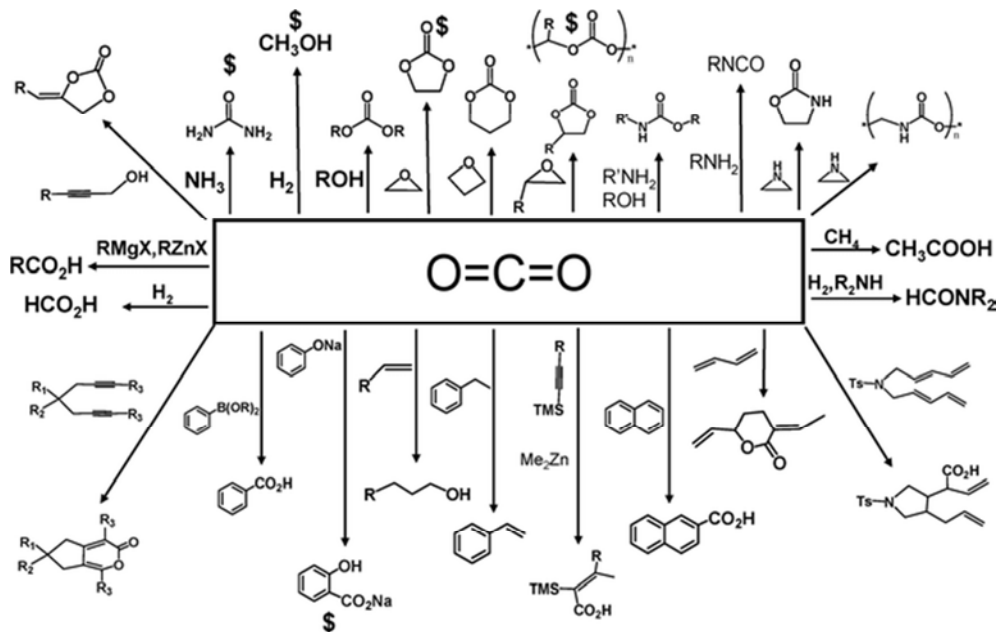
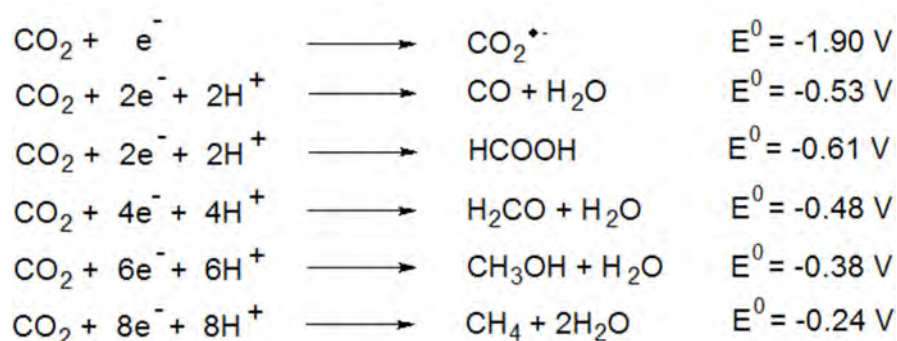


Figure 6 Possible reaction routes and materials from CO₂ as feedstock in the CCU approach.^[11]

Besides generation of various chemicals like for example cyclic carbonates^[12] (for the application in cosmetics or adhesives) or polymers^[13] where CO₂ is an essential feedstock for the industrial processes, also production of artificial fuels from CO₂ is of high interest.^[8,14,15,16] Nevertheless, generation of desired compounds follows in most cases the chemical reduction of CO₂. Equation 2 shows possible reduction routes of CO₂ towards C1-chemicals and the corresponding theoretical potentials or energy amounts respectively required for the reaction.



Equation 2 Theoretical standard redox potentials for the reduction of CO₂ vs. NHE in aqueous solution at pH 7.

The potentials depicted here, however, are theoretical values at thermodynamic equilibrium and are valid for aqueous solutions at pH 7. In reality those potentials are higher due to overpotentials. Such overpotentials are required for compensation of influences from experimental parameters and electrochemical setup such as distance of electrodes, resistivity of the electrolyte or membrane diffusion.

Chemical reduction of CO₂ needs, as seen in Equation 2 from the corresponding potentials, energy input or delivery of electrons respectively to drive the reactions. To overcome those energy barriers, either high potentials and/or high temperatures^[17, 18] can be used or catalysts have to be applied to lower the activation barrier of the reduction processes.

Especially the use of different catalytic materials in approaches, where the required energy input is delivered from an electrochemical system, has been widely discussed and investigated in the last three decades. Application of catalysts offers the possibility of energetically favorable processes due to lowering of the energy barrier. Further since catalysts are not consumed irreversibly during reactions, such reactions are economically and environmentally favored.

Combining CO₂ reduction catalysts with electrochemically provided energy furthermore is regarded as one of the feasible routes to convert renewable energies into artificial fuels. Electrochemical CO₂ reduction reactions, driven by for example solar- or wind energy, constitute a sustainable method of reducing CO₂ and storing those renewable energies as chemicals or fuels at the same time. Thus it makes renewable energy sources independent from time and place of utilization.^[8] This idea basically describes an artificial photosynthesis approach by mimicking the task of plants by the electrochemical CO₂ reduction.^[19, 20, 21, 22, 23]

In an early approach, Hawecker et al. presented in 1986 the application of (2,2'-Bipyridine)tricarbonylchlororhenium(I) and related complexes in photochemical and electrochemical reduction of carbon dioxide to carbon monoxide (CO). They reported 98% faradaic efficiencies according to the conversion to CO. This research initiated further investigations of this catalytic compound and derivatives. Cosnier et al. showed results on the Re(2,2'-bipyridine)(CO)₃Cl complex applied to polypyrrole electrodes as well as alkylammonium and pyridinium group-containing polypyrroles for CO₂ reduction.^[24, 25, 26] Later approaches on organo-metallic catalysts comprising pyridine groups were done by Kubiak et al. Besides butyl-substituted Re(bipy) compounds they examined substitution of Re by other metals in the application of electro- and photochemical CO₂ reduction processes.^[27, 28, 29, 30] Moreover Portenkirchner et al. presented results on the application of alkynyl substituted Re(bipy) complexes, electropolymerized on electrodes, for electrochemical CO₂ reduction.^[31, 32] Recently Cole et al. used pyridinium itself as homogenous catalyst for the selective reduction of carbon dioxide to methanol in aqueous media with faradaic efficiencies up to 22 %.^[33] This approach was reproduced later by Portenkirchner et al. reaching 14% faradaic efficiency. They further compared observations to results obtained from using pyridazine instead of pyridine as catalytic species.^[34]

Besides utilization of organic and organo-metallic catalysts, also metal electrodes and nanoparticles were explored for electrochemical CO₂ reduction processes. Mizuno et al. show the use of copper electrodes for the electrochemical reduction of CO₂ at low temperatures in methanol.^[18] Baruch et al. present the influence of tin electrodes on electrochemical CO₂ reduction using in situ ATR-FTIR spectroscopy.^[35] Application of transition metal surfaces was examined by Kuhl et al.^[36] Investigations on nanoparticles and nanocrystals for CO₂ reduction were presented by the groups of Bachmeier and Chaudhary.^[37, 38]

However, all these artificial catalytic systems are not as selective as natural catalysts and need further development. Compared to other catalytic systems, biocatalysts are highly selective according to the product generated which results in a high yield and reproducibility for CO₂ reduction.

In the following chapters the CO₂ reduction using microorganisms and enzymes as biocatalysts will be discussed.

1.3. Microorganisms as Catalysts

From natural processes microorganisms are known for their capability to reduce CO₂ to different products via intrinsic multistep reactions. Further, living systems such as microorganisms offer the opportunity of self-regeneration and are therefore highly suitable for long-term performance systems without degradation of the catalysts.

Reduction reactions using microorganisms as biocatalysts are reported to happen due to exoelectrogenic microorganisms, capable of transferring electrons over the cell membrane. This transfer usually happens via extracellular electron transport within two mechanisms: electron-shuttling via cytochromes (proteins that enable redox reactions) on the outer membrane of the cell and due to endogenous (in the cell) or exogenous (outside the cell) mediators.^[39, 40, 41, 42]

Microorganisms and corresponding cultures differ in several parameters. Depending on the kind of microorganisms and correlated metabolisms, such systems need certain conditions (pH, temperature, aerobic or anaerobic environment, etc.) to survive and for performing an ideal metabolism. With regard to microorganisms, appropriate for the reduction of CO₂, reactions mainly occur at ambient temperature, atmospheric pressure and neutral pH, making those systems highly attractive for large-scale application.

According to the cultures used, generation of different reduction products can be tuned. Bokinsky et al. for example show the generation of advanced biofuels, namely fatty acid ethyl esters, butanol and pinene from engineered *Escherichia coli*.^[43] Xin et al. report on the production of methanol from the reduction of CO₂ by resting cells of a methanotropic bacterium.^[44] Moreover Tracy et al. investigated the diverse potential of clostridia towards generation of several biofuels and their application in biorefinery. They show, that depending on the source of substrate (e.g. CO₂, cellulose, glycerol), conversion to distinct products is favored (Figure 7).^[45]

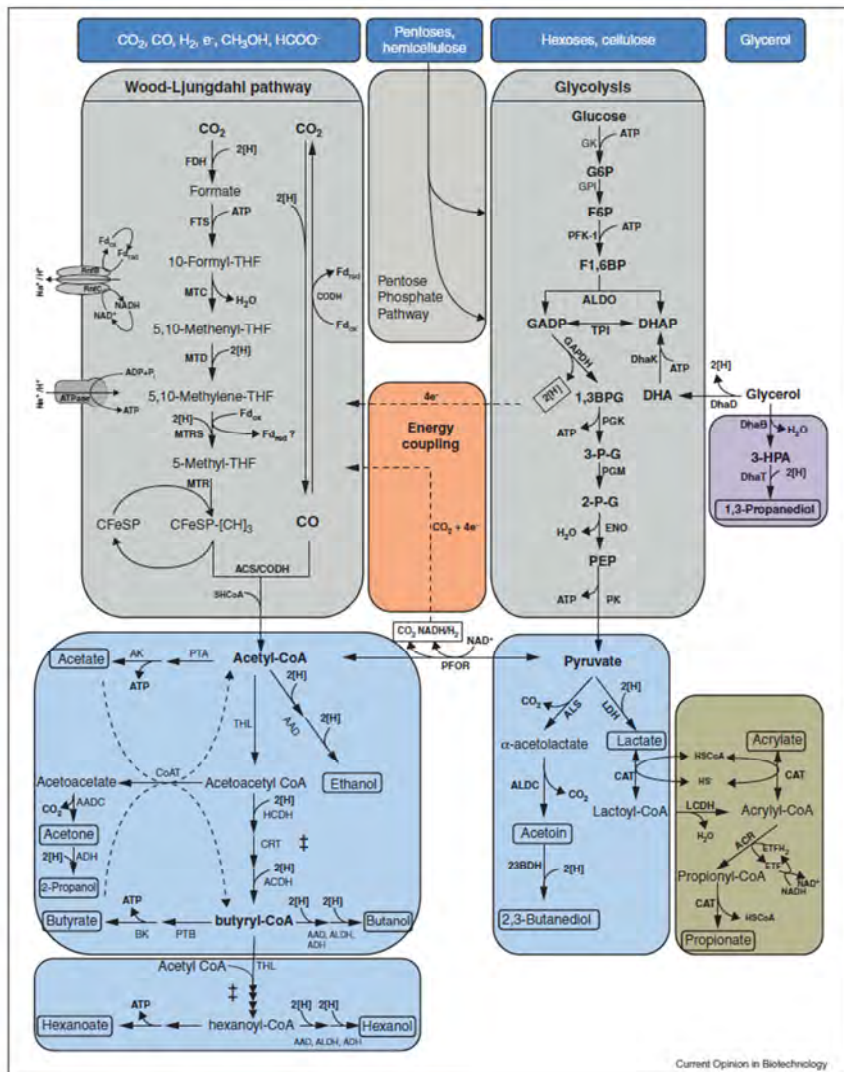
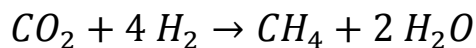


Figure 7 Metabolic pathway of clostridia towards various products depending on the source of substrate to be metabolized, presented by Tracy et al.^[45]

In case of reduction of CO₂ especially methanogenic microorganisms, that convert CO₂ within anaerobic processes to methane (CH₄), are of high interest. The living organisms used for these applications usually consist of several subcultures that co-exist and metabolize CO₂ reduction to some extent symbiotically. Such methanogenic mixed cultures are known from anaerobic reactors in sewage and biogas plants. Sewage, biomass and CO₂ can serve as carbon-source for the microorganisms to be converted to CH₄ and water in anaerobic digesters. The well-known metabolic pathways^[46, 47, 48, 49] result due to the following overall reaction equation (Equation 3).



Equation 3 Reaction pathway for the reduction of CO₂ with H₂ added artificially, catalyzed by anaerobic microorganisms.

However, approaches for the reduction of CO₂ to methane usually require hydrogen or hydrogen-equivalents that have to be added artificially. This poses the problem of increased energy supply and costs, since the H₂ added has to be generated from external electrolysis processes first and subsequently stored, transported and added to the reduction site.

In more recent works electrochemical reactions are investigated using electrotrophic microorganisms that take up electrons directly from an electrode since they prefer electrons for their growth. Nowadays research focuses intensively on the electrochemical application of different microorganisms for the reduction of CO₂.^[50]

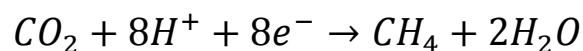
The first report on bio-electrochemically synthesized methane from CO₂ without any electron shuttles or mediators needed was presented by Cheng et al. in 2009.^[51] Van Eerten-Jansen et al. further studied the performance of a methane-producing microbial electrolysis cell for a long-term performance of 188 days.^[52] The maximum energy efficiency obtained in this study was 51.3% in a yield test. Villano et al. showed high methane production rates by using a microbial biocathode based on a hydrogenophilic methanogenic culture.^[53] Sato and co-workers discussed in several works the possible implementation of bio-electrochemical conversion of CO₂ to methane for geological storage reservoirs. It was shown that electro-methanogenic CO₂ reduction can be achieved by biocathodes based on methanogens.^[54, 55, 56, 57] In a different approach Li et al. investigated genetically modified microorganisms for the electromicrobial conversion of CO₂ to higher alcohols like isopropanol and 3-methyl-1-butanol.^[58]

Great focus has further been put on the optimization of biocathodes to enable efficient immobilization of the microorganisms and therefore improving electron uptake for CO₂ reduction.

Patil et al. report on the application of osmium polymer modified electrodes as a cathode material. They report on the efficient wiring of non-exoelectrogens on the electrode.^[59] Further Jourdin et al. present the utilization of nanotube-modified scaffolds.^[60]

Especially big electrode surfaces are desired for a sufficient immobilization or growth of microorganisms on the electrode respectively. Recently Jiang et al. showed a bio-electrochemical approach using methanogenic mixed culture for the simultaneous production of methane and acetate from CO₂. Electroactive microorganisms were grown on a carbon felt electrode by applying a potential. The CO₃²⁻ rich medium as well as gaseous CO₂ acted as carbon based nutrients. Further they adapted microorganisms to a carbon nutrient only metabolism by reducing stepwise the hydrogen amount added.^[61] However, the approaches presented here show either the application of genetically modified microorganisms, requirement of artificially added hydrogen or utilization of other or additional C-sources with regards to gaseous CO₂.

In this work an approach on direct electron injection into methanogenic mixed cultures within a microbial electrolysis cell (MEC) and the reduction of carbon dioxide to methane is shown. This work demonstrates the direct electron uptake and methane generation without any H₂ added artificially. In contrast to the work of Jiang et al., who were adding sodium hydrogen carbonate (NaHCO₃) and CO₂, here the system was saturated with gaseous CO₂ only to serve exclusively as carbon source. Further microorganisms were used directly from a sewage suspension. This approach provides a controlled supply of the carbon source and direct electrochemical conversion of gaseous CO₂ following Equation 4:



Equation 4 Reaction pathway for the reduction of CO₂ within microbial electrolysis, without H₂ added artificially.

Addition of H₂ was ceased due to adaption to direct electron injection. Microbial electrolysis cells were investigated for different adaption methods and for long-term performance using different potentials for two MEC's that were investigated.

Besides the application of living-catalysts in microbial electrolysis cells for the reduction of CO₂ to methane, also the non-living biocatalysts, namely enzymes, are of high interest.^[62] As shown in Figure 7 presented by Tracy et al.^[45] the conversion of CO₂ to fuels within a metabolic pathway of microorganism basically consists of a multistep reaction where each step is catalyzed by a corresponding enzyme.

In addition to investigations of microorganisms for CO₂ reduction, the utilization of dehydrogenase enzymes for reduction reactions is investigated in this work. The theory of enzymatic and enzymatic electrochemical reduction will be described in the following.

1.4. Dehydrogenase Enzymes as Catalysts

Dehydrogenase enzymes are well known from natural processes, where they catalyze for example the conversion of CO₂. Application of such enzymes offers the opportunity to produce selectively valuable chemicals and fuels with high yields from the greenhouse gas CO₂. Possible products from CO₂ reduction using dehydrogenase enzymes are formate, formaldehyde, methanol or carbon monoxide, depending on the corresponding enzymes.^[29, 63, 64, 65]

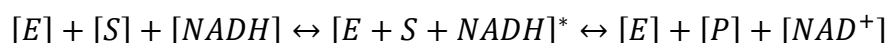
Especially the conversion of CO₂ to hydrocarbons, like via the three step reduction reaction of CO₂ to methanol, is of peculiar interest. In this reaction cascade, each step is catalyzed by a certain enzyme to the corresponding intermediate or final product respectively. As a first step of the reduction of CO₂ formic acid is generated with the aid of formate dehydrogenase (F_{ate}DH), followed by a reduction to formaldehyde by formaldehyde dehydrogenase (F_{ald}DH). Last formaldehyde is reduced to methanol via alcohol dehydrogenase (ADH). Each of those steps is obtained by a two electron reduction. In natural processes those electrons are delivered from the oxidation of a sacrificial co-enzyme such as Nicotinamide adenine dinucleotide (NADH).

Several approaches have been done for mimicking this natural process using dehydrogenase enzymes to catalyze the reduction of CO₂. Ruschig et al. presented already in 1976 a work on

enzymatic reduction of CO₂ to formate using formate dehydrogenase and nicotinamide adenine dinucleotide (NADH) as co-enzyme.^[66]

Those enzymes are favorable since reactions occur ideally at ambient conditions, neutral pH and aqueous media. However, to ensure performance of the biocatalysts and further to provide reusability of the enzymes, several works on immobilization of enzymes have been done. First approaches of enzyme immobilization were reported by Heichal-Segal et al. using alginate-silicate gel matrices for glucosidase immobilization to prevent it from thermal and chemical denaturation.^[67] Later on Aresta et al. investigated enzymes immobilized in agar as well as polyacrylamide, pumice and zeolite materials concerning stability and activity of the carboxylase enzyme to be used for the synthesis of benzoic acid from phenol and CO₂.^[68, 63] Obert and Dave first presented the immobilization of dehydrogenase enzymes for chemical CO₂ reduction in silica sol-gel matrices.^[69] Furthermore also the groups of Lu and Wu investigated the immobilization of dehydrogenases in beads of an alginate-silica hybrid gel for the chemical CO₂ reduction to methanol and formate.^[70, 71] In the work of Dibenedetto et al. NADH regeneration and the use of new hybrid technologies, by merging biological and chemical technologies, for the conversion of CO₂ to methanol with the dehydrogenase cascade, co-immobilized in alginate based beads, was investigated.^[72] Among different immobilization techniques especially encapsulation of enzymes in gels and gel beads is advantageous. Such gels yield a large surface area, provide high chemical stability for the enzymes and reduce costs due to possible reusability of the biocatalysts.

However, in all these enzymatic CO₂ reduction approaches using dehydrogenase enzymes, NADH has been used as electron and proton donor for the reduction reactions. Basically reactions of such processes follow Michaelis-Menten equation for enzyme kinetics and are demonstrated in Equation 5.



Equation 5 Reaction pathway based on Michaelis-Menten equation for enzyme kinetics.

In this equation E denotes the enzyme, S the substrate (such as CO₂ and its intermediate reduction products), and P the final product.^[73] As common in enzyme kinetics the use of dehydrogenase enzymes for CO₂ reduction with NADH can be described with the formation of an intermediate state with dehydrogenase enzymes and substrates. During this state substrate and co-enzyme both link to the (metal) active site of the enzyme. This is crucial for the reduction of the substrate due to enabled proton and electron transfer via the active site of the enzyme during the intermediate state. Nevertheless, in those processes NADH is irreversibly converted to its oxidized form NAD⁺, as a sacrificial co-factor. This irreversible NADH oxidation limits enzyme applications for CO₂ reduction to small scale experiments due to high costs for co-factor synthesis and regeneration (Figure 8A).

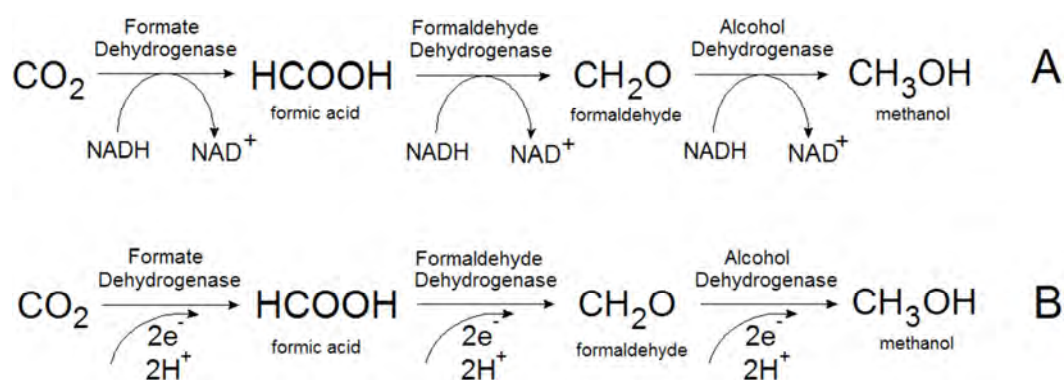


Figure 8 Reduction mechanisms of CO₂ catalyzed by dehydrogenase enzymes. 3-step reduction of CO₂ to methanol with NADH as sacrificial co-enzyme (A) and via a direct electron transfer to the enzyme without any co-enzyme (B).

Therefore, an appropriate substitution for co-enzymes like NADH as electron donors is necessary. Particularly the application of electrochemical processes and direct electron injection into enzymes instead of NADH as electron donor is of great interest. Figure 8B demonstrates the possible reduction route using direct electron injection from an electrode instead of NADH as electron and proton donor. In the electrochemical process protons are delivered from aqueous electrolyte solution. An approach according to address enzymes electrochemically has been presented e.g. by Addo et al. They showed that dehydrogenase enzymes can be electrochemically addressed and depicted this technique for the

bio-electrocatalytic regeneration of NADH.^[74] Amao and Shuto demonstrated the application of viologen modified FateDH immobilized on a indium-tin oxide electrode for the reduction of CO₂ to formate in an artificial photosynthesis approach.^[75] Further, for the direct reduction of CO₂ Kuwabata et al. presented an electrochemical approach for the conversion to methanol using dehydrogenase enzymes and methylviologen as well as pyrroloquinolinequinone as electron mediators.^[76] Reda et al. later demonstrated the electrochemical CO₂ reduction using formate dehydrogenase adsorbed on glassy carbon without any electron shuttle needed, yielding Faradaic efficiencies of 97% and higher. They moreover proposed a mechanism for the electron transfer to the enzyme and subsequent reduction of CO₂ depicted in Figure 9.^[77]

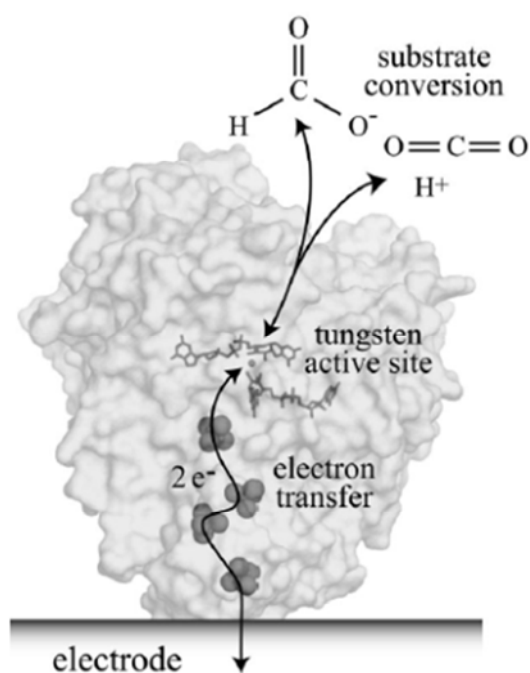


Figure 9 Proposed electron transfer from an electrode to formate dehydrogenase during reduction of CO₂ to formate, reported by Reda et al.^[77]

Such approaches of electrochemical reduction of CO₂, utilizing immobilized dehydrogenase enzymes on carbon felt electrodes without any co-enzyme or mediator required depict a sustainable route towards biocompatible reduction of the greenhouse gas CO₂. It offers

further the possibility of renewable energy storage since renewable energy sources can be used as electrical source for the electrochemical processes. This approach possibly could substitute the expensive electron donor NADH by direct electron injection into the enzymes.

In this work experiments for the conventional reduction reactions catalyzed by dehydrogenase enzymes with NADH as electron and proton donor were done. Further the same systems were investigated for the direct electrochemical reduction. Three different approaches, examining individual dehydrogenase enzymes as well as the combination of all three dehydrogenases, were performed. As a first approach the initial step of the reduction of CO₂ to formate via formate dehydrogenase is shown. In further experiments co-immobilization of all three dehydrogenase enzymes for the reduction of CO₂ all the way to methanol is demonstrated using NADH as well as finally the direct electron injection from an electrode. Last the reduction reaction of butyraldehyde to butanol catalyzed by alcohol dehydrogenase is presented as an approach towards higher alcohols. Especially the conversion of CO₂ directly to methanol using bio-electrocatalytic systems is of particular interest.

Furthermore, investigation of the conventional method using NADH and comparing it to direct electron injection into the same systems delivers valuable information about the reduction processes and activity of the enzymes on the one hand and proofs further the possibility of addressing dehydrogenase enzymes directly by immobilization on an electrode.

2. Experimental

2.1. Microbial Electrolysis for CO₂ Reduction

2.1.1. Setup

Electrochemical reduction of CO₂ using methanogenic microorganisms was investigated in two approaches using two microbial electrolysis cells (MEC1 and MEC2). All experiments were performed in two compartment cells (2 x 100 mL) or H-cells respectively with anode and cathode chamber separated by a Nafion membrane, allowing proton transport.

Nafion membrane was prepared from commercially obtained Nafion sheet cut to a circular shape (ϕ 3 cm). The membrane was stored in 3 M HCl solution for 2 h for soaking. Subsequently the membrane was rinsed with water and put into purified 18.2 MΩ water and boiled for 30 min. The membrane was fixed between cathode and anode chamber with the aid of a clamp.

As an anode or counter electrode respectively platinum foil with a total area of 8 cm² (4 x 1 cm) was used in the anode compartment. In the cathode compartment carbon felt (CF) with a size of 2.5 x 6 x 0.6 cm, with a platinum wire as electrical contact, served as working electrode and a Ag/AgCl in 3 M KCl electrode(MF 2079), purchased from BASi, was applied as reference electrode. Figure 10 shows the setup for the microbial electrolysis cells with anode compartment on the right hand side and cathode compartment on the left hand side, separated by a Nafion membrane in between.

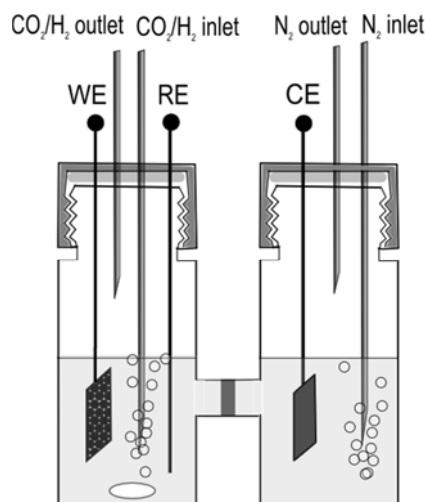


Figure 10 Microbial electrolysis cell. Photograph on the left hand side and schematic of the cell on the right hand side display the setup used. Setup shows anode compartment (right) and cathode compartment (left) separated by membrane which was fixed between the compartments using a clamp. Electrical contacts for the electrodes as well as gas in- and outlets were implemented via septa.

Methanogenic microorganisms were added for the reduction of CO₂ to methane at the cathode side. Those microorganisms are anaerobic and therefore require sterile conditions and a strict exclusion of oxygen. Anaerobic conditions were obtained by sealing the two compartment cell with caps and septa. Establishment of the setup was done after water-steam sterilization of the two compartment cell, caps, septa, counter- and working electrode in an autoclave. The reference electrode was wiped with 70% isopropanol. The cell was then put together in a N₂ flow box, which was previously sterilized with 70% isopropanol. As an electrolyte solution 20 mM phosphate buffer (3 g L⁻¹ KH₂PO₄, 2.5 g L⁻¹ K₂HPO₄) was used. For the anode compartment 80 mL of the buffer were added as prepared. For the cathode compartment Cheng medium was added, consisting of the same phosphate buffer with trace elements and vitamins added. Trace element solution (pH 7, adjusted with KOH, Table 1) and vitamin solution (Table 2) were obtained from PROFACTOR GmbH within the project REGSTORE and were prepared according to Cheng et al.^[51] Table 3 shows the concentration of all components added for Cheng medium.

Trace elements	concentration (g L ⁻¹)
Nitrilotriacetic acid	1.50
MgSO ₄ · 7 H ₂ O	3.00
MnSO ₄ · 7 H ₂ O	0.50
NaCl	1.00
FeSO ₄ · 7 H ₂ O	0.10
CoSO ₄ · 7 H ₂ O	0.18
CaCl ₂ · 2 H ₂ O	0.10
ZnSO ₄ · 7 H ₂ O	0.18
CuSO ₄ · 7 H ₂ O	0.01
KAl(SO ₄) ₂ · 12 H ₂ O	0.02
H ₃ BO ₃	0.01
Na ₂ MoO ₄ · 2 H ₂ O	0.01
NiCl ₂ · 6 H ₂ O	0.03
Na ₂ SeO ₃ · 5 H ₂ O	0.30

Table 1 Compounds and corresponding concentrations in trace element solution required for medium and electrolyte solution of the MEC respectively, provided by PROFACTOR GmbH.

vitamins	concentration (mg L ⁻¹)
Biotin	2.00
Folic acid	2.00
Pyridoxine-HCl	10.00
Thiamine-HCl · 2 H ₂ O	5.00
Riboflavin	5.00
Nicotinic acid	5.00

D-C-panthothenate	5.00
Vitamin B₁₂	0.10
p-Amino benzoic acid	5.00
Lipoic acid	5.00

Table 2 Compounds and corresponding concentrations in vitamin solution required for medium and electrolyte solution of the MEC respectively, provided by PROFACTOR GmbH.

Substance	Amount
NaCl	0.13 g L ⁻¹
NH₄Cl	0.31 g L ⁻¹
Trace element solution	12.5 mL L ⁻¹
Vitamin solution	5 mL L ⁻¹

Table 3 Concentrations of components added to 20 mM phosphate buffer for obtaining a medium according to Cheng.

Phosphate buffer solution for the anode compartment as well as Cheng medium for the cathode compartment were prepared with a neutral pH value of around 7. Sewage suspension, containing methanogenic microorganism, obtained from sewage plant Asten (Linz AG Kläranlage, 4481 Asten), was centrifuged and provided by PROFACTOR GmbH. About 9 mL of suspension were added to the cathode compartment. Figure 11 shows a microbial electrolysis cell after inoculation of sewage suspension that contained methanogenic microorganisms. The suspension obtained was originally of grey to green-brown color and therefore made the electrolyte solution or medium respectively look turbid.



Figure 11 Microbial electrolysis cell after inoculation of sewage suspension containing microorganism to the cathode compartment (right-hand side).

The cell was sealed with caps and septa and connected outside the N₂ flow box to a Jaisle P-M 100 potentiostat for electrochemical operation. The cathode compartments were stirred permanently during growing, adaption and long-term performance.

2.1.2. Growing of Methanogenic Microorganisms

Growing and immobilization respectively of the methanogenic microorganisms was obtained simply by applying a constant potential of -700 mV vs. Ag/AgCl for MEC1 and -850 mV vs. Ag/AgCl for MEC2.

MEC1

In MEC1 the cathode compartment was purged with CO₂ and H₂ (1:1) for at least 5 h per day for 4 days to achieve sufficient growth and breeding of the microorganisms on the electrode. The immobilization of the microorganisms was obtained only due to application of charge to the electrode, which is supposed to be favorable. This kind of auto-immobilization of the microorganisms was desired for sufficient electron transport to the microorganisms for

efficient reduction of CO₂. After 4 days growing was completed since biofilm formation on the working electrode was sufficient.

MEC2

As an approach to enrich the biofilm further, glucose was added to the cathode compartment in the MEC2 setup and the cathode compartment was purged with CO₂ and H₂ in a ratio of 1:1 as well. However, purging was performed for MEC2 for 2 weeks before further steps were conducted. In contrast to MEC1, where growing was performed within 4 days, growing was performed for a longer period of 2 weeks for MEC2 to enhance biofilm formation.

After growing procedures the electrolyte solution at the cathode chamber was exchanged in both approaches (MEC1 and MEC2) to fresh Cheng medium.

2.1.3. Microbial Electrolysis

The microbial electrolysis cells (MEC1 and MEC2) were both established the same way but operated at two different potentials, as described previously. Both systems were investigated for CO₂ reduction to methane (CH₄). Microbial electrolysis was conducted steadily at potentiostatic mode. In MEC1 microbial electrolysis was investigated at -700 mV of operation potential. In the second experiment (MEC2) electrolysis at -850 mV was performed.

For CO₂ only performance microorganisms had to be adapted to operate without requiring the artificial addition of H₂. Two different techniques were considered and are described in the following.

Adaption with CO₂/H₂

MEC1 was investigated in a first approach for the adaption by subsequent decrease of the hydrogen amount added. The procedure was performed within three cycles of 5 days each. First adaption cycle was done by purging the cathode side of the microbial electrolysis cell

with CO₂ and H₂ at a ratio of 1:1 for about 5 h per day. After two days of no purging cycle 2 was conducted with a ratio of 2:1 for CO₂ and H₂. In the last adaption cycle ratio was changed to 3:1 for CO₂:H₂.

Adaption with Glucose

In a later approach sewage suspension and non-adapted microorganisms respectively were added to the adapted MEC1 and the system was purged with CO₂/H₂ to reconstitute an initial, non-adapted state of the microorganism.

The microorganisms then were adapted by adding 0.1 mL of saturated glucose solution and purging electrolyte solution with CO₂/H₂ for about 5 days and 5 h per day. Glucose is known further for supporting the growth and breeding of the microorganisms. Adaption was further performed by reducing the H₂ amount in the ration of CO₂:H₂ within 3 cycles of 5 days of purging and 2 days of break each. After 3 weeks electrolyte solution was refreshed by exchanging two third of the volume. This adaption technique was used for the adaption of MEC2 as well.

For the long-term procedure of both adapted setups (MEC1 and MEC2), electrolyte solution or Cheng medium in the cathode compartment was refreshed by exchanging about 80% of the liquid every 2 weeks, to provide steadily required vitamins and trace elements. Further, after adaption, both setups were purged with CO₂ as the only C-source for about 5 h per day and 5 days a week in long-term experiments with duration of several months.

2.1.4. Preparation of Catalyst Covered Anode

Procedure of catalyst formation was done in collaboration with Dr. A. Fuchsbauer and MSc D. H. Apaydin based on results of Nocera et al. and according to the recipe used by Dr. Fuchsbauer as reported in her PhD thesis.^[78, 79]

Experiments were done in a two compartment cell with anode and cathode chamber separated by a frit. As a counter electrode and anode respectively platinum foil (4 x 1 cm)

served. In the cathode compartment a Ag/AgCl (in 3 M KCl) reference electrode from BASi (MF 2079) and a 4 x 1 cm platinum foil as working electrode were mounted. A 0.1 M phosphate buffer of neutral pH, containing 0.5 mM $\text{Co}(\text{NO}_3)_2 \cdot 6\text{H}_2\text{O}$ (obtained from Sigma Aldrich), served as electrolyte solution.

In a first step film formation was done by cycling the potential between 0 mV and +1200 mV with a scan rate of 50 mV s^{-1} for 100 cycles.

Subsequently potentiostatic measurement was conducted by keeping the potential at +1200 mV for about 1 h.

2.1.5. SEM-EDX Analysis

SEM-EDX Analysis was performed in courtesy of Fachhochschule Wels in collaboration with DI D. Salaberger et al. within REGSTORE project (Regio13 program). EDX was used in order to characterize the surface constitution of the Nocera catalyst covered platinum electrode prepared as described in 2.1.4. For the measurement a TESCAN Vega2 LMU scanning electron microscope was used together with an energy dispersive X-ray spectroscopy detector. The electrode was used for the measurement as prepared. The electrode was applied as anode in the microbial electrolysis cell after investigation with SEM-EDX.

2.1.6. Anodic Oxygen Evolution with Nocera Catalyst

The obtained electrode covered with the Co^{2+} Nocera catalyst was applied as anode during the long-term performance of MEC1. The microbial electrolysis was performed constantly during several months at a constant potential of -700 mV vs. Ag/AgCl applied to the cathode. The catalyst covered anode was applied to the anode compartments to combine the cathodic methane production with an anodic oxidation of water to O_2 at the same time.

2.1.7. Analysis of Methane

For investigation of the constitution of headspace and gaseous products from microbial electrolysis respectively, 2 mL headspace samples were taken using a gas tight syringe and analyzed in a Thermo Scientific Trace GC Ultra gas chromatograph with N₂ as carrier gas. Samples were injected manually. Qualification and quantification was done by injection of test gas samples at different dilutions with N₂ gas. For detection a thermal conductivity detector was used. Determination of H₂, O₂, CH₄ and CO₂ could therefore be obtained. The method for measuring gas samples followed the procedure described in Table 4.

step	duration
T= 30°C	10 min
Heating to 250°C	5 min
T= 250°C	6 min

Table 4 Method for analysis of headspace gas samples in gas chromatography.

Methane generation and headspace constitution during long-term performance was analyzed daily.

2.1.8. Determination of Efficiency

Faradaic efficiency of both microbial electrolysis cells was calculated from potentiostatic electrolysis experiments that were performed for a certain time of 4 h and were samples

were taken of the headspace before and after electrolysis. Gas samples were investigated in gas chromatography. Calculation was done by determining the area of the current–time plot obtained from electrolysis, which corresponds to the number of charges (Q) consumed during applying constantly the negative potential. This area corresponds to Ampere seconds (A s) or Coulombs (C).

The number of moles n that could theoretically be obtained in the experiment was calculated from

$$n = \frac{Q}{zF}$$

with the Faraday constant as $F=96485.33 \text{ C mol}^{-1}$ and the number of charges z defining the number of electrons required for the reduction reaction according to Equation 2.

The number of charges obtained from electrolysis (Q) was divided by F and delivered the amount of electrons flowing. Dividing by $z=8$, according to the 8 electron process for the reduction of CO_2 to CH_4 , gave then the theoretical amount of methane produced. From GC analysis methane content from the experiment was achieved. Experimental amount of mol divided by the theoretical amount in mol delivered the faradaic efficiency.

2.2. Enzyme Catalyzed Reduction Reactions

Besides the application of living biocatalytic systems as described above for the application of methanogenic microorganisms, utilization of non-living biocatalyst, namely enzymes, was investigated. All chemicals were obtained from Sigma Aldrich if not stated differently.

2.2.1. Immobilization of Enzymes

Matrix Preparation

For chemical stabilization of the enzymes and further to enable application of enzymes on an electrode, enzymes were immobilized. Thus also sufficient charge transport to the biocatalysts in electrochemical approaches was obtained. As immobilization matrix an alginate-silicate hybrid sol-gel was chosen. Preparation of immobilization matrix was performed the same way for all experiments. Alginic acid sodium salt (0.1 g) (Figure 12) was dissolved in 3 mL of purified water (18.2 MΩ). The solution was then mixed vigorously with 1.5 mL of tetraethylorthosilicate (TEOS) (Figure 12). After some minutes a two-phase system was obtained with the upper phase as remaining TEOS that was not miscible with the alginate solution. The upper phase was therefore removed (1 mL).

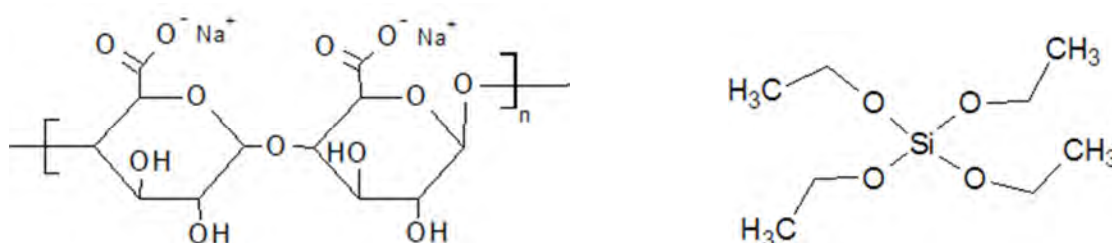


Figure 12 Molecular structures of alginic acid sodium salt (left hand side) and tetraethylorthosilicate (right hand side).

Immobilization of Formate Dehydrogenase for the Reduction of CO₂ to Formate

Formate dehydrogenase (F_{ate}DH) from *Candida boidinii* (0.88 u/mg solid, 4 mg) was dissolved in 500 µL of aqueous 0.05 M Tris(hydroxymethyl)-aminomethane-HCl (TRIS-HCl) (Figure 13) buffer (pH 7.65) and added to the alginate-silicate solution.

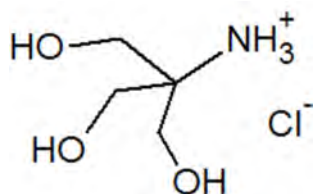


Figure 13 Molecular structure of tris(hydroxymethyl)-aminomethane-HCl (TRIS-HCl).

TRIS-HCl buffer was prepared by dissolving TRIS in 18.2 MΩ water to obtain a 0.05 M solution. The pH value was then adjusted to 7.65 using 3 M HCl.

Immobilization of Dehydrogenase Enzymes for the Reduction of CO₂ to Methanol

For co-immobilization of the dehydrogenase enzymes about 20 mg of formate dehydrogenase (F_{ate}DH), 10 mg formaldehyde dehydrogenase (F_{ald}DH) (from *Pseudomonas putida*, 1-6 units/mg solid) and about 10 mg of alcohol dehydrogenase (ADH) were dissolved together in 500 µL of 0.05 M TRIS-HCl buffer (pH 7.65) or, in another approach, in 500 µL 1 M phosphate buffer (PB) (pH 7.64). Phosphate buffer of pH 7.64 was prepared from 136.09 g L⁻¹ of K₂HPO₄ and 174.2 g L⁻¹ of KH₂PO₄. For both approaches the enzyme containing buffer solution was added to the alginate matrix for further use. Experimental steps were done in a N₂ flow cell for highly pure conditions and to prevent enzymes from degradation.

Immobilization of Alcohol Dehydrogenase for the Reduction of Butyraldehyde to Butanol

Alcohol dehydrogenase (ADH) from *Saccharomyces cerevisiae* (415 u/mg solid, 4 mg) was dissolved in 500 µL of aqueous 0.05 M TRIS-HCl buffer (pH 7.65) and added to the alginate-silicate solution.

Preparation of Beads for Reduction Reactions using NADH

Preparation of alginate-silicate hybrid gel beads was performed the same way for all experiments. Alginate-silicate hybrid gel solution, prepared as described previously, was dropped into 0.2 M CaCl₂ solution via a syringe for precipitation in bead-like shape with an approximate size of 4 mm diameter. Bead-like shape offers high, rather uniform and controllable surface area and offers the opportunity of sufficient diffusion of substrate, co-enzyme and product. For sufficient precipitation the beads were kept in the solution for 20 min. Afterwards beads were rinsed with highly pure water (18.2 MΩ) and directly used for the reduction experiments. Figure 14 displays the stepwise procedure of preparing the beads as described previously.

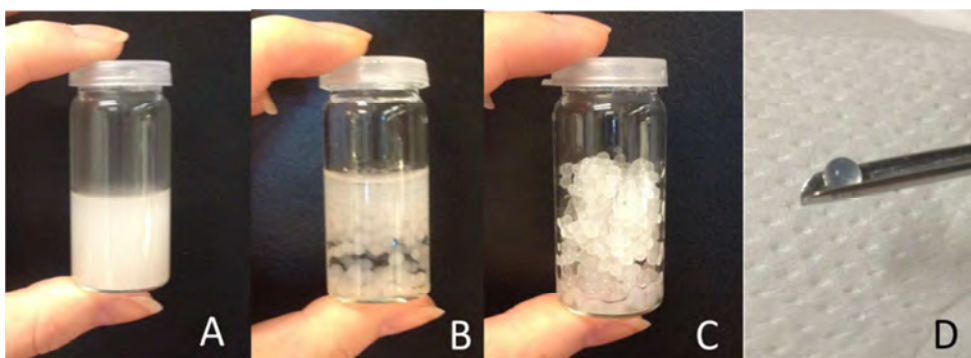


Figure 14 Preparation of alginate based beads. Solution of alginate-silicate hybrid sol-gel (A) was dropped into 0.2 M CaCl₂ solution for precipitation (B). After 20 min of precipitation, obtained beads (C and D) were rinsed and used directly for experiments.

Preparation of Electrodes for Electrochemical Approaches

For improved charge transport to the enzymes carbon felt electrodes were modified with equally prepared alginate matrix containing the enzymes.

Therefore carbon felt (CF), purchased from SGL Carbon GmbH with a size of 0.6 x 3 x 0.6 cm, was soaked like a sponge with the alginate-silicate hybrid gel solution and subsequently stored in 0.2 M CaCl₂ solution for 20 min to obtain sufficient precipitation. The electrode then was rinsed with purified, 18.2 MΩ water and directly applied as working electrode in

the electrochemical setup. The corresponding steps of the preparation procedure for the electrode are depicted in Figure 15.

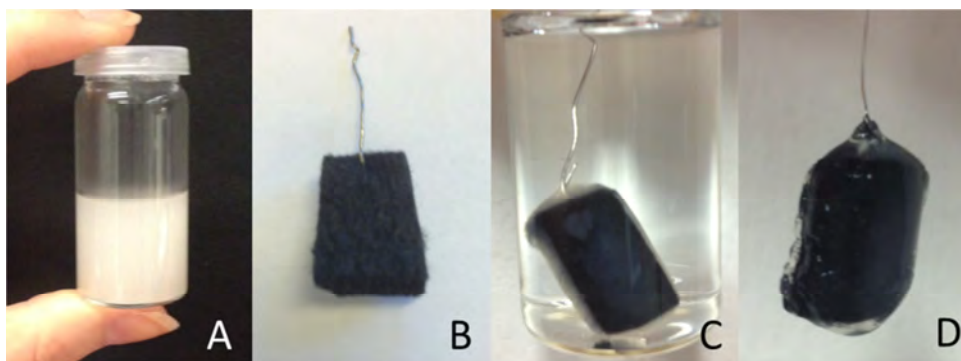


Figure 15 Preparation of a carbon felt electrode modified with alginate-silicate hybrid sol-gel. The carbon felt electrode (B) was soaked with the prepared matrix gel (A) and precipitated in 0.2 M CaCl₂ solution for 20 min (C). The obtained gel covered electrode (D) was used as working electrode in electrochemical measurements.

2.2.2. Reduction Reaction Using NADH

For enzyme activity testing and for general investigation of the immobilization method as an appropriate method, experiments with free floating alginate beads, and with the aid of NADH as electron and proton supplier were conducted. Figure 16 depicts the experimental setup for reduction reactions using NADH. The beads prepared previously as described in 2.2.1 were transferred to a round flask containing 4 mL of buffer solution. As a buffer solution 0.05 M TRIS-HCl (pH 7.65) was used. For experiments with all three dehydrogenase enzymes immobilized also 0.05 M phosphate buffer was investigated. The buffer solutions containing the gel-beads were purged with N₂ for about 1 h, followed by addition and dissolution of around 7 mg NADH. For the reduction of butyraldehyde to butanol using ADH subsequently an excess volume of butyraldehyde (0.1 mL) was added. For the reduction experiments of CO₂ to formate with F_{ate}DH and the reduction of CO₂ to methanol via the 3-step cascade using F_{ate}DH, F_{ald}DH and ADH, the systems were subsequently saturated with CO₂ for about 1 h.

Purging of the system with N_2 or CO_2 respectively was done via syringes and needles acting as gas in- and outlet. Butyraldehyde addition was done via syringe and needle as well. NADH was stored in a tube under anaerobic conditions prior to addition via the tube.

Reduction reactions were conducted for 8 h or 16 h respectively. Samples for analysis in liquid injection gas chromatography (LGC) for butanol and methanol detection and capillary ion chromatography (LGC) for analysis of formate, were taken before combining substrate and NADH in the solution, immediately after combination and start of the reaction respectively and after 8 h of reaction time for generation of butanol and methanol or after 16 h for generation of formate.

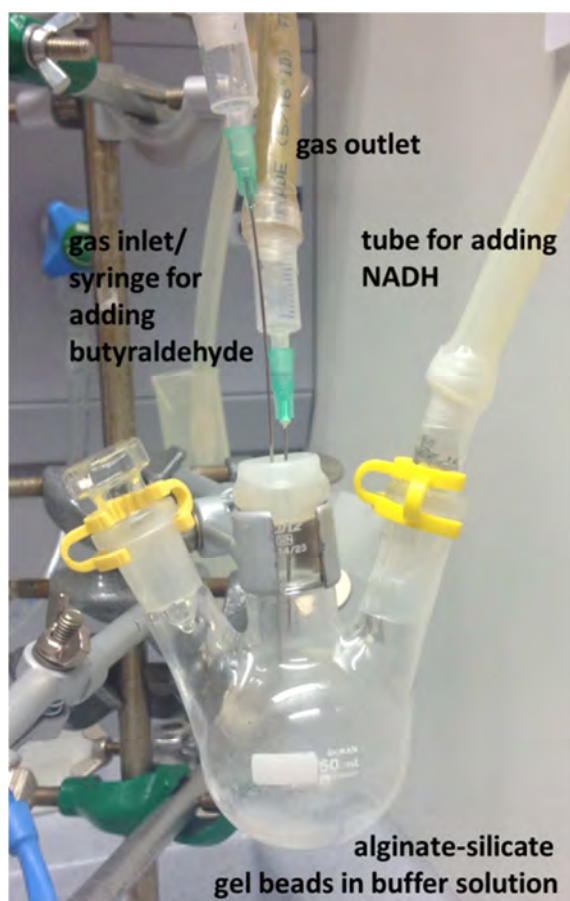


Figure 16 Setup for reduction reaction using alginate-silicate gel beads and NADH as electron and proton donor.

2.2.3. Enzymatic Electrochemical Reduction Reaction

Setup

Enzymatic electrochemistry measurements were done using a two-compartment-cell (H-cell, 2 x 25 mL) as demonstrated in Figure 17. Cathode and anode compartment were separated by a frit to avoid re-oxidation of the reduction product at the anode. The previously prepared carbon felt electrode, modified with alginate-silicate hybrid gel was applied as working electrode or cathode respectively in the cathode compartment, where the reduction reactions take place. Further a Ag/AgCl in 3 M KCl reference electrode was mounted next to the working electrode in the cathode compartment as well. In the anode compartment Pt foil was used as counter electrode. Purging of the cathode compartment to obtain inert N₂ conditions or for the supply with CO₂, to be reduced, was performed via needles in the septum as gas in- and outlet respectively. In experiments with butyraldehyde, addition was performed with syringe and needle via the septum. Samples for analysis in capillary ion chromatography (CAP-IC), liquid injection gas chromatography (LGC) and gas chromatography (GC) were taken from the cathode compartment via the septum as well.

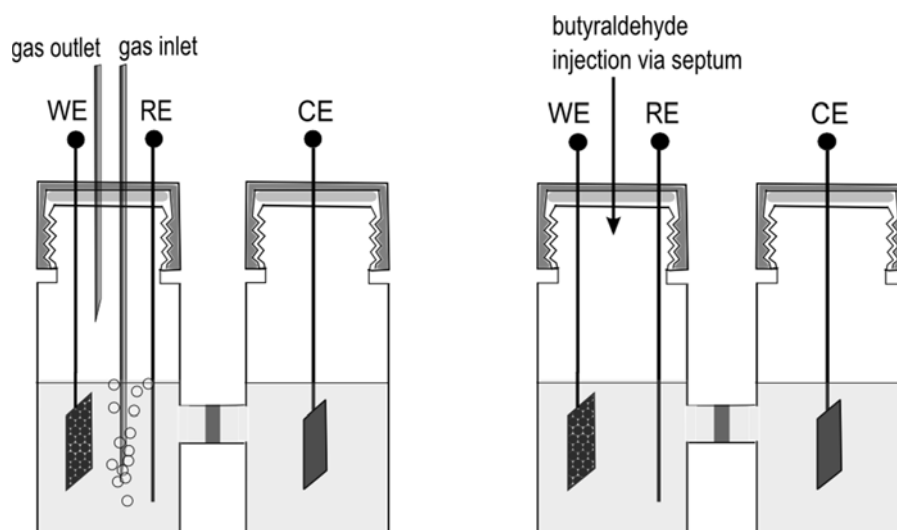


Figure 17 Two-compartment-cells for enzymatic electrochemistry measurements. The left-hand side schematic depicts the setup for purging and saturating with gases. The right-hand side setup shows a schematic for the addition of liquid components like butyraldehyde to the setup.

Electrochemical Measurements for the Reduction of CO₂ to Formate using F_{ate}DH

Electrochemical characterization of the carbon felt electrode modified with FateDH containing alginate-silicate hybrid gel was done by recording cyclic voltammograms (CV) with scan rates of 5 and 50 mV s⁻¹. The potential was swept between 0 mV and -1200 mV vs. Ag/AgCl according to the reduction potential shown in Equation 2 with overpotentials taken into account. CV's were recorded for comparison first after 30 min of saturation with N₂. Afterwards the system was purged 30 min with CO₂ and characterization was repeated. For efficient reduction reaction and sufficient generation of product from the reduction reaction potentiostatic electrolysis was performed after another 30 min of purging with CO₂ at -1200 mV vs. Ag/AgCl for 11 h. For comparison electrolysis was repeated at the same potential but after 30 min of N₂ purging for 13 h. All electrochemical measurements were done using a JAISLE Potentiostat-Galvanostat IMP 88 PC. Liquid samples of the cathode compartment were taken before and after electrolysis experiments were performed and were analyzed using capillary ion chromatography (CAP-IC).

Electrochemical Measurements for the Reduction of CO₂ to Methanol using Dehydrogenase Enzymes

The reduction of CO₂ to methanol using the enzymatic electrochemistry approach with all three dehydrogenase enzymes immobilized was performed using two different electrolyte solutions for comparison. All electrochemical measurements were done with JAISLE Potentiostat-Galvanostat IMP 88 PC.

First a 0.05 M TRIS-HCl buffer solution (pH 7.65), as also used for measurements with F_{ate}DH or ADH only, was chosen as electrolyte solution. In a second approach a 0.05 M phosphate buffer solution (pH 7.62) served as electrolyte solution.

Electrochemical measurements were performed identically for both electrolyte solutions. Cyclic voltammograms were recorded for characterization of the electrochemical performance of the modified carbon felt electrode with enzymes immobilized. Cyclic voltammetry was carried out by sweeping the potential between 0 and -1200 mV vs. Ag/AgCl

with scan speeds of 5, 10, 20, 50 and 100 mV s^{-1} after saturating the system for 30 min with N_2 or CO_2 respectively. Further electrolysis experiments were performed under potentiostatic conditions at $-1200 \text{ mV vs. Ag/AgCl}$ for 4 h after 30 min N_2 or CO_2 saturation respectively. Further electrolysis experiments were conducted under the same conditions using modified carbon felt electrodes without any enzymes immobilized for both buffers as electrolyte solutions. Samples were taken before and after electrolysis and were analyzed using liquid injection gas chromatography (LGC) for liquid samples and gas chromatography (GC) for samples of the headspace.

Figure 18 shows a schematic of setup and reactions for this approach demonstrating the electrochemical procedure for the reduction of CO_2 to methanol using the dehydrogenase enzyme cascade immobilized on the electrode. The same schematic basically also applies for the reduction of CO_2 to formate and butyraldehyde to butanol.

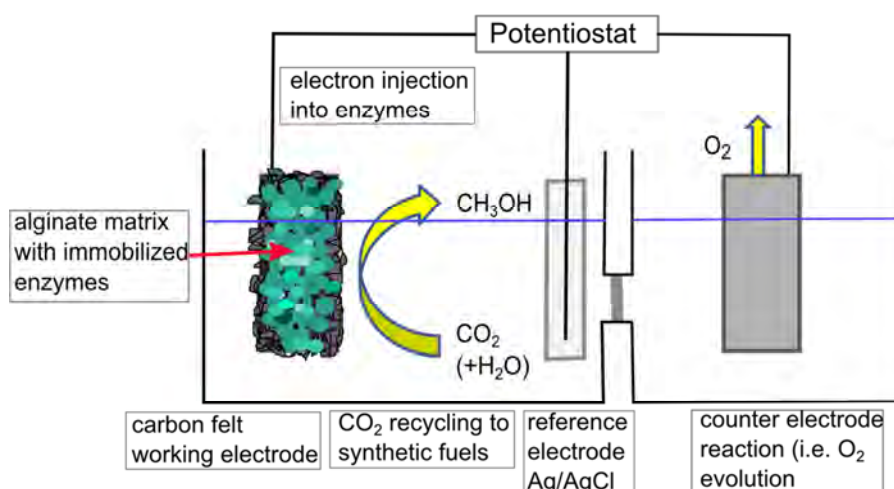


Figure 18 Schematic of the electrochemical CO_2 reduction using enzymes. Electrons are injected directly into the enzymes, which are immobilized in alginate-silicate hybrid gel (green) on a carbon felt working electrode. CO_2 is reduced at the working electrode. Oxidation reactions take place at the counter electrode.

Electrochemical Measurements for the Reduction of Butyraldehyde to Butanol using ADH

For the electrochemical measurement a JAISLE Potentiostat-Galvanostat IMP 88 PC was used. TRIS-HCl buffer (0.05 M, pH 7.65) was chosen as electrolyte solution. Measurements were done after saturating the system with N₂ for 30 min and after adding 0.1 mL butyraldehyde to the electrolyte solution of the cathode compartment for the reduction reactions. Cyclic voltammograms (CV) were recorded for the electrode with immobilized enzyme and an identically prepared electrode but without any enzyme added for comparison. The potential was swept between 0 mV and -600 mV vs. Ag/AgCl with a scan rate of 5 and 50 mV s⁻¹. Further electrolysis experiments were carried out for 8 h at -600 mV vs. Ag/AgCl for significant butanol production. The same experiment was repeated but without adding any butyraldehyde to the electrolyte solution and simply saturating the system with N₂. Further electrolysis was performed with the same parameters but with the electrode without enzyme immobilized. Liquid samples from before and after the electrolysis experiments were analyzed in liquid injection gas chromatography.

2.2.4. Analysis of Products

Qualification and quantification of products from the reduction reactions for the enzymatic approaches were done using chromatography methods. All used techniques are discussed in the following:

Liquid samples from the electrolyte solution were analyzed in liquid injection gas chromatography (LGC) and capillary ion chromatography (CAP-IC) before and after electrolysis was performed. Gaseous samples were investigated using gas chromatography (GC).

Liquid Injection Gas Chromatography (LGC)

Liquid injection gas chromatography (Thermo Scientific, Trace 1310, TR-Wax column 30 m x 0.32 mm ID x 0.50 μ m film) is suitable for detection and quantification of alcohols and aldehydes and was therefore used for proof of substrates and products from reduction reactions of butyraldehyde and CO₂. Analysis in LGC followed a method starting at 50 °C of injection temperature for 1 min followed by an increase to 250 °C within 10 min and keeping that temperature for further 10 min. Liquid samples were taken from the setup for the reduction reaction with needle and syringe and were injected as obtained. Injection was done using an auto sampler calibrated for injecting sample volumes of 1 μ L into the chromatograph. For detection a flame ionization detector (FID) was used.

Identification and quantification of expected substances was done by injecting standard solutions containing concentration between 0.1 and 100 ppm of the substance.

Capillary Ion Chromatography (CAP-IC)

Capillary ion chromatography (Dionex ICS 5000, conductivity detector, AG19, CAP, 0.4 x 50 mm pre-column, AS19, CAP, 0.4 x 250 mm main column) with potassium hydroxide (KOH) as eluent for isocratic chromatography is justified for analysis of anionic substances such as salts from organic acids, halogenic salts, phosphates or sulfates. This method was therefore used for the detection and quantification of possibly generated formate as reduction products from CO₂. Liquid samples were diluted 1:10 with highly purified 18.2 M Ω water for the injection. Injection was performed by injecting 1 mL of diluted sample with a syringe. During measurement method the eluent generation was kept at 10 mM for 10 min, followed by increasing the concentration to 45 mM within 15 min and keeping the concentration at 45 mM for further 2 min. A conductivity detector was used for signal detection.

In CAP-IC the focus for products from CO₂ reduction was on formate mainly. Therefore retention time identification of formate was done by recording chromatograms using standard solutions containing 1, 10 and 100 ppm of formic acid.

Gas Chromatography (GC)

Gas chromatograms for samples of the headspace gas were analyzed as described already in 2.1.7 for the microbial electrolysis experiments.

2.2.5. Calculation of Efficiency

Efficiencies concerning generation of reduction products were calculated for both, the non-electrochemical processes using the co-enzyme NADH as electron donor and for electrochemical processes with direct electron injection from an electrode.

Efficiencies in approaches using a co-enzyme were calculated according to the amount of NADH added. Referring to Figure 8, there is one molecule of NADH required for a 2-electron reduction. That means that for every NADH molecule consumed, one molecule of product can be generated within one 2-electron reduction step. The amount of NADH added (in mg) was divided by the molar mass of NADH as $665.45 \text{ g mol}^{-1}$ to obtain the number of moles which corresponds to the theoretical number of mol of the product. From analytics and quantification using standard calibration the experimentally obtained number of mol was calculated. Dividing the experimentally obtained number by the theoretical value delivers the percentage value for the conversion efficiency.

For the electrochemical experiments faradaic efficiencies were determined according to paragraph 2.1.8 where the efficiency calculation is discussed in detail.

The real, experimentally achieved number of mol was determined from analytical measurements. Quantification was done using calibration standards with different but known amounts of the investigated reduction product. Dividing this value by the calculated, theoretical value delivers the percentage of faradaic efficiency.

2.3. Microscopic Characterization of Carbon Felt

Carbon felt was used as material for the working electrode in both, microbial and enzymatic, electrochemical approaches. This material offers favorable properties such as high surface area and high availability at low price. Further its sponge-like constitution makes it highly suitable for the immobilization of biocatalysts. Characterization of pristine carbon felt was done in scanning electron microscopy using a Zeiss 1540XB SEM instrument (by courtesy of Dogukan Apaydin). Images of a carbon felt sample were taken with 84 and 3000 fold magnification. Imaging was done at 5 kV and an aperture size of 30 μm . Further pristine carbon felt was imaged using incident light microscopy performed with Nikon Eclipse LV100ND microscope at 5 fold magnification. An alginate-silicate gel modified carbon felt was further also investigated using this microscopy technique with the same magnification as well as in Scanning Electron Microscopy done at 20 kV with 120 fold magnification and 10 kV with 2000 fold magnification, in courtesy of JEOL.

3. Results and Discussion

3.1. Microbial Electrolysis for CO₂ Reduction

3.1.1. MEC 1-Microbial Electrolysis at Lower Potential

As an initial step for microbial electrolysis, growing of microorganisms from the sewage suspension on the carbon felt electrode was investigated and conducted for four days in the approach of MEC1. Since there was a constant potential of -700 mV vs. Ag/AgCl applied and the system was purged with CO₂ and H₂ at a ratio of 1:1 during the whole procedure, it was expected to generate methane from the reduction of CO₂ already during the growing process. Analysis of headspace gas samples in gas chromatography supported this expectation and shows the increase of methane concentration with progressing time of growth. Figure 19 features the recorded gas chromatograms from day 1 to day 4 of the growing procedure. An increasing peak is observed at the corresponding retention time of methane at 0.48 min.

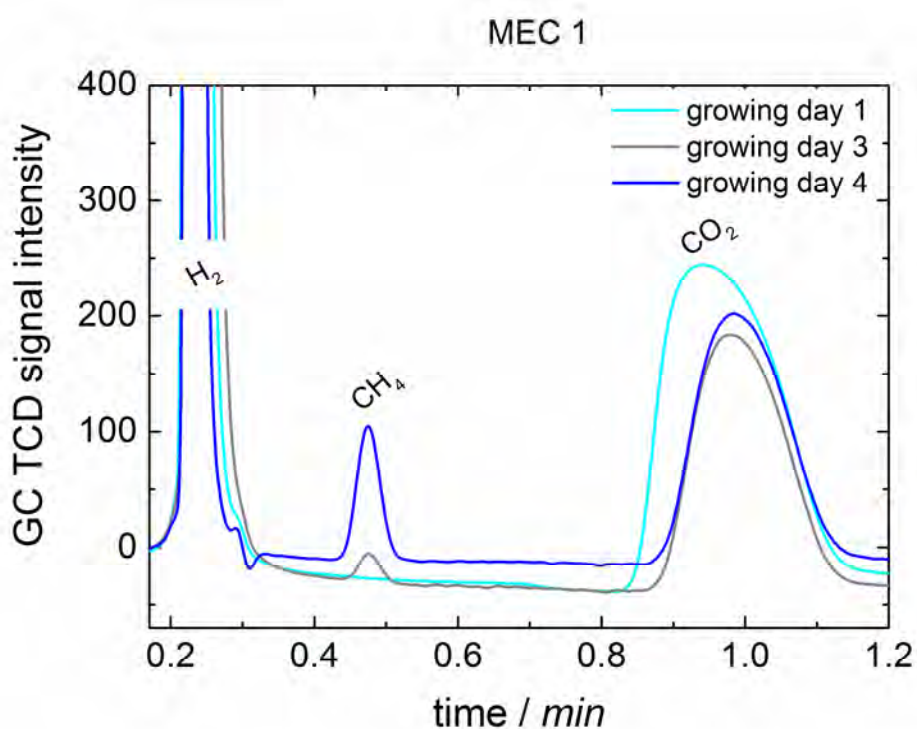


Figure 19 Gas chromatograms of the headspace constitution of the cathode compartment in MEC1. Chromatograms show the development of amount of reduction product during the growing process. An increase of methane concentration is observed within four days of growing of microorganisms on the carbon felt electrode.

The sudden development of the methane peak on day 4 is supposed to appear due to an obtained stabilization of the microorganisms on the electrode after adding them as homogenous catalyst (as a content of sewage suspension) to the electrochemical system.

The observed attachment of the microorganisms occurs only when there is a negative potential applied to the carbon felt electrode. This effect is supposed to happen due to the electron uptake of the microorganisms via the direct or indirect extracellular electron transfer.^[61] The electron transfer is basically described to happen due to electrothrophic or exoelectrogenic properties of the microorganisms. Electrothrophic mechanisms are regarded as part of the energy metabolism of the microorganisms, in which they take up the electrons from the electrode.^[80] Exoelectrogenic mechanisms are described to be dependent on enzymes and charge carriers in the gram-negative cells of the microorganisms. Those

enzymes and corresponding charge carriers influence the electron transfer to or from the cell-wall surface as a sort of energy transduction.^[41]

Biofilm formation on the carbon felt electrode was observed after about 24 h of potentiostatic performance in a CO₂/H₂ saturated system as an algae-like growth (Figure 20) and was enhanced after 4 days of growing procedure.



Figure 20 Biofilm formed after proceeding growth of the microorganisms on the electrode for 3 days. The red circle displays the microorganisms grown on the electrode.

Microorganisms, grown as biofilm on the electrode, require in that state artificially added H₂ in addition to electrons from the electrode for the reduction reaction of CO₂ to methane. After the growing procedure therefore adaption of the microorganisms to CO₂ only performance was initiated. An early characterization of the biocathode was done with cyclic voltammetry to display electrochemical mechanisms occurring. Measurements were recorded at the beginning of the adaption. Characterization after purging CO₂ and H₂ in a ratio of 1:1 shows a strong increase in reductive current from -300 mV vs. Ag/AgCl (Figure 21). Further, cyclic voltammetry performed with the biocathode but in a N₂ saturated system does not show a remarkable increase in reductive current. In addition application of a pristine, blank carbon felt electrode, without microorganisms grown on it, was investigated

under the same conditions and by using the same parameters. Again no increase in reductive current is observed for the N₂ and also for the CO₂/H₂ saturated system.

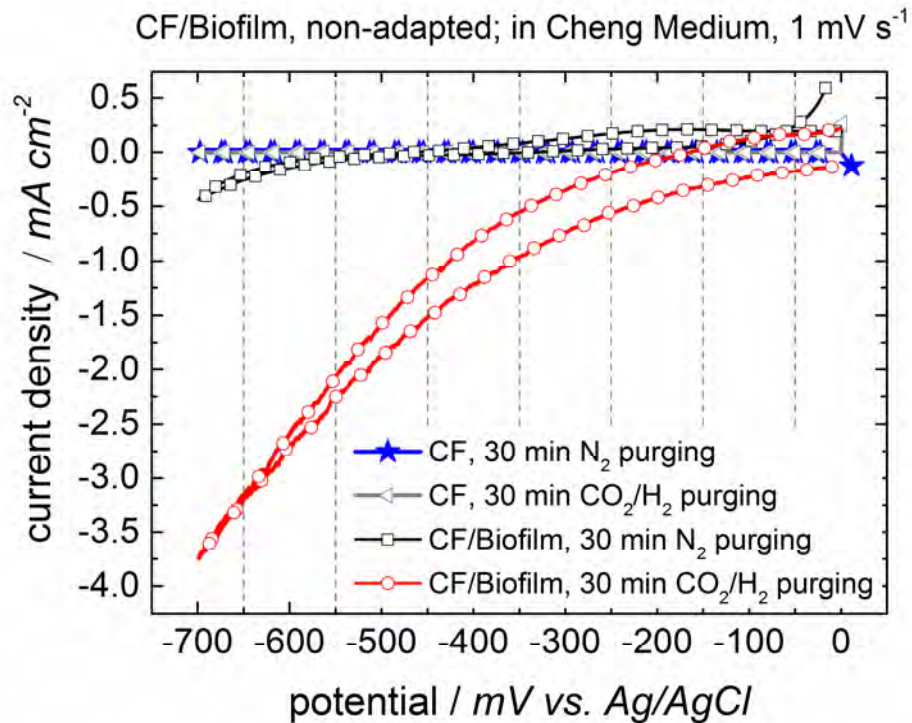


Figure 21 Cyclic voltammograms of the biocathode in the non-adapted state. The biocathode was electrochemically characterized after purging and saturating the system with N₂ or CO₂/H₂ respectively. Further for comparison the same measurements were performed for a pristine carbon felt electrode without biofilm.

The microbial electrolysis cell was then investigated during adaption cycles and for long-term performance after adaption was completed.

Figure 22 shows the constant methane generation from the reduction of CO₂ even due to decrease of H₂ added with increasing number of cycles. This indicates stabilization of the microorganisms to a CO₂ only performance without any H₂ needed.

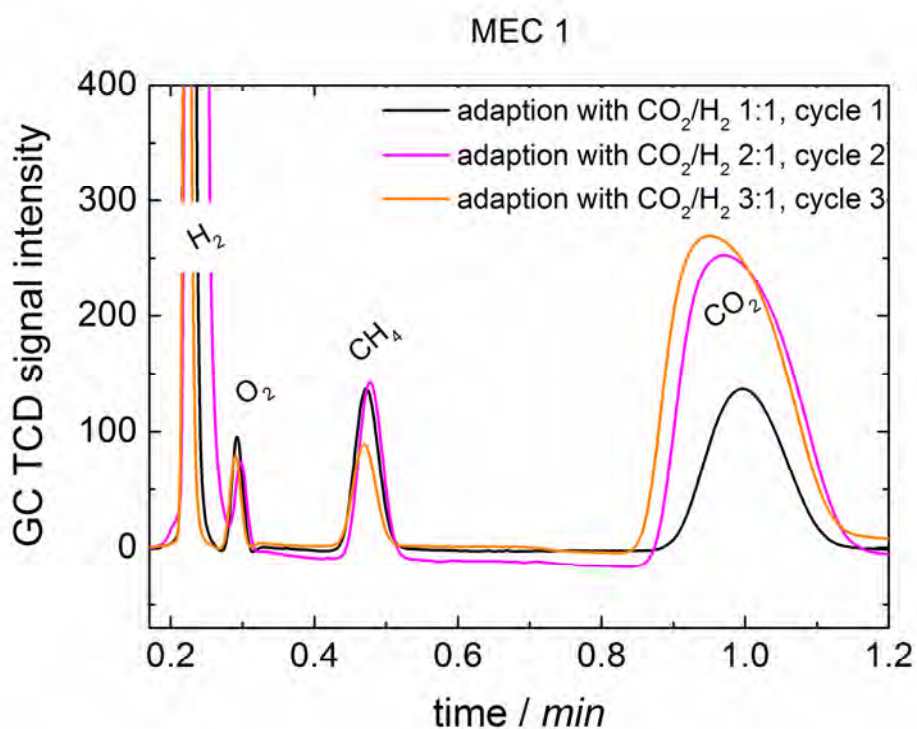


Figure 22 Gas chromatograms featuring the development of the headspace gas constitution during adaption with CO₂ and H₂. Concentration of H₂ added was reduced subsequently with every cycle. Adaption was performed within 3 cycles and 3 weeks respectively.

The performance of this adapted biocathode in microbial electrolysis with CO₂ as the only C-source and without requiring any H₂ added artificially was then investigated over several weeks. The microbial electrolysis cell therefore was conducted steadily under potentiostatic conditions. The cell was purged only with CO₂ daily for several hours. Methane production was subsequently analyzed in gas chromatography about 24 h after saturation with CO₂. Figure 23 shows the methane production from long-term microbial electrolysis for the reduction of CO₂ over 22 weeks.

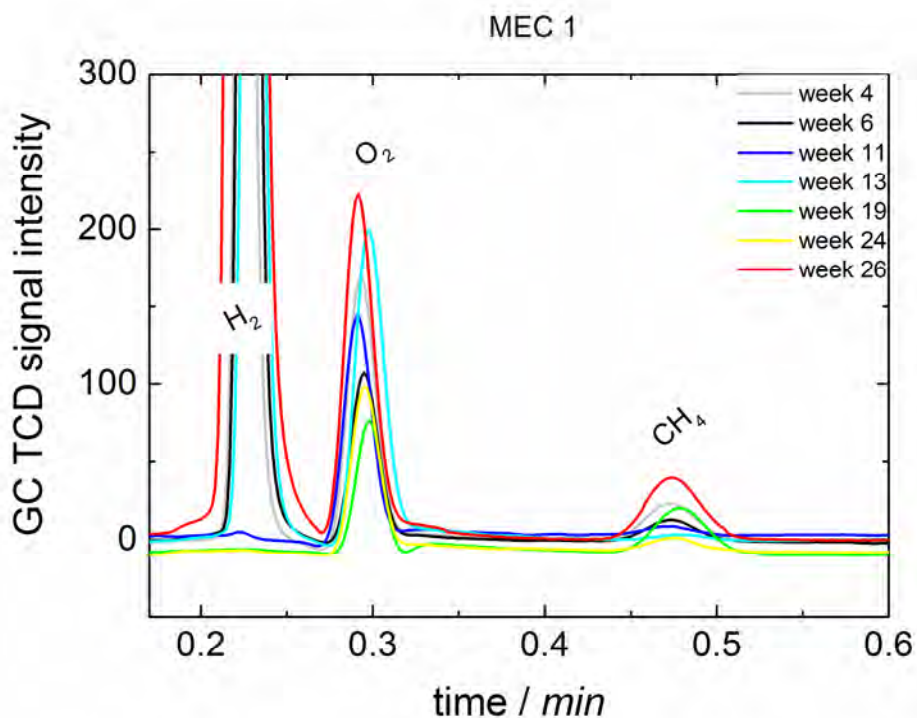


Figure 23 Gas chromatograms showing long-term performance of MEC1 after completed adaption with CO₂ and H₂. Methane production in general decreased, in comparison to performance immediately after adaption. However, methane generation was rather constant within 22 weeks of performance despite of lower concentration, as seen for the methane peaks at 0.48 min of several records in gas chromatography.

In addition to the reduction of CO₂ to methane, hydrogen generation is observed to be performed from the microorganisms themselves. Since there was steadily potential applied to the system, one would expect a constant generation and constant amount of H₂. According to the H₂ signal of the gas chromatograms in Figure 23 fluctuation of the peak intensity are obvious. For several measurements amounts of H₂ were not even detectable. In contrast, methane generation could be detected steadily. However, even though performance of the microbial electrolysis cell was rather constant over several weeks according to methane generation from CO₂ reduction, concentrations were rather low. Therefore re-adaption with a different approach, using glucose, and enhancement of the biofilm on the carbon felt cathode was intended.

The microorganisms immobilized on the electrode were therefore established back to a non-adapted state, by adding sewage suspension containing microorganisms and by purging again with CO₂ and H₂ as well, as described in the experimental section. Adaption to CO₂ only

performance was done once again but with a different approach adding glucose in addition to purging with CO₂ and H₂ and reducing the amount of H₂ within 3 cycles. Adding saturated glucose solution supports enhancement of the biofilm as it is a favorable C-source for the microorganisms. Moreover glucose does not compete with CO₂ as C-source in the further performance but even improves productivity without H₂ and CO₂ only. Figure 24 shows the recorded gas chromatograms of the headspace of MEC1 during adaption with glucose and CO₂/H₂. Methane production is increased during adaption in comparison to methane performance before the repeated adaption shown in Figure 23 as it is obvious from the rising peak at the retention time of methane at 0.48 min.

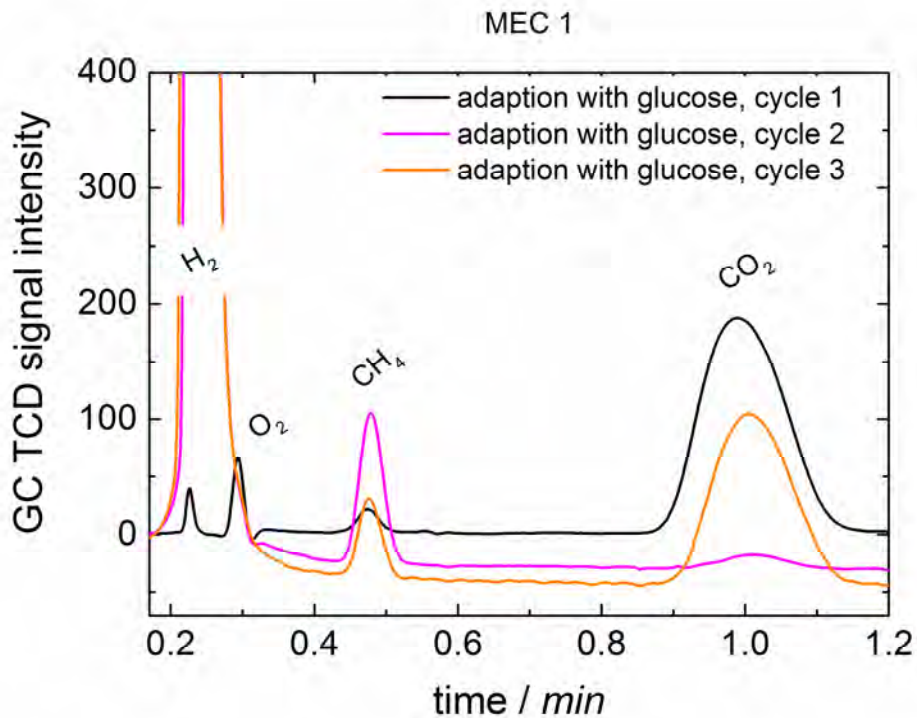


Figure 24 Gas chromatograms showing the development of methane generation within adaption of the microorganisms using glucose.

After completed second adaption, long-term performance of the microbial electrolysis cell was investigated over several months with a constant applied potential of -700 mV vs. Ag/AgCl as it was done after first adaption procedure as well. Regularly recorded gas

chromatograms of headspace gas samples from the cathode compartment show an improved productivity of methane generation in comparison to performance before repeated adaption in Figure 23. Constant potentiostatic electrolysis after repeated adaption delivered amounts of methane generated from CO₂ reduction that have been about double that high compared to amounts produced before the second adaption procedure. Figure 25 shows records of gas chromatograms of headspace gas samples of MEC1 after adaption with glucose for long-term performance of 25 weeks.

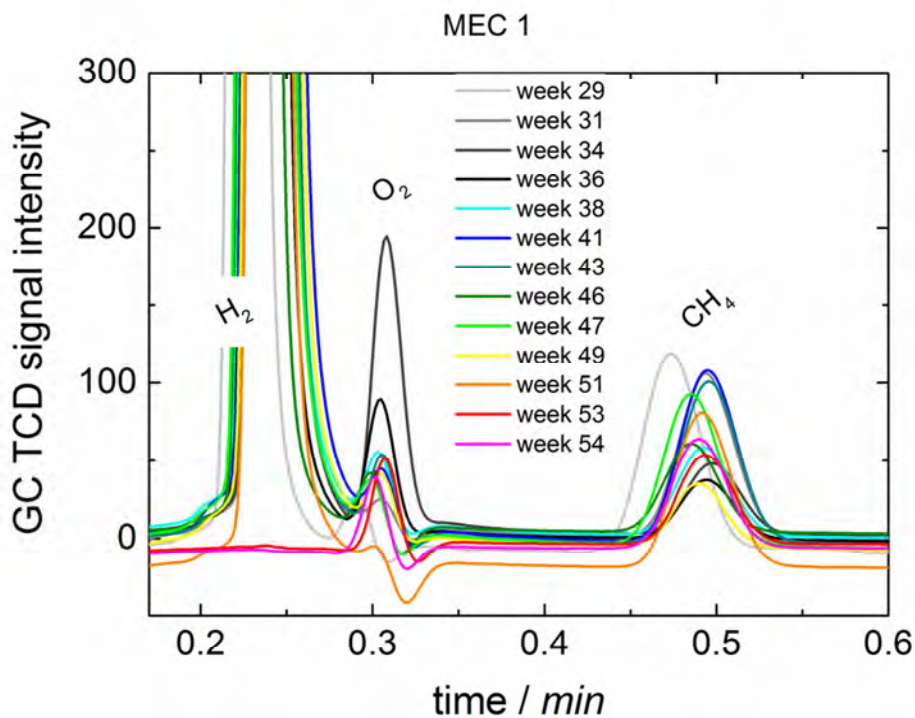


Figure 25 Gas chromatography records for the long-term performance of MEC1 after repeated adaption with glucose. Production of methane from CO₂ reduction shows a remarkable increase in comparison to results from long-term performance before adaption with glucose.

As it was observed for previous results after adaption with CO₂/H₂, methane generation stayed rather constant during long-term performance for the glucose adapted biocathode as well. For hydrogen production the same fluctuations were observed as for the first long-term investigation. However it is expected that the H₂ is not only produced but also partly used by the microorganism for their metabolism and the reduction of CO₂ to methane.

Correlation of detected amounts of H₂ and CH₄ from headspace gas samples of the cathode compartment of MEC1 over that time shows that fluctuations of H₂ and CH₄ concentration were mainly parallel (Figure 26). Peak values of concentrations for both were reached at approximately the same time during the long-term performance. This indicates the regenerative behavior of the living biocatalysts, occurring rather regularly every 2-3 weeks. However, H₂ generation follows much stronger fluctuations over time in contrast to the generation of methane, where fluctuations in concentrations over time are much less intense.

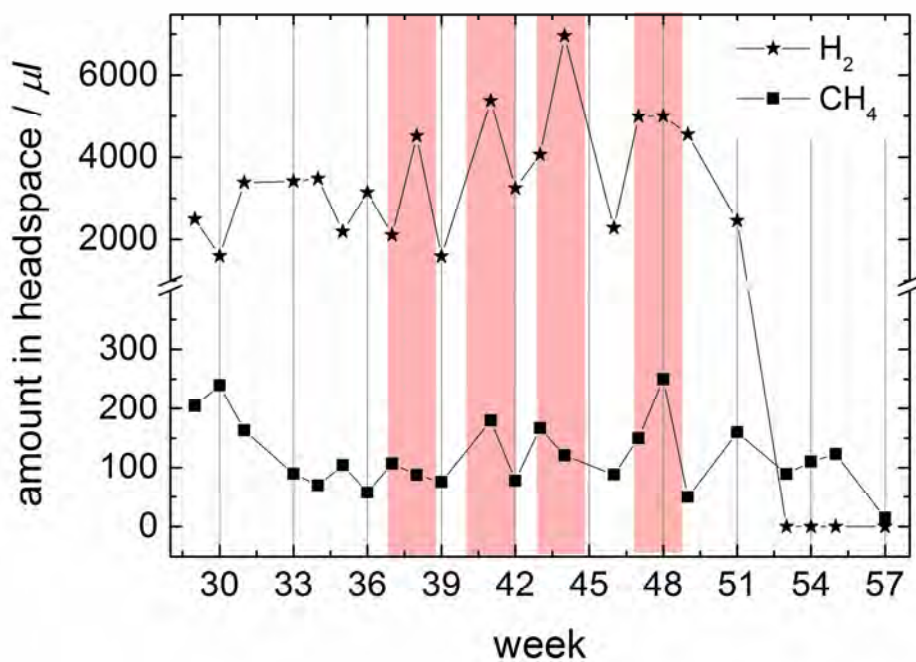


Figure 26 Correlation of amounts of H₂ and CH₄ in the headspace of the cathode compartment of MEC1 during long-term performance after the second adaption.

Figure 27 displays cyclic voltammograms that were recorded for characterization of the adapted biocathode after 8 weeks of long-term performance. There is an increase in reductive current from -300 mV vs. Ag/AgCl observed only for the CO₂ saturated system for the adapted biocathode. Saturation with N₂ and experiments without biofilm did not deliver

an increase in reductive current which indicates that the predominant reaction of the microbial electrolysis is the reduction of CO_2 to methane. In comparison to Figure 21, displaying such CV's of the biocathode just after growing and after purging with CO_2 and H_2 , current densities are smaller for the adapted biocathode. This is believed to occur due to steady regeneration of the microorganisms, as it is a living system. Further adaption procedures and long-term performance were done between electrochemical characterization of the non-adapted and the adapted microbial electrolysis cell, which makes a direct comparison of cyclic voltammograms not reasonable.

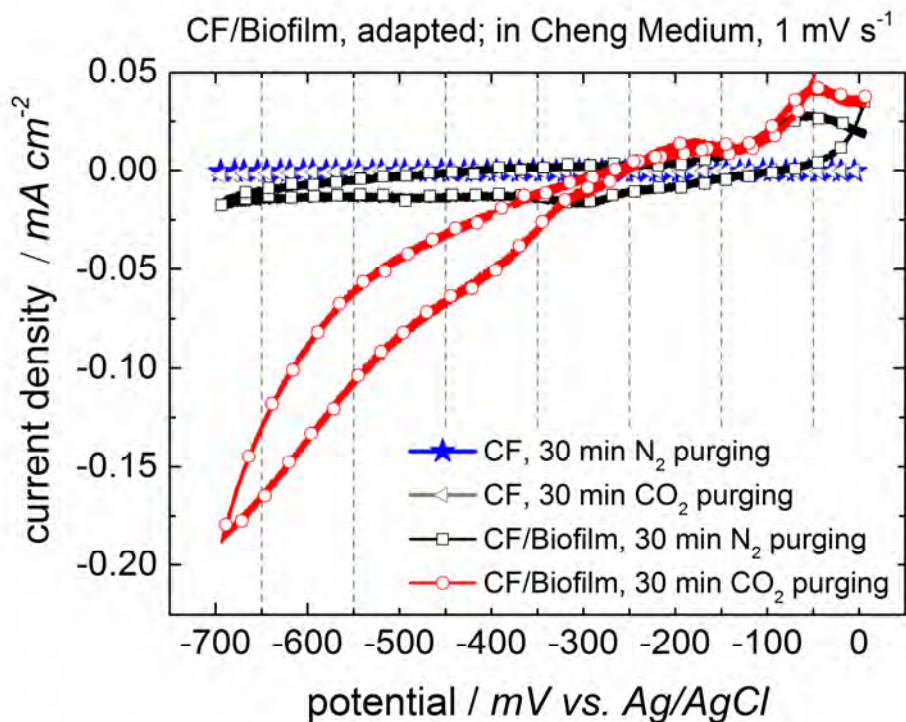


Figure 27 Cyclic voltammograms of the adapted biocathode in MEC1 in N_2 and CO_2 saturated system. An increase in reductive current is only observed after the system was purged with CO_2 . Further comparison with a pristine carbon felt electrode without any biofilm supports that CO_2 reduction only occurs when there are microorganisms apparent.

For comparison and to proof the necessity of electron supply for the reduction reaction, gas chromatograms were recorded further for samples of the headspace of the adapted MEC1 when no potential was applied. Chromatograms of samples after saturation of the system

with CO₂ and after 20 h without any potential applied are shown in Figure 28. At the retention time of methane at around 0.48 min, there is no increase of a peak observed. This indicates that methane is only generated in the microbial system from reduction of CO₂ when potential was applied and electrons were provided therefore.

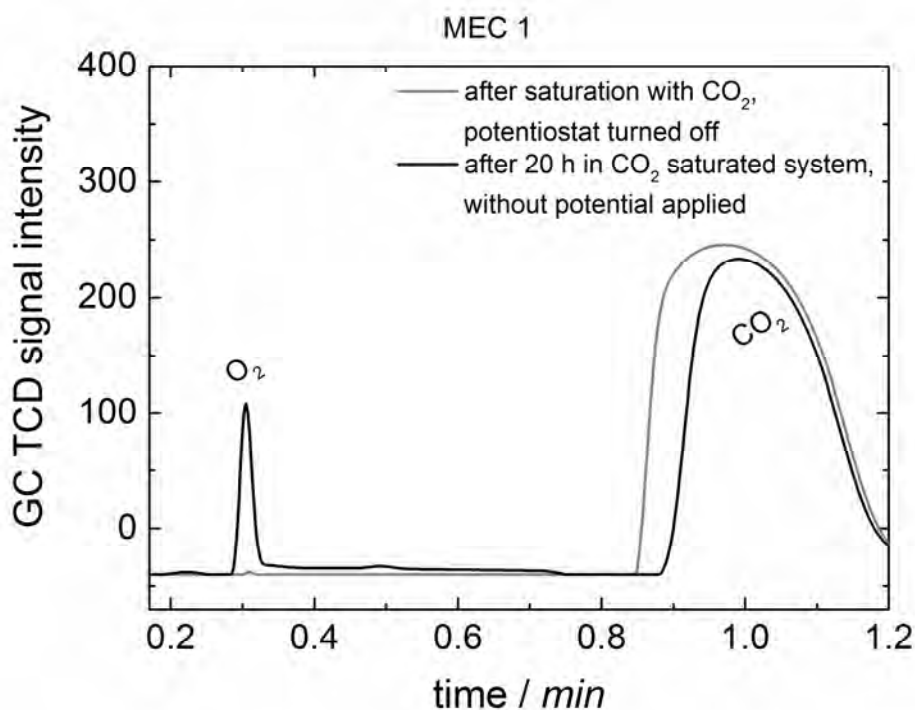


Figure 28 Gas chromatograms of the cathode compartment when there was no potential applied. Chromatograms were recorded after saturating the system with CO₂ and after 20 h when there was no potential applied. There is no methane formation observed.

Efficiencies for MEC1 were determined from potentiostatic electrolysis when the system was saturated with CO₂ and headspace samples were analyzed in gas chromatography before and after electrolysis. According to the number of charges consumed within 4 h (39 C) a faradaic efficiency of 22% was calculated for 17.5 μL of methane detected for the headspace volume of the cathode compartment. However, it is expected, that due to low kinetics generation of methane from that time of electrolysis would be actually higher but cannot be detected immediately after electrolysis, since metabolism of the microorganisms for sufficient CO₂ conversion takes a longer time after completing supply of electrons.

3.1.2. MEC2-Microbial Electrolysis at Higher Potential

In addition to MEC1 an identical setup (MEC2) was driven at a constant potential of -850 mV vs. Ag/AgCl. Microorganisms were grown on a carbon felt electrode with the same procedure as it was done for MEC1. Additionally, since it was observed in experiments with MEC1 to enhance the biofilm formation and performance, 0.1 mL of saturated glucose solution were added to the electrolyte solution (Cheng Medium) of the cathode compartment, containing the biofilm electrode and the system was purged with CO₂/H₂. The biofilm on the cathode was enriched within 4 weeks before adaption procedure to a CO₂ only performance was started. Figure 29 depicts recorded chromatograms of headspace gas samples from the cathode compartment of MEC2. A sample after completed growing of microorganisms on the electrode is compared to samples from enrichment procedure of the biofilm with glucose. A small increase in intensity of the peak for methane at 0.48 min is observed after 4 weeks of enhancing the biofilm.

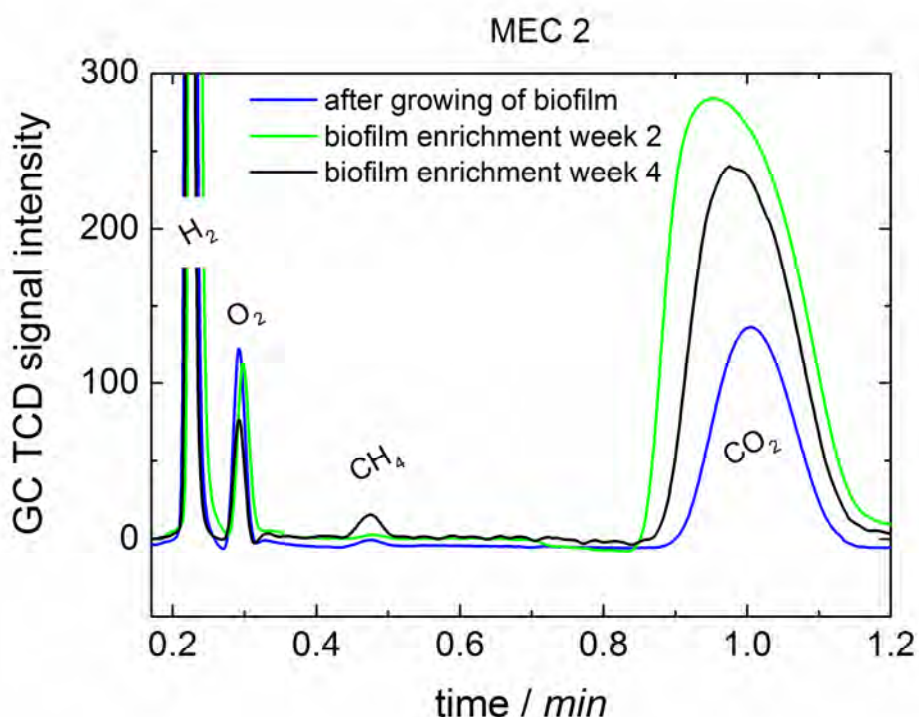


Figure 29 Gas chromatograms of headspace gas samples after growth of microorganisms on the carbon felt electrode and during enrichment of the biofilm. Analysis shows a slow and small increase of methane concentration after 4 weeks of enhancing the biofilm.

Adaption of MEC2 was also performed according to results observed in experiments with MEC1. Due to more promising results obtained with the adaption method using glucose in addition to saturation of the system with CO_2/H_2 , this method was chosen for application to MEC2 as well. Methane production was observed during the whole adaption procedure. However, amount of methane detected from the headspace was remarkably lower than for the same procedure performed with MEC1 at a lower potential, shown previously in Figure 24. In Figure 30 gas chromatograms of headspace gas samples during different cycles of the adaption mechanisms and after completed adaption are compared. During adaption an increase of the methane peak at 0.48 min and increase of methane concentration respectively was observed. Nevertheless, after completed adaption, methane concentration decreased slightly.

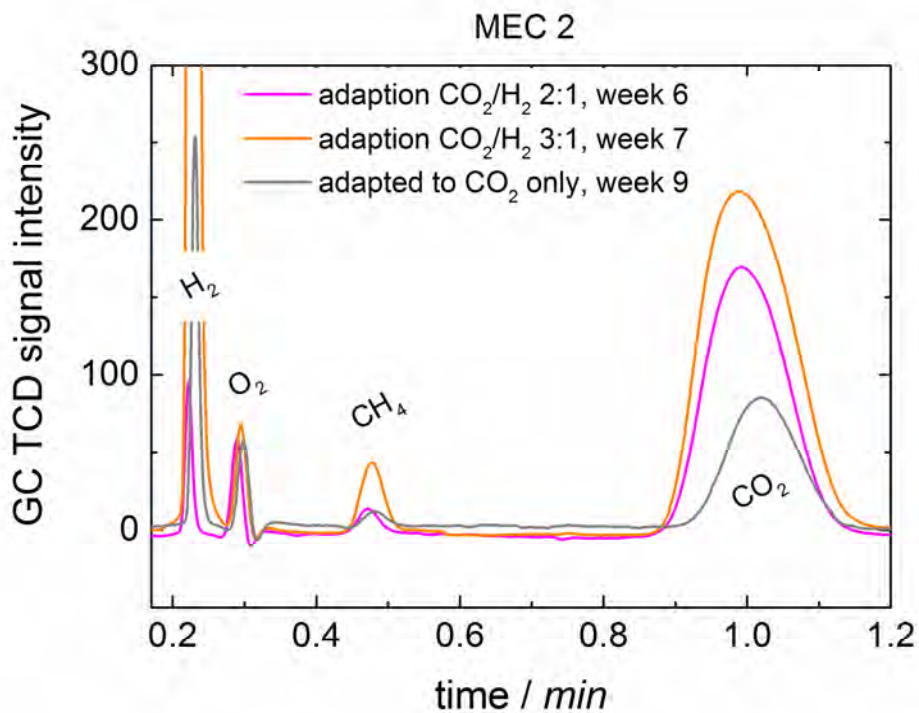


Figure 30 Gas chromatograms of headspace gas samples from MEC2 during adaption with glucose and CO_2/H_2 . Methane formation was observed already during adaption as can be seen for the peak at 0.48 min corresponding to the retention time of methane.

However, long-term performance of MEC2 in the adapted state with CO₂ purging only, depicts a strong increase for the first 3 weeks. Methane concentration then decreased in the following 3 weeks back to initial values, as achieved directly after adaption. Further methane concentration was increasing and decreasing within the same time periods. This development is shown in Figure 31. Moreover, H₂ concentration during long-term performance displayed a similar behavior as it was also investigated for MEC1. Concentrations are intensively fluctuating over time and can therefore be correlated to a generation process occurring due to the microorganisms but not from water splitting due to the negative potential applied.

For MEC2 fluctuations of H₂ as well as of CH₄ are particularly more intense as it was seen from results of MEC1. Especially concentrations of H₂ are increasing and decreasing strongly during long-term performance of MEC2. Correlation of fluctuations in the amounts of H₂ and CH₄ detected, however, can be done for MEC2 as well as it was done for MEC1 in Figure 26.

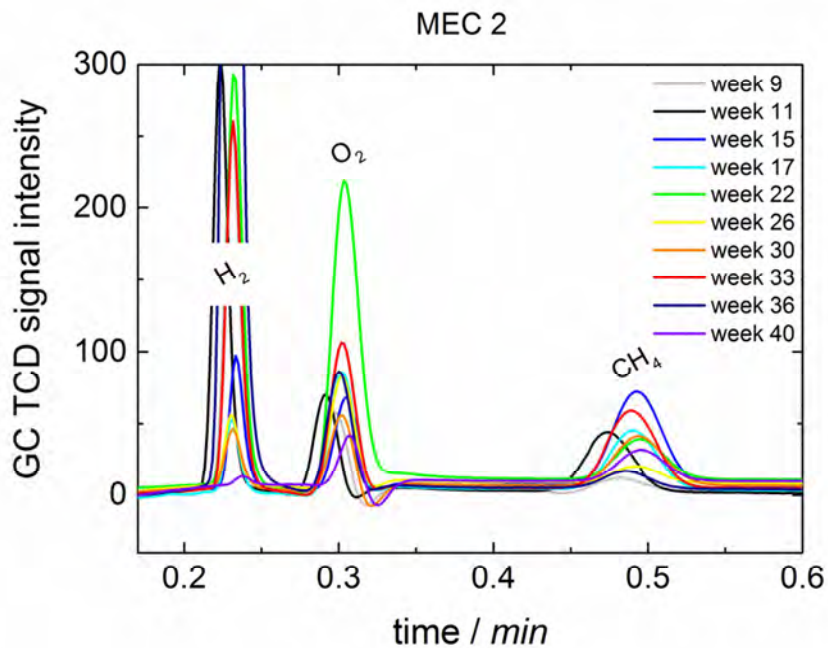


Figure 31 Gas chromatograms of headspace gas samples of MEC2 during long-term performance with CO₂ only after adaption. A periodic increase- and decrease-behavior is observed for the methane peak intensity and concentration respectively at 0.48 min.

Figure 32 features concentration values of the two analytes. Increasing or decreasing concentration of H_2 can mainly be directly correlated to the same effects in CH_4 concentration.

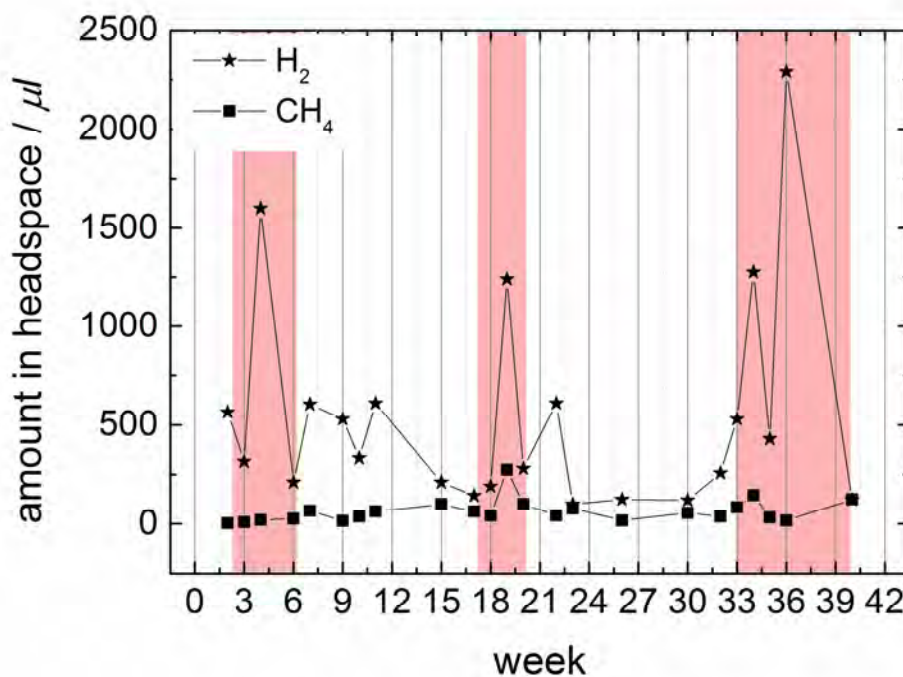


Figure 32 Correlation of concentration values of H_2 and CH_4 during long-term performance over several weeks.

Besides investigations according to performance in methane production, the system was characterized electrochemically using cyclic voltammetry. The enriched but non-adapted biocathode further was characterized prior to adaption procedure using cyclic voltammetry. Cyclic voltammograms of the biocathode in a N_2 or CO_2/H_2 saturated system, before adaption was performed, were compared to the same measurements done after adaption of the biocathode in N_2 or CO_2 saturated electrolyte solution. These measurements were proceeded the same way as it was done previously for MEC1, except for sweeping to a higher negative potential of -850 mV vs. Ag/AgCl. However, as obvious from Figure 33, current densities were very low in comparison to cyclic voltammograms recorded previously for MEC1. Further, the highest increase in reductive current is seen for the adapted biocathode after saturation with CO_2 . The same electrode in N_2 saturated solution does not deliver a comparable increase in reductive current. Moreover, cyclic voltammograms of the

non-adapted biocathode show even lower current densities, in contrast to results obtained from electrochemical characterization of MEC1, where the non-adapted system delivered the higher current densities than the adapted system (Figure 21 and Figure 27).

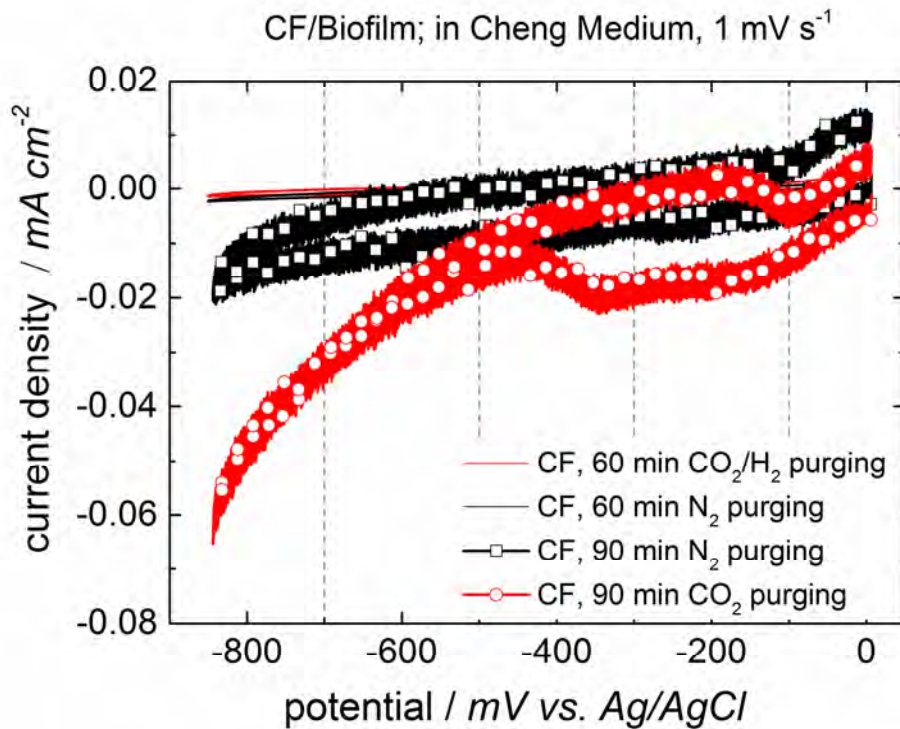


Figure 33 Cyclic voltammograms of a biocathode and a pristine carbon felt electrode.

Efficiencies for MEC2 were calculated from potentiostatic electrolysis for 3 h in the adapted state. Samples were taken before and after electrolysis from the headspace and were analyzed in gas chromatography. During electrolysis 11.23 C were consumed which corresponds to a theoretical amount of $1.45 \cdot 10^{-5}$ mol or 329 μ L of methane to be produced. GC analysis delivered 2 μ L of methane generated during the experiment and therefore gives an efficiency of 0.6%. This faradaic efficiency seems to be very low in comparison to efficiencies reported in literature earlier.^[58, 61] It is expected that the microbial reduction of CO₂ happens via a quite slow process and electrolysis for 3 h does not indicate an appropriate time scale for such processes. However, longer electrolysis experiments did not deliver much higher faradaic efficiencies. Comparison of methane production during

potentiostatic performance over 24 hours (after saturation with CO₂), where approximately 173 C were consumed, delivered 3.4% of faradaic efficiency according to 170 μL of methane produced. Comparing results of MEC1 and MEC2 shows similar behaviors according to growing, adaption and constant product generation. However, remarkable differences in faradaic efficiencies are not expected to correlate with the potential applied. From observations of the biofilm formation and long-term investigations, it has been seen that the quality of the biofilm and therefore number of microorganisms immobilized plays an initial role. The higher efficiencies achieved for MEC1 might come due to repeated adaption and re-inoculation of microorganisms for the second adaption. This means, more microorganisms were grown as a biofilm on carbon felt. Further, determination of faradaic efficiencies might not be suitable for living biocatalyst. Slow kinetic processes during the reduction reactions and slow metabolism of the microorganisms respectively make it difficult to correlate the indeed amount of methane generated. In order to obtain a realistic number of methane generated one has to take into account, that after electrolysis there might be a remarkable number of electrons and CO₂ be taken up by the microorganisms but being located in the metabolism and therefore would not appear as methane generated in the headspace.

Nevertheless, both approaches show a constant production of methane over a long-term performance of one year, which depicts a reliable, bio-sustainable system with stable catalysts. Improvement of efficiency and optimization of such processes opens the way for large-scale applications with bio-based, cheap and high capability supply of catalyst.

3.1.3. Anodic Oxygen Evolution with Nocera Catalyst

During performance of microbial electrolysis it was also intended to utilize the oxidation potential of the anode compartment as a parallel ongoing counter reaction for CO₂ reduction. For this purpose oxygen evolution reaction (OER) was decided as the oxidation reaction of choice. To catalyze anodic water splitting according to oxygen evolution reaction a catalyst was applied. A favorable catalyst known to be very suitable for the oxidation

reaction is the Co^{2+} based so-called Nocera-catalyst (presented by D. Nocera et al.^[22]), which was applied to the platinum anode by electropolymerization.

For electropolymerization of the catalyst on Pt, the electrode was applied as cathode in the electropolymerization setup. Figure 34 displays cyclic voltammograms for potentiodynamic electropolymerization as a first step, obtained from cycling 100 times by sweeping the potential between 0 mV and +1100 mV vs. Ag/AgCl. With increasing number of cycles current densities are increasing, indicated by the arrow. Such an increase is due to changed resistivity of the electrode during formation of the catalyst film on the Pt electrode. Subsequently to potentiodynamic electropolymerization potentiostatic electropolymerization was conducted by applying constantly +1100 mV vs. Ag/AgCl for around 1 h as it was demonstrated in Figure 35.

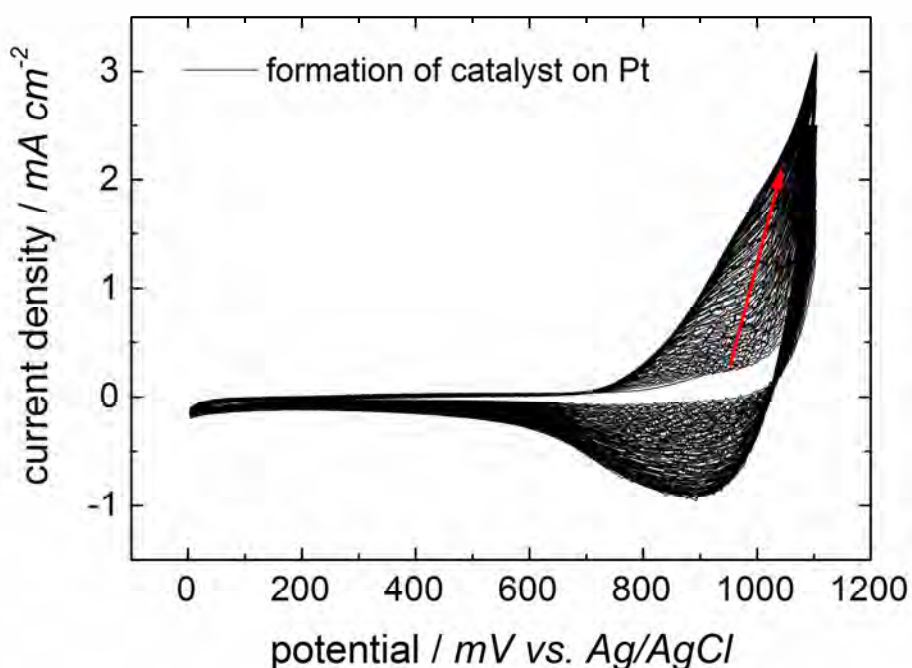


Figure 34 Electropolymerization of the Co^{2+} Nocera catalyst on Pt. Increasing number of cycles results in an increase of current densities due to changed resistivity of the electrode due to film formation on the electrode.

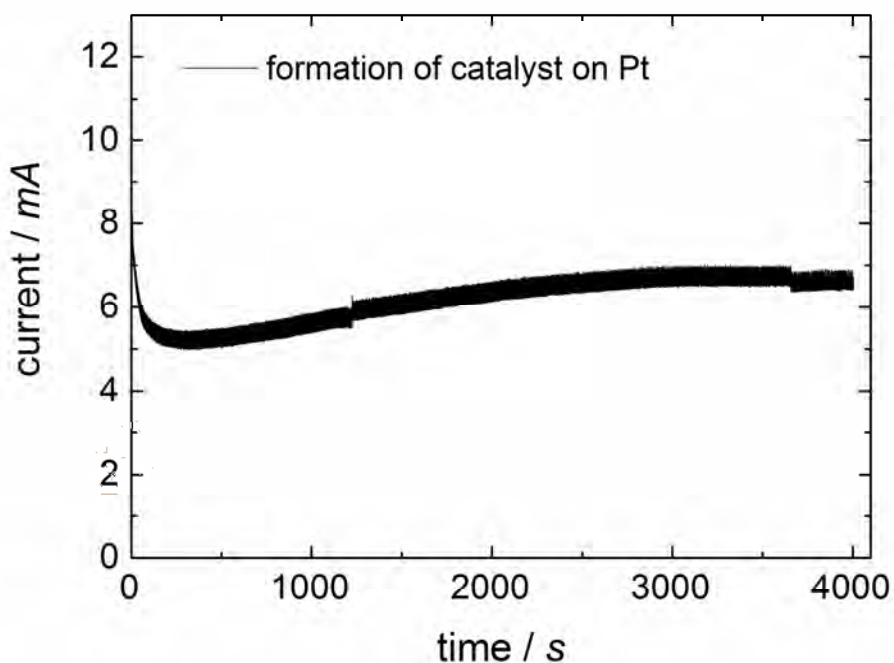


Figure 35 Potentiostatic electropolymerization subsequent to potentiodynamic film formation. Application of +1100 mV vs. Ag/AgCl for about 1 h features a constant current flowing.

Constant application of the positive potential delivers a constant flow of current which indicates a stabilized film of catalyst, since there are no changes in current or resistivity respectively obtained. A picture of the achieved platinum electrode covered with the Co^{2+} Nocera catalyst is shown in Figure 36.



Figure 36 Photograph of the obtained Pt electrode covered with Nocera catalyst after electropolymerization procedure.

After completed electropolymerization technique the electrode was rinsed with highly pure 18.2 M Ω water and dried for subsequent characterization in SEM-EDX analysis. SEM measurements demonstrated in Figure 37 and Figure 38 show the island-like constitution of the catalyst on the surface. Further, white spots on the islands are expected to correlate to salt residues from electrolyte solution remaining due to insufficient rinsing. Elementary constitution in Figure 38 delivered from SEM imaging shows mainly Co and Pt as components across the points analyzed in detail (indicated as 1, 2 and 3 in Figure 37). As expected, also traces of phosphate and potassium were found, which are due to remains of the phosphate buffer electrolyte solution, used for electropolymerization. Precise constitution in percentage values for the three different spots across the catalyst electrode is found in Table 5.

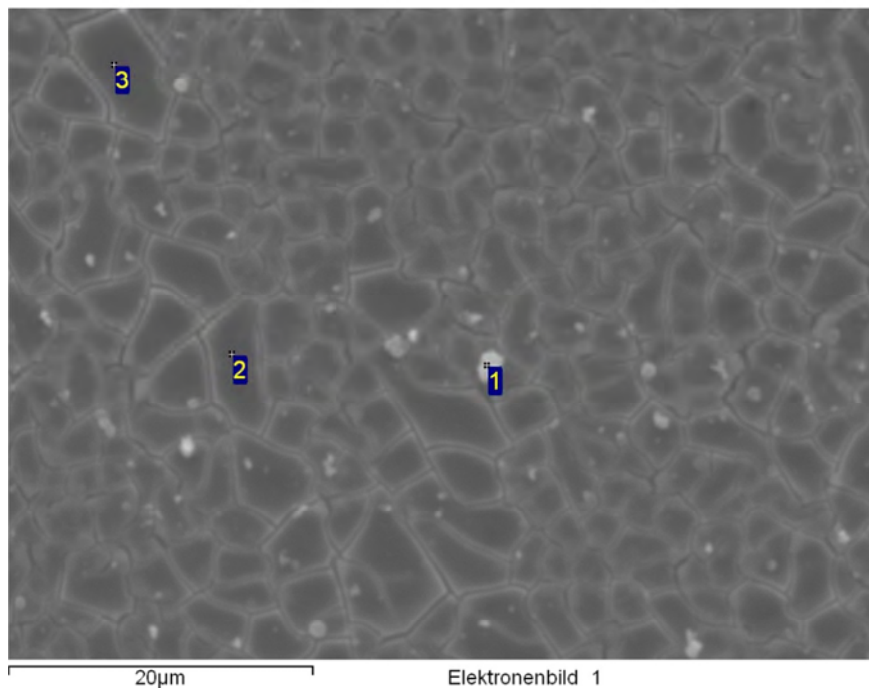


Figure 37 SEM surface image depicting island-like constitution of the Co-based Nocera catalyst. Besides islands white spots are observed that are expected due to salt residues from electropolymerization procedure.

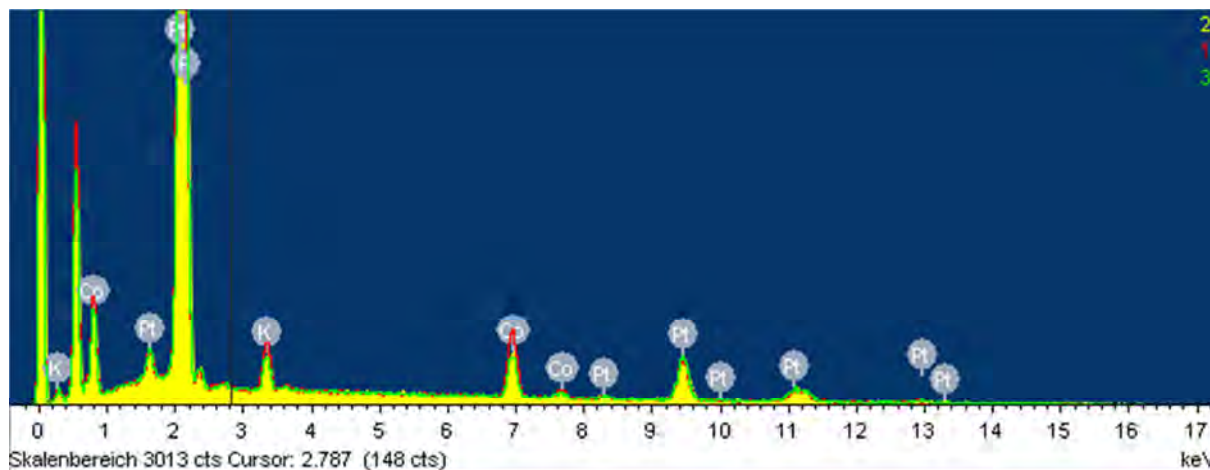


Figure 38 Elementary constitution of the islands and white spots from SEM image. Constitution depicts high amounts of cobalt and platinum as expected for the catalyst film. Besides there are hardly any impurities detected. Small traces of potassium and phosphate were also expected due to the phosphate buffer electrolyte solution.

Spectrum	P (in %)	K (in %)	Co (in %)	Pt (in %)
1	2.35	4.35	15.13	78.18
2	0.65	3.37	10.69	85.29
3	0.15	3.24	9.98	86.62

Table 5 Corresponding values in percentage for the elementary constitution determined from SEM-EDX analysis.

The previously characterized catalyst covered Pt electrode was applied to the anode compartment of MEC1 as counter electrode. Oxygen evolution was investigated during the common microbial electrolysis long-term performance at -700 mV vs. Ag/AgCl. The electrolyte solution in the anode compartment was kept as 20 mM phosphate buffer solution. Headspace gas samples from the anode compartment were analyzed in gas

chromatography measurements before and after 5 h of electrolysis at -700 mV vs. Ag/AgCl, applied to the biocathode for the reduction of CO₂.

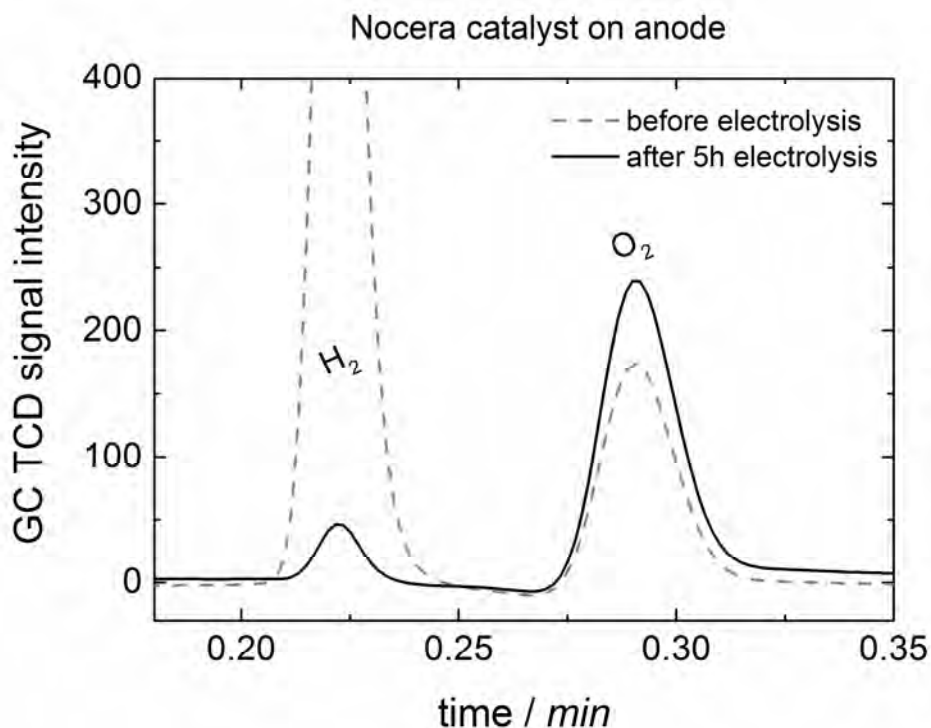


Figure 39 Gas chromatography of headspace gas samples from the anode compartment of MEC1. Chromatograms are shown for samples taken before and after 5 h of potentiostatic electrolysis.

From gas chromatograms demonstrated in Figure 39 a small increase for the oxygen peak at 0.29 min of retention time is shown. What is even more obvious is that the H₂ peak at 0.22 min is decreasing remarkably. This is supposed to occur due to proton conduction over the Nafion membrane, which is favorable in the direction from anode to cathode compartment. Oxygen evolution, however, was even observed by eye due to formation of bubbles exactly on the surface of the catalyst electrode, as demonstrated in Figure 40. However, due to the observed presence of hydrogen and oxygen at the same time in the compartment, for future approaches there is strict separation of H₂ and O₂ required to prevent oxyhydrogen (“knallgas”) reactions or explosions respectively.



Figure 40 Oxygen evolution on the surface of the Nocera catalyst electrode due to catalyzed oxidative water splitting reaction in the anode compartment of MEC1.

3.2. Enzyme Catalyzed Reduction Reactions

3.2.1. Formate Dehydrogenase for CO₂ Reduction to Formate

As a first approach for the reduction of CO₂ utilizing dehydrogenase enzymes, the first step in the 3step reduction cascade was investigated. On doing so, formate dehydrogenase was immobilized in alginate-silicate hybrid gel beads for experiments using NADH as reduction equivalent. Capillary ion chromatography was used for determination of formed formate as reduction product from CO₂. Figure 41 shows chromatograms recorded immediately after NADH was added to the CO₂ saturated system containing the enzyme beads, and after completed reduction. At the determined retention time of formate at 5.75 min the initial sample shows a small peak. It is expected that the reduction reaction using NADH occurs quite fast and therefore makes the detection of a small peak reasonable. After 16 h, where the reduction reaction was expected to be completed totally, another sample was investigated in CAP-IC. At the same position of the peak, previously detected, an even higher peak was observed which is correlated to the sufficient reduction of CO₂ to formate.

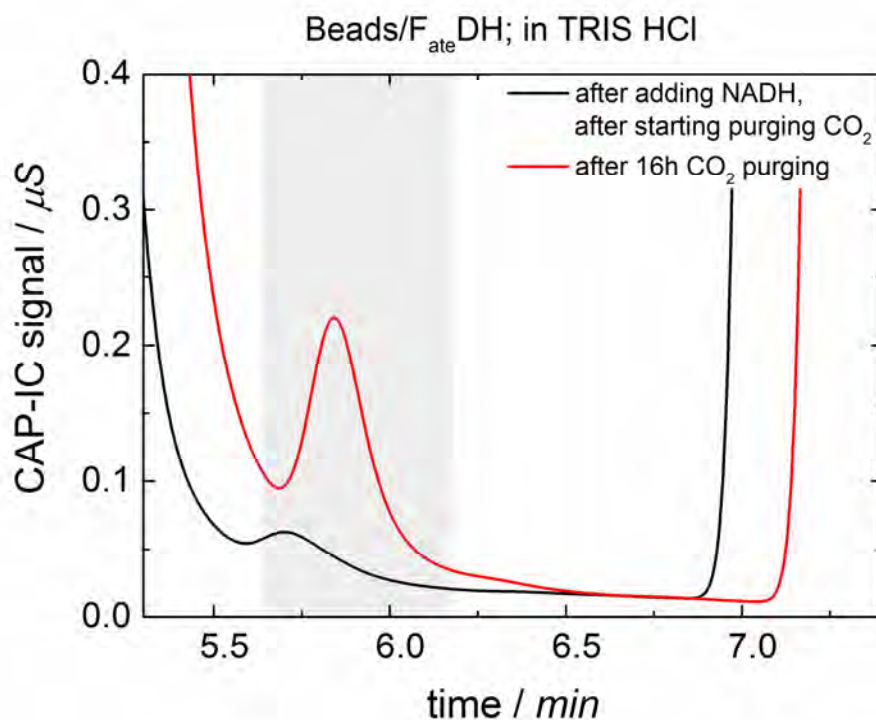


Figure 41 Chromatogram from CAP-IC comparing samples from directly after starting the reduction reaction and after completed reduction.

According to the amount of NADH added (6 mg) the theoretical value for formate that could be produced is $9 \cdot 10^{-6}$ mol. The amount detected in CAP-IC was determined as around 1 ppm corresponding to $7 \cdot 10^{-8}$ mol. Conversion efficiency according to NADH added therefore was determined as 0.8%. Efficiency as low as the value obtained are unusual according to results presented earlier by several groups.^[70, 71] Such low values are assumed to be due to experimental difficulties. F_{ate} DH as well as NADH are known as very air sensitive substance and chemically rather unstable. It is therefore expected that experiments were not conducted in sufficiently oxygen free environment.

3.2.2. Enzymatic Electrochemical CO₂ Reduction to Formate Using F_{ate}DH

Electrochemistry

Electrochemical characterization was done by recording cyclic voltammograms at different scan rates and for the N₂ as well as for the CO₂ saturated system. Independently from the scan rate, CV's recorded for the CO₂ saturated system did not deliver higher reductive currents in comparison to CV's done for the N₂ saturated system. Since F_{ate}DH is the most sensitive and chemically unstable molecule of the enzyme cascade and further known as less active in comparison to ADH or F_{ald}DH it is expected that cyclic voltammetry, even at slow scan rate like 5 mV s⁻¹, is no appropriate method for characterizing electrodes with F_{ate}DH immobilized to display reductive reactions. However, for the electrode containing F_{ate}DH the same decrease of current density with increasing number of cycles interpreted as degrading effect was seen for a faster scan rate at 50 mV s⁻¹. Figure 42 and Figure 43 demonstrate the electrochemical behavior of the alginate modified CF electrode containing F_{ate}DH at different scan rates.

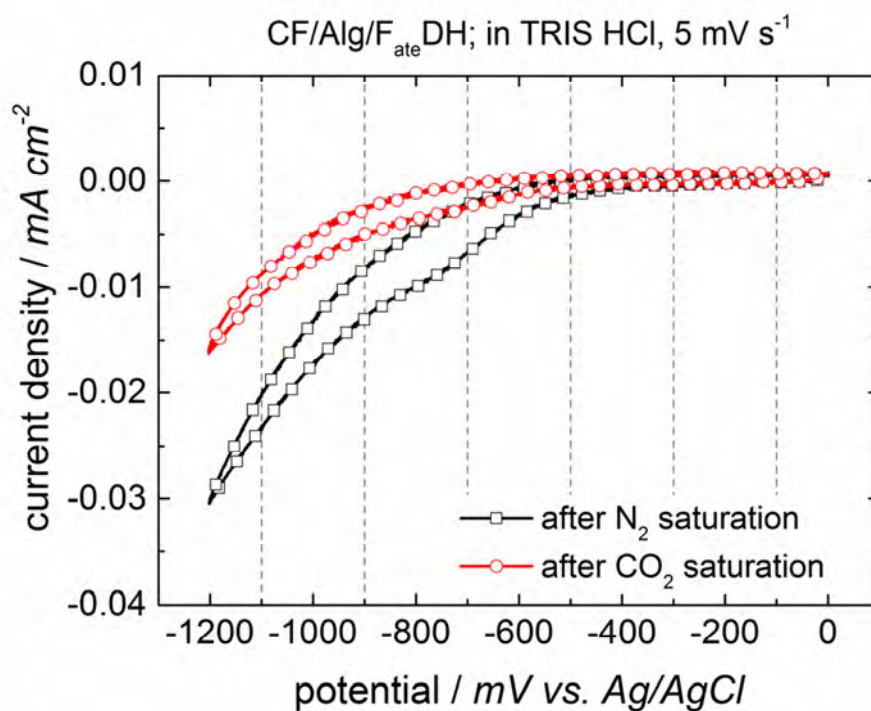


Figure 42 Cyclic voltammogram of an alginate modified carbon felt electrode with $F_{ate}DH$ immobilized at a scan rate of 5 mV s^{-1} and cycling between 0 mV and -1200 mV vs. $Ag/AgCl$ after saturation with N_2 as well as after saturation with CO_2 . CV for the N_2 saturated system depicts even higher current densities than CV after saturating with CO_2 .

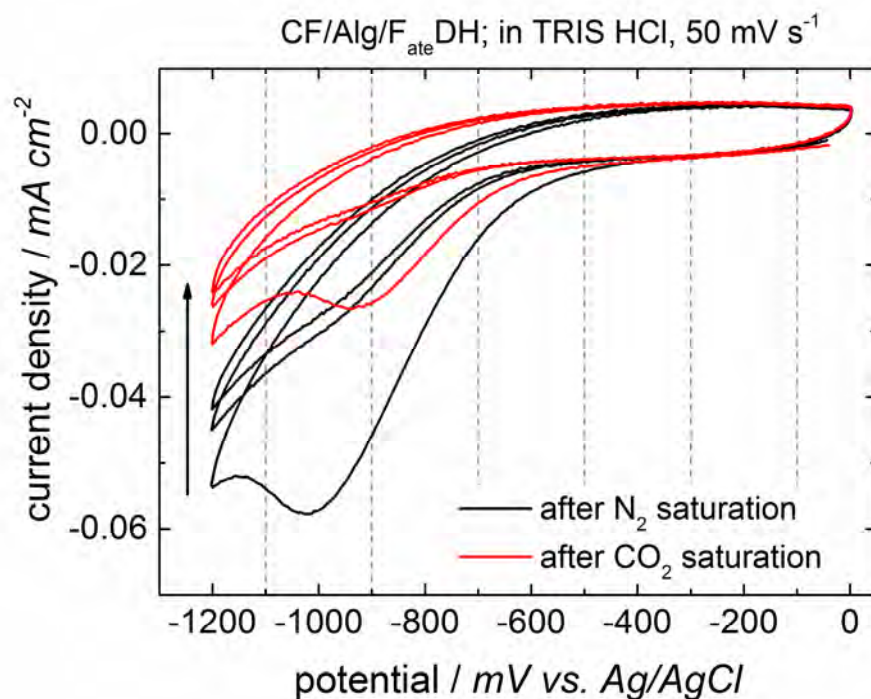


Figure 43 Cyclic voltammograms of an alginate modified carbon felt electrode containing $F_{ate}DH$ at a scan rate of 50 mV s^{-1} . CV's were recorded after saturating the electrochemical cell with N_2 and after saturation with CO_2 . A decrease in current densities is observed with increasing number of cycles.

However, even though there was no increase in reductive current observed for the CO₂ saturated system, reduction of CO₂ was investigated further by potentiodynamic electrolysis experiments. This electrochemical method was expected to be more appropriate than cyclic voltammetry, which makes it difficult to display kinetically slow reactions using catalysts with slow conversion rate. Figure 44 demonstrates the current time plots of an experiment using a carbon felt electrode with F_{ate}DH immobilized during potentiostatic electrolysis in a N₂ saturated system compared to a plot of the same experiment using an identical prepared electrode in a CO₂ saturated system.

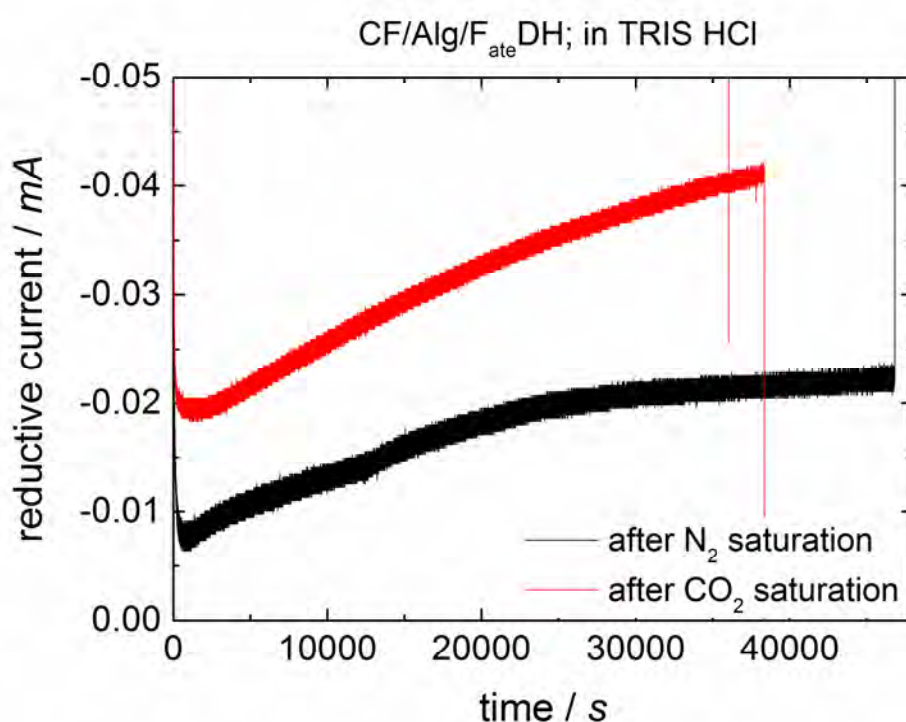


Figure 44 Current-time plot of the electrolysis experiment in a N₂ saturated system and the same experiment in CO₂ saturated system using a formate dehydrogenase containing gel modified CF electrode.

Application of a constant potential (-1200 mV vs. Ag/AgCl) for over 10 h in each experiment delivered higher currents for the CO₂ saturated system than for the N₂ saturated system. These results are in contrast to what has been observed in cyclic voltammetry. This observation might be due to approaching a more appropriate time scale provided for the reduction reaction (10 h of applying exactly the reduction potential vs. 4 min in the reductive range during cyclic voltammetry). The increased reductive current for the N₂ saturated

system as well is expected due to competing water splitting reaction occurring at such high potentials. Calculation of the charges consumed during electrolysis delivered 1.183 C for electrolysis in the CO₂ saturated system and 0.631 C in the N₂ saturated systems. This gives 0.55 C that could be consumed for the reduction of CO₂ to formate only, corresponding to a theoretical amount of $2.86 \cdot 10^{-6}$ mol of formate that could be generated in the most ideal case (100% efficiency).

Analytics

Figure 45 depicts chromatograms from injection to capillary ion chromatography before electrolysis was started, after 8 h and after 18 h of electrolysis using an alginate modified CF electrode with F_{ate}DH immobilized. There is a peak increasing with increasing time of electrolysis at the retention time of formate. Comparison experiment in a N₂ saturated system using the same parameters and an identically prepared electrode did not deliver an increasing peak. However for the N₂ experiment there was also small peak observed at the retention time of formate, which was already there before electrolysis and which did not increase after electrolysis and therefore was not interpreted as formate generation but as artefact or impurity in the chromatography device. Such a small peak is also seen in the chromatogram of the sample before electrolysis was started.

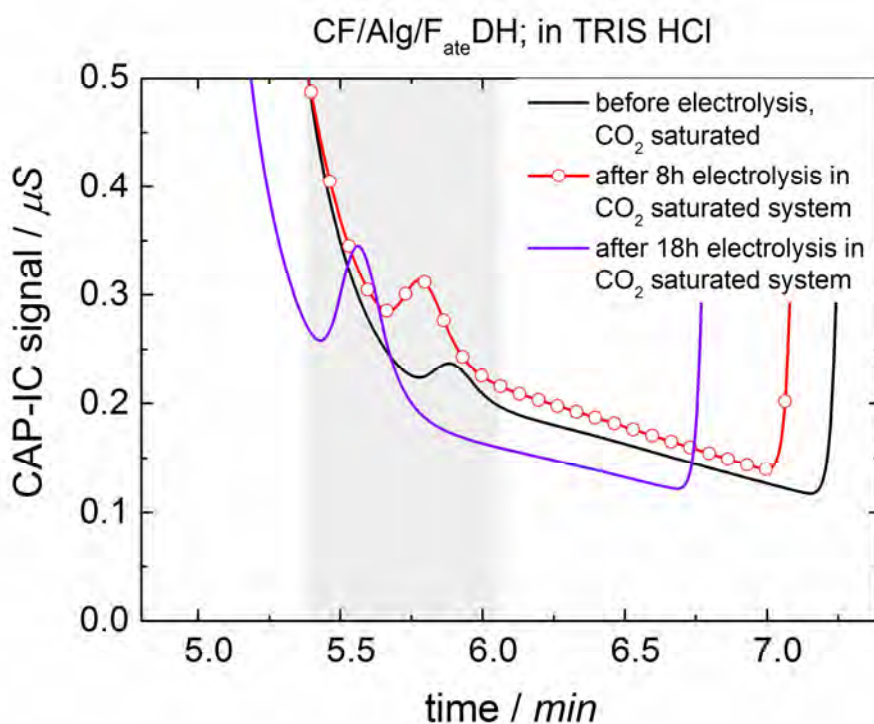


Figure 45 Capillary Ion chromatograms before and after electrolysis in a CO₂ saturated system using a gel-modified electrode with immobilized F_{ate}DH. At the retention time of around 5.75 min a peak is rising after electrolysis in comparison to a sample before electrolysis. This indicates formate generation from potentiostatic electrolysis.

Amounts generated were quantified in CAP-IC using standard calibration. Subtracting the artefact value of the initial injection before electrolysis, 8 h of electrolysis delivered around 0.2 ppm of formate. This corresponds to $1.1 \cdot 10^{-7}$ mol produced and a faradaic efficiency of 4% (according to 0.55 C consumed).

3.2.3. Dehydrogenase Enzymes for CO₂ Reduction to CH₃OH

After investigating reduction reactions using F_{ate}DH and ADH individually, combination of all three dehydrogenase enzymes, namely F_{ate}DH, F_{ald}DH and ADH, for the 3-step reduction cascade with regards to the direct reduction of CO₂ to methanol was studied. As a first approach again reduction was performed using the co-enzyme NADH as known from natural processes. Experiments were done in two different buffer solutions (TRIS-HCl and phosphate

buffer PB) with pH 7.62-7.65 for comparison. TRIS-HCl has been reported as appropriate buffer solution for reduction reactions using dehydrogenase enzymes and NADH. Figure 46 displays chromatograms recorded for the reaction in TRIS-HCl after several stages of the experiment. In addition to the liquid samples taken from the setup during the experiment, blank TRIS-HCl buffer solution was injected. As indicated by the dashed line in Figure 46 the pristine buffer solution shows a peak at the retention time of methanol at 1.87 min as well. Regarding the molecular structure of TRIS it is assumed that from the injection in the gas chromatograph and heating to 250°C, according to the method used for analysis in the chromatograph, the molecule decays. The hydroxymethyl groups of the molecule are therefore supposed to give a feature in the chromatogram at the same retention time of methanol. After purging the system with N₂ (black line) and CO₂ subsequently (pink line) no increase in the peak intensity was observed. However, a peak starts to evolve and increase after NADH was added to the CO₂ saturated system (grey line). After 4 h (red line) and 8 h (dark red line) with both, NADH and CO₂ apparent in the system, samples were taken to investigate the reduction progress. The peak value of methanol generated was obtained after 8 h (dark red line).

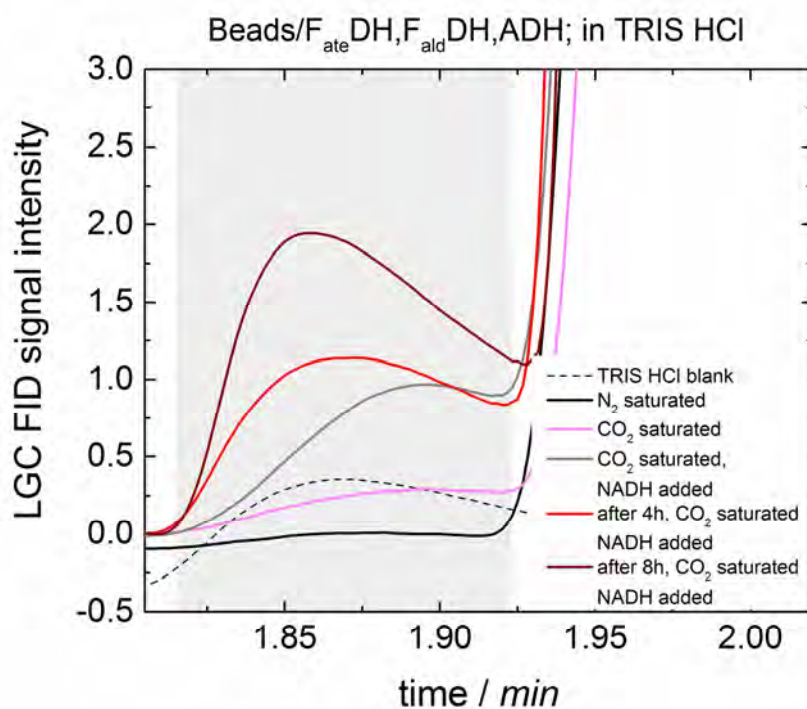


Figure 46 Liquid injection gas chromatograms of a non-electrochemical control experiment in TRIS-HCl buffer using enzyme containing alginate gel-beads and NADH as co-enzyme. A peak is observed to evolve and to increase at the retention time of methanol at 1.87 min after addition of NADH indicating CO₂ reduction to be started (grey, red and dark red line). However, a peak at that retention time is also observed for the TRIS-HCl buffer solution itself (dashed line).

Due to 6.8 mg of NADH added a corresponding theoretical amount of $3.41 \cdot 10^{-6}$ mol of methanol were calculated. From analysis in chromatography generation of around 7 ppm was determined which corresponds to $2.18 \cdot 10^{-6}$ mol of methanol produced. Conversion efficiency according to the amount of NADH therefore can be calculated at 65%. This is in the order of magnitude of values stated earlier^[70]

For comparison the same experiment was repeated but with PB instead of TRIS-HCl buffer. TRIS-HCl was further substituted for the preparation of the beads, where buffer solution was added for stabilizing the enzymes and providing a neutral pH in the beads. Figure 47 shows chromatograms from LGC with PB as buffer solution at different states of the experiment, with regard to the experiment using TRIS-HCl.

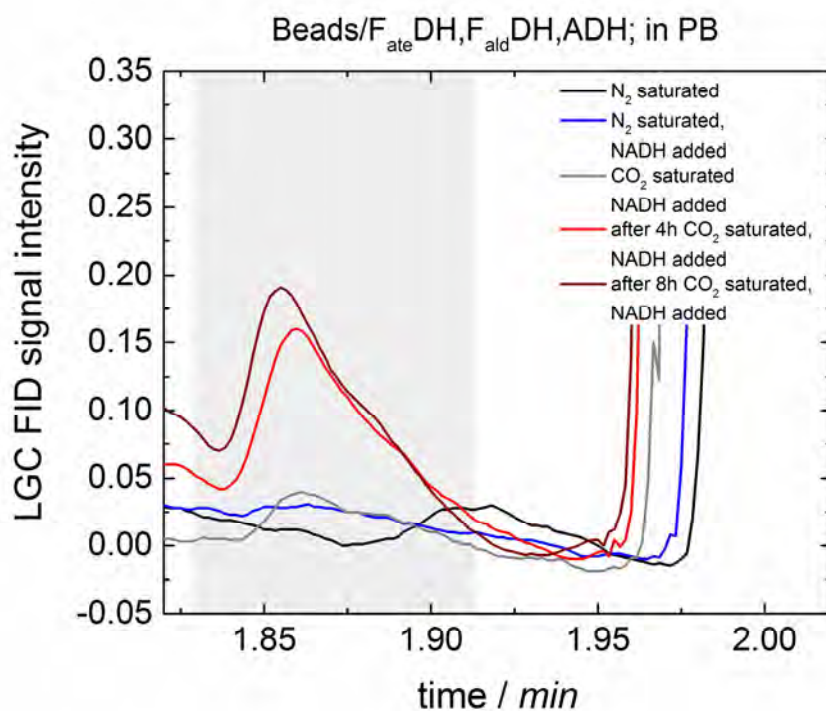


Figure 47 Liquid injection gas chromatograms of a non-electrochemical control experiment using enzyme containing alginate gel-beads and NADH as co-enzyme in PB buffer solution. An increasing peak is obtained at the retention time of methanol at 1.86 min after addition of NADH indicating CO₂ reduction to methanol (grey, red and dark red line). There is no peak observed as long as NADH was not added as electron donor.

Saturation of the PB solution with N₂ as well as adding NADH subsequently did not deliver any increasing peak (black and blue line). However, after saturating the system with CO₂ a small peak is evolving at 1.86 min (grey line). After 4 h and 8 h of reaction time with CO₂ and NADH added to the system, maximum peak intensities were obtained (red and dark red line). However, efficiency according to the amount of NADH added was lower in comparison to experiments using TRIS-HCl buffer solution. From 7 mg of NADH added $3.51 \cdot 10^{-6}$ mol methanol were calculated as theoretical amount obtainable. From LGC 0.2 ppm ($9 \cdot 10^{-8}$ mol) of methanol were determined as peak amount produced. Calculated efficiency was only around 2.5%. However, since it is stated by the provider of NADH (Sigma Aldrich) it is not recommended to store NADH in phosphate buffer due to degradation. Regarding the low efficiency obtained in this experiment, degradation of NADH is assumed due to the performance of the experiment in PB.

3.2.4. Enzymatic Electrochemical CO₂ Reduction to CH₃OH Using Dehydrogenase Enzymes

Electrochemistry using TRIS HCL buffer solution

After non-electrochemical experiments using NADH, application of the alginate matrix containing the three dehydrogenase enzymes to a carbon felt electrode for electrochemical measurements was investigated. A first approach was done using TRIS-HCl as buffer and electrolyte solution respectively. Cyclic voltammetry was again chosen as technique for characterization of the electrochemical process. Cycles were recorded between 0 mV and -1200 mV vs. Ag/AgCl with scan rates of 10 mV s⁻¹ and 50 mV s⁻¹. Figure 48 shows cyclic voltammograms of the electrochemical system after saturation with N₂ as well as after saturation with CO₂. Cyclic voltammograms recorded under the different conditions do not show a remarkable difference between the curves. A similar effect was previously observed for the approach using F_{ate}DH only (Figure 42). It is assumed, that also for the electrochemical reduction of CO₂ using all three enzymes immobilized, cyclic voltammetry is no appropriate method to display the reductive process. However, there is a small increase in reductive current observed from -700 mV vs. Ag/AgCl for both CV's, after N₂ and CO₂ as well, which is presumed to come due to water splitting found to take place at potentials higher than -1000 mV vs. Ag/AgCl.

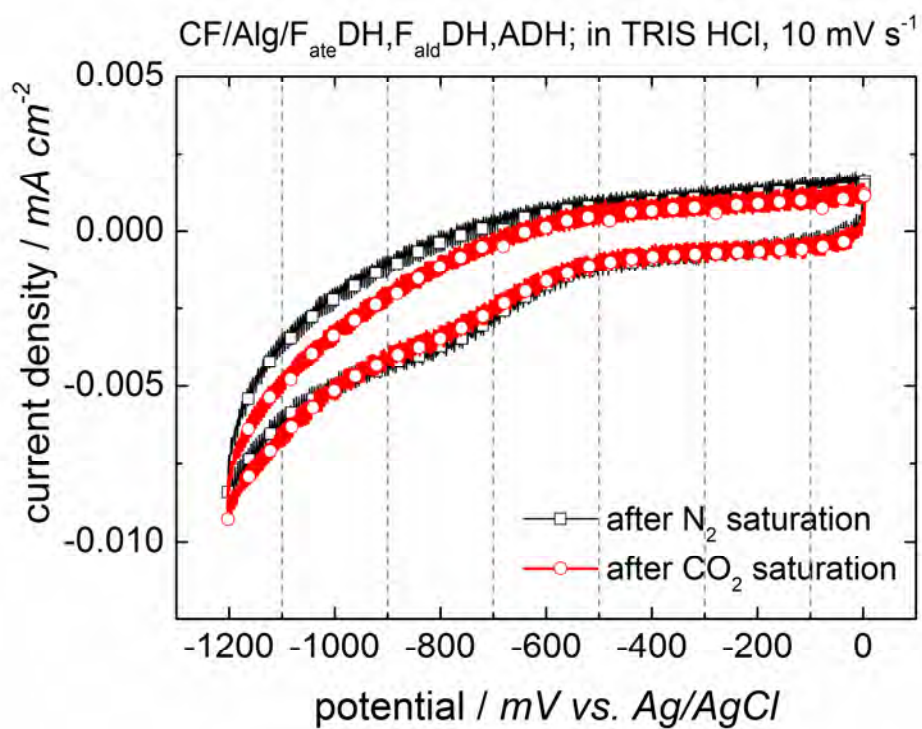


Figure 48 Cyclic voltammograms at a scan rate of 10 mV s⁻¹ of an alginate modified carbon felt electrode containing all three dehydrogenase. TRIS-HCl was used as buffer solution. CV's were recorded after saturating the electrochemical cell with N₂ as well as after saturation with CO₂. There is no remarkable difference observed.

Higher scan rates for recording CV's delivered the same observation as shown in Figure 49. There is no increase in reductive current observed also for higher scan rates.

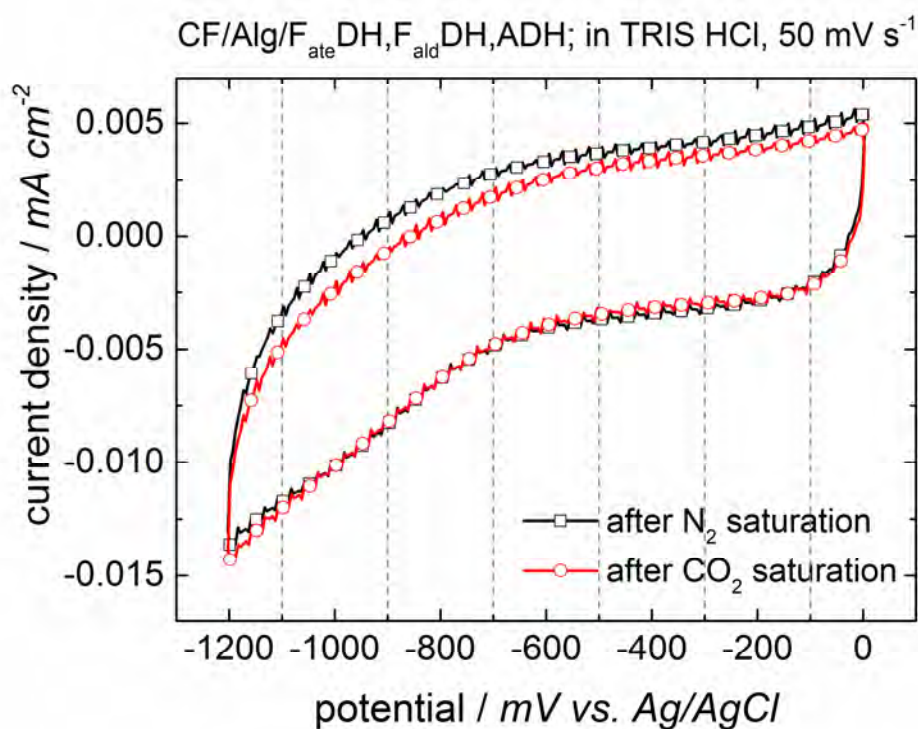


Figure 49 Cyclic voltammograms at a scan rate of 50 mV s⁻¹ of an alginate modified carbon felt electrode containing all three dehydrogenases. TRIS-HCl was used as buffer solution. CV's were recorded after saturating the electrochemical cell with N₂ as well as after saturation with CO₂. There is no remarkable difference observed.

However, comparison of cyclic voltammograms at different scan rates, demonstrated in Figure 50 for the CO₂ saturated system, displays an increase in current densities for increasing scan rates. Such effects usually are observed for diffusion controlled processes where the occurring reduction reaction depends on the diffusion of substance to be reduced to and diffusion of the product from the electrode. However, since there is no distinct oxidative or reductive peak observed but rather a simple increase in current density this process cannot be regarded to be totally diffusion controlled. Increase in current density due to the increase of scan rate without any distinct oxidative and reductive peaks increasing correspondingly, can be interpreted as capacitive process. That means that the alginate modified electrode behaves as a capacitor that is charged more or less according to the scan rate applied. Taking both interpretations into account it can be assumed that either way such modified electrodes depict a very complex system.

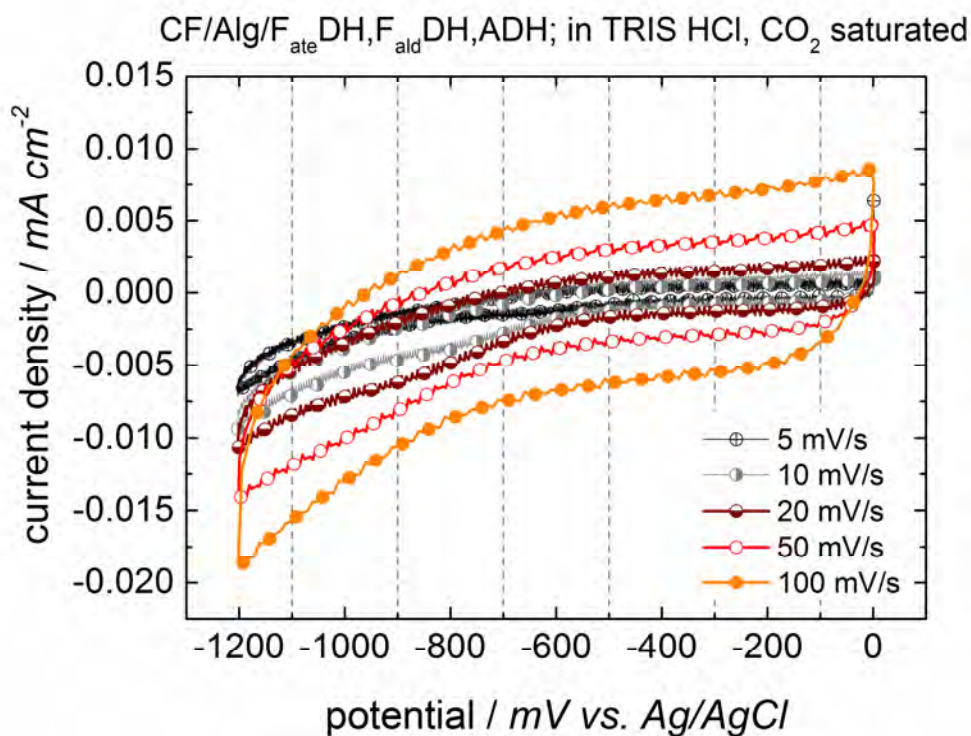


Figure 50 Cyclic voltammograms of the carbon felt electrode modified with enzyme containing alginate at different scan rates between 5 and 100 mV s^{-1} using TRIS-HCl as buffer solution. Currents are increasing with increasing scan rates. This is assumed for diffusion controlled processes as it is also expected for processes occurring on such a gel modified electrode.

Apart from cyclic voltammetry measurements potentiodynamic electrolysis was performed for 4 h for a N_2 saturated system as well as for a CO_2 saturated system. Current time plots in Figure 51 show the overlapping curves of both measurements. This is according to what has been observed for electrochemical characterization in cyclic voltammetry. However, liquid samples of both experiments were taken before and after electrolysis was conducted and analyzed in LGC.

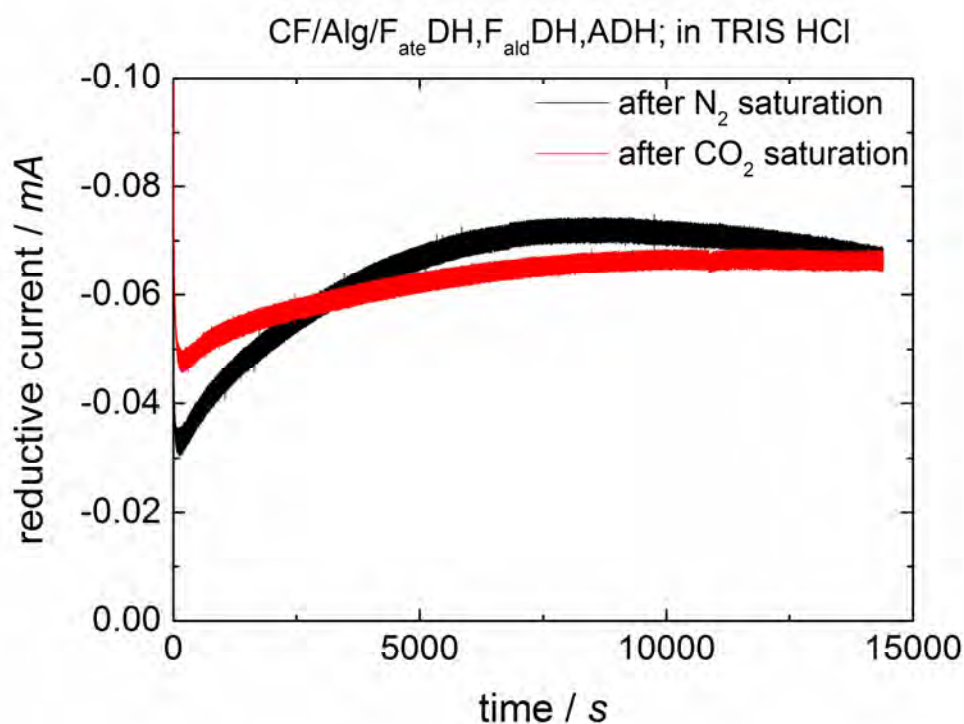


Figure 51 Current-time curves from electrolysis of a carbon felt electrode, modified with enzyme containing alginate. Experiments were conducted potentiostatic at a constant potential of -1200 mV vs. Ag/AgCl in a N₂ or CO₂ saturated TRIS-HCl electrolyte solution. Current behavior over time for the N₂ saturated system shows a certain basic current due to competing reactions taking place independently from the CO₂ reduction for all electrochemical experiments.

Determination of charges consumed during electrolysis in the CO₂ saturated system, assuming all charges to be used for CO₂ reduction and regardless of charges consumed due to competing processes occurring even in N₂ saturated systems, delivered 0.9 C according to the area below the current-time plot. This corresponds to $1.55 \cdot 10^{-6}$ mol methanol possibly generated.

Analytics using TRIS HCl buffer solution

Chromatograms in liquid injection gas chromatography were recorded for samples taken before and after electrolysis experiments were conducted for the alginate modified CF electrode with all three dehydrogenase enzymes immobilized. Figure 52 displays the comparison of a sample before electrolysis as well as samples after potentiostatic

electrolysis in the N_2 saturated system and in the CO_2 saturated system respectively. Further, a liquid sample was investigated after electrolysis in a CO_2 saturated system with a modified electrode but without any enzymes immobilized.

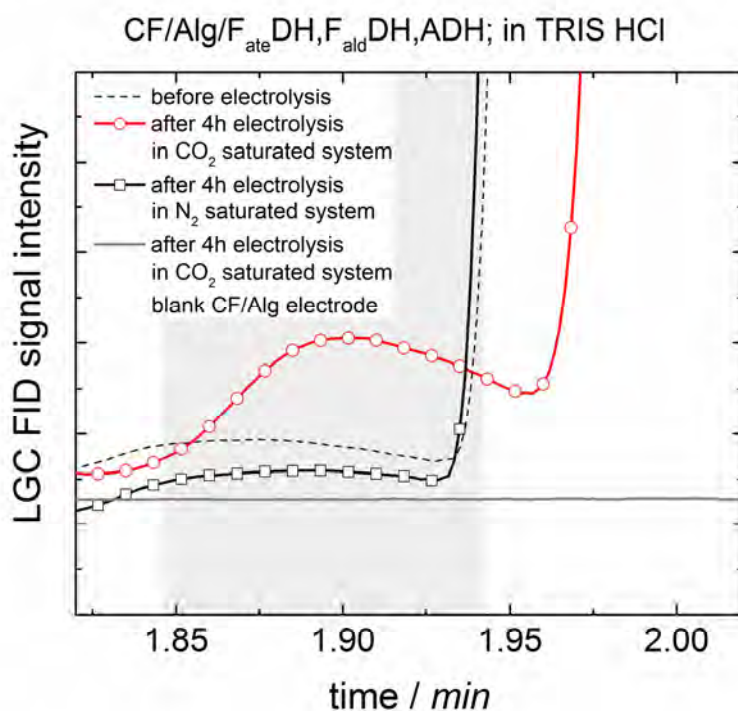


Figure 52 Liquid injection gas chromatograms before and after electrolysis in CO_2 saturated TRIS-HCl electrolyte solution using a CF electrode with all three enzymes immobilized compared to reference measurements without CO_2 (black symbols) or without enzyme (grey line). At the retention time of around 1.9 min a peak is rising after electrolysis, indicating methanol generation.

As it was also observed for chromatograms of the non-electrochemical bead experiment with NADH using TRIS-HCl buffer, there is a small peak observed at the retention time of methanol at around 1.9 min already for the sample taken before electrolysis was started. The same peak was also observed for the sample after N_2 electrolysis. However, an increasing peak corresponding to methanol generation is only observed for the CO_2 saturated system when there was an electrode used with enzymes immobilized. This observation is contrary to what has been expected from electrochemical measurements as cyclic voltammetry or potentiostatic electrolysis did not show any indication for CO_2

reduction. Nevertheless, as it was assumed previously, cyclic voltammetry might not be an appropriate method for electrochemical characterization of those systems. Almost equivalent currents, compared to CO₂ experiments, obtained for N₂ electrolysis are assumed to occur due to water splitting reaction, competing with CO₂ reduction reaction. Water splitting further seems to suppress the ongoing reduction of CO₂ to methanol to be displayed in an electrochemical measurement like potentiostatic electrolysis.

Determination of methanol amount produced by standard calibration gave round 1 ppm which corresponds to $7.8 \cdot 10^{-7}$ mol. Faradaic efficiency according to charges consumed during electrolysis (0.9 C) was therefore determined at about 50%. Taking into account that there was about the same amount of charges flowing during electrolysis in the N₂ saturated system, faradaic efficiency according to methanol generation is estimated lower in reality than calculated.

Electrochemistry using Phosphate buffer solution

The same electrochemical measurements as reported previously using TRIS-HCl buffer were done for the alginate modified carbon felt electrode containing all three enzymes in phosphate buffer (PB) as electrolyte solution. Figure 53 shows cyclic voltammograms of the enzyme electrode in phosphate buffer solution after saturation with N₂ as well as after saturation with CO₂ at a scan rate of 10 mV s⁻¹. Comparison with Figure 48 of the same measurement but with TRIS-HCl buffer as electrolyte solution shows that substitution of electrolyte solution does not influence electrochemical behavior. For both approaches, with TRIS-HCl buffer as well as for PB, the same electrochemical characteristics were obtained. There is again no remarkable difference observed between the cycle recorded after N₂ saturation and the cycle recorded after CO₂ saturation.

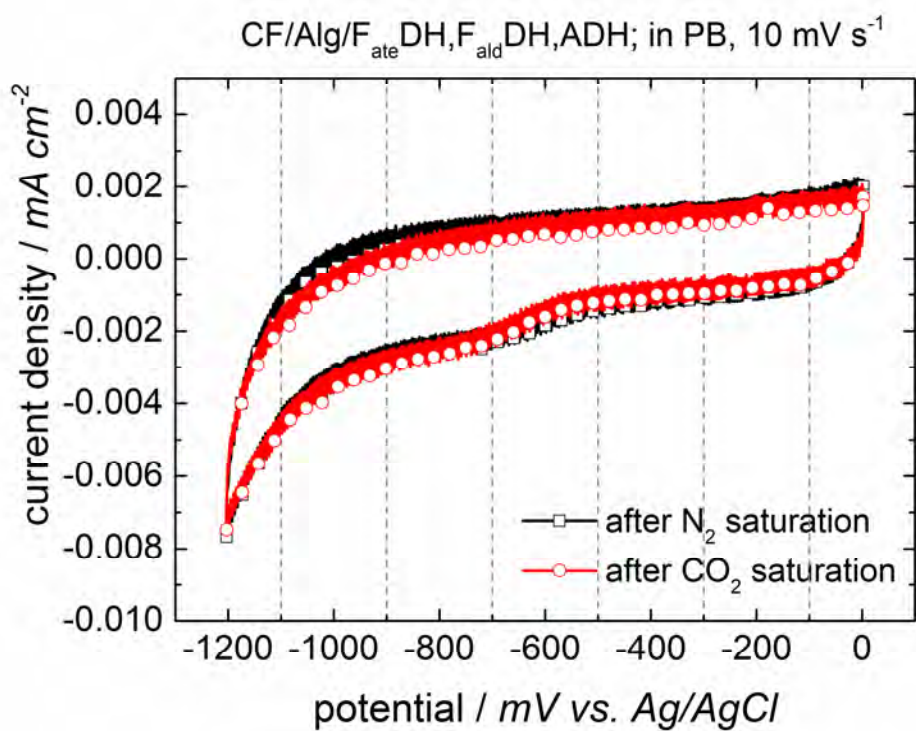


Figure 53 Cyclic voltammograms at a scan rate of 10 mV s⁻¹ of an alginate modified carbon felt electrode containing all three dehydrogenases. PB was used as buffer solution. CV's were recorded after saturating the electrochemical cell with N₂ as well as after saturation with CO₂. There is no remarkable difference observed.

Characterization at higher scan rates as shown for 50 mV s⁻¹ in Figure 54 delivered a small increase of reductive current for the CO₂ saturated system from -700 mV vs. Ag/AgCl

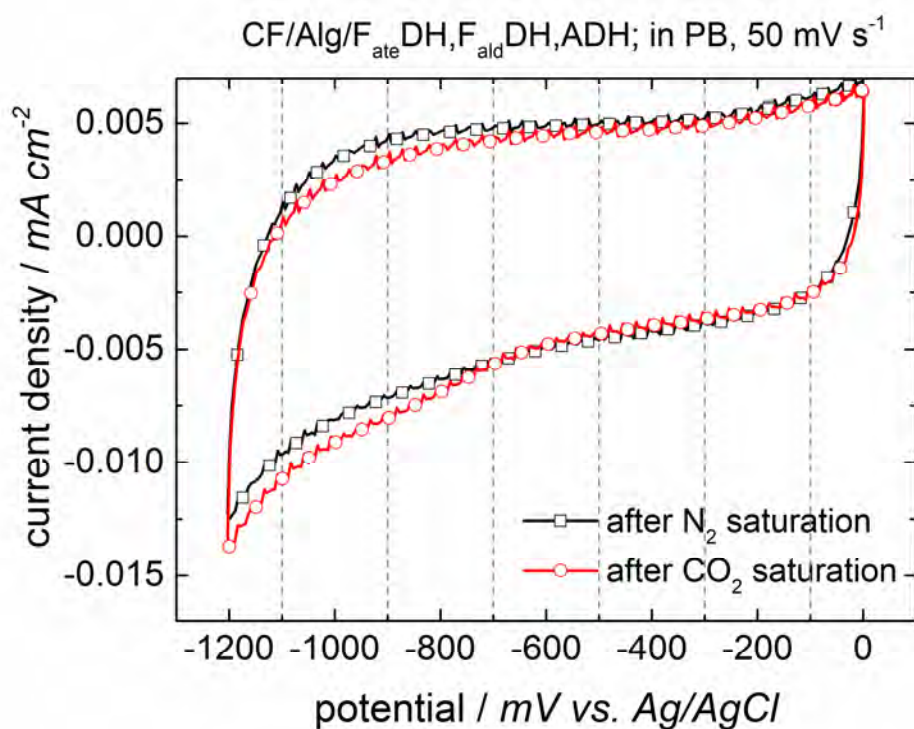


Figure 54 Cyclic voltammograms at a scan rate of 50 mV s^{-1} of an alginate modified carbon felt electrode containing all three dehydrogenases. PB was used as buffer solution. CV's were recorded after saturating the electrochemical cell with N_2 as well as after saturation with CO_2 . There is no remarkable difference observed.

Comparing cyclic voltammograms recorded at different scan rates in Figure 55 for the CO_2 saturated system, as it was done in Figure 50 for TRIS-HCl buffer depicts the same behavior of increasing current densities. This states that reaction processes, that possibly could be diffusion controlled or capacitive as well, are not dependent on the electrolyte solution and therefore do occur due to the constitution of the electrode itself.

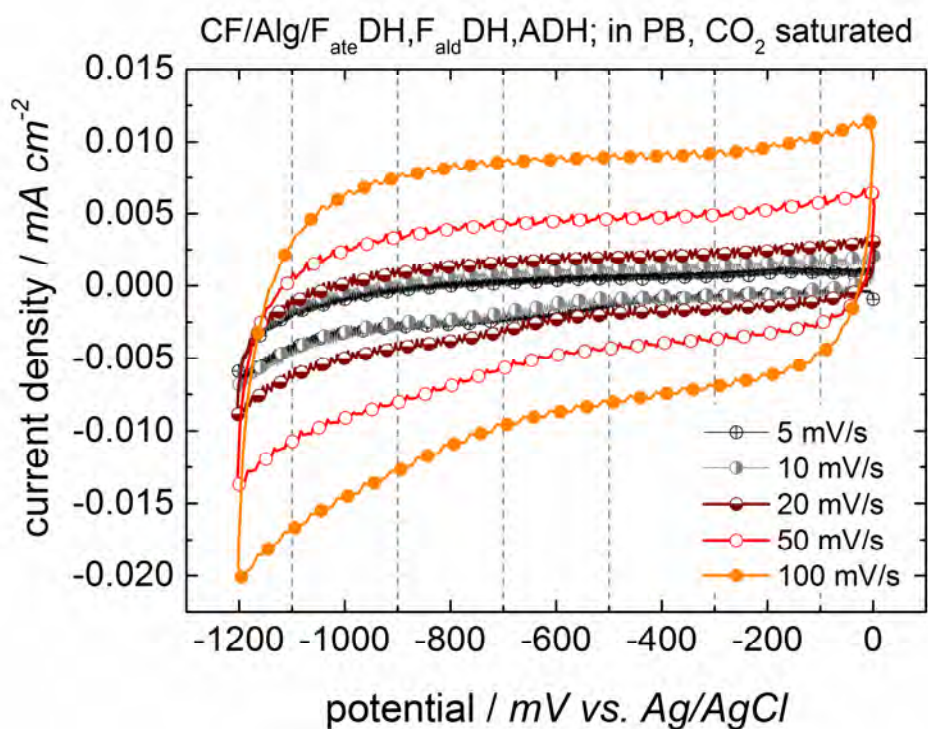


Figure 55 Cyclic voltammograms of the carbon felt electrode modified with enzyme containing alginate at different scan rates between 5 and 100 mV s⁻¹ using PB as buffer solution. Currents increase with increasing scan rates. This is assumed for diffusion controlled processes as it is also expected for processes occurring on such a gel modified electrode.

Potentiostatic electrolysis experiments were performed for 4 h at -1200 mV vs. Ag/AgCl after saturation of the PB electrolyte solution with N₂ or CO₂ respectively. In contrast to results obtained from experiments using TRIS-HCl buffer shown in Figure 51 there was a remarkably higher current obtained after saturation with CO₂ as obvious from Figure 56. A small increase in reductive current for the electrolysis in the N₂ saturated system is correlated to competing water splitting reaction.

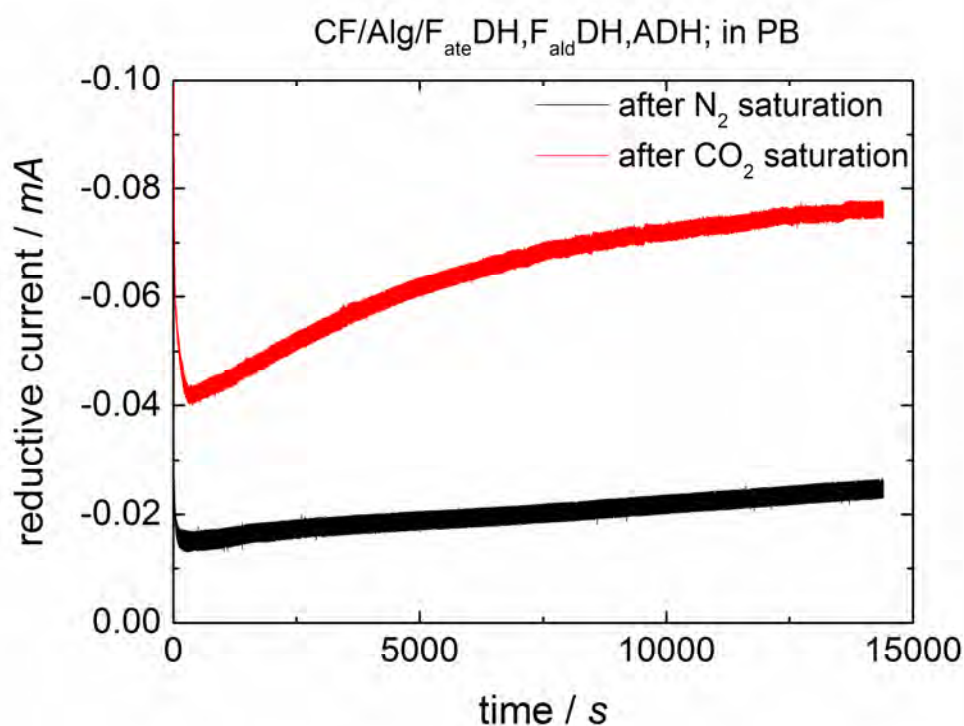


Figure 56 Current-time curves from electrolysis of a carbon felt electrode, modified with enzyme containing alginate. Experiments were conducted potentiostatic at a constant potential of -1200 mV vs. Ag/AgCl in a N₂ or CO₂ saturated TRIS-HCl electrolyte solution. Current behavior over time for the N₂ saturated system shows a certain basic current due to competing reactions taking place independently from the CO₂ reduction for all electrochemical experiments.

Charges consumed during electrolysis in the N₂ saturated system were calculated as 0.288 C, corresponding to the area under the curve. For the electrolysis in the CO₂ saturated system 0.926 C were consumed. Assuming 0.288 C used for water splitting, 0.638 C are assigned to CO₂ reduction which corresponds to $1.1 \cdot 10^{-6}$ mol of methanol theoretically generated.

Analytics using Phosphate buffer solution

Samples after potentiostatic electrolysis experiments were investigated in LGC. For comparison, a sample after electrolysis in CO₂ saturated electrolyte solution using an alginate modified CF electrode without enzymes immobilized was analyzed. Further, to exclude that reduction of CO₂ occurs due to in situ formation of H₂ while water splitting and

reaction of CO₂ with H₂ without requiring a potential applied, samples of a comparison experiment without potential applied were investigated. Figure 57 shows comparison of chromatograms from sample injected in LGC.

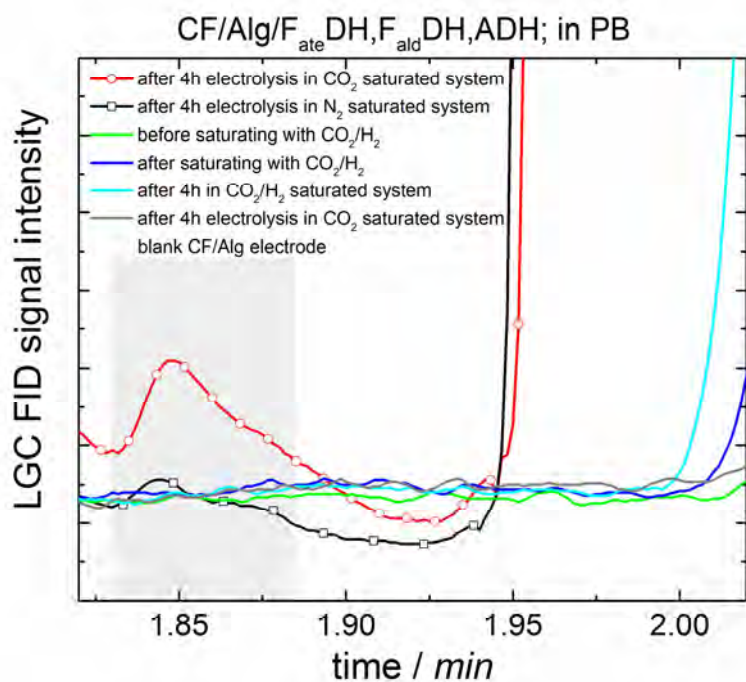


Figure 57 Liquid injection gas chromatograms before and after electrolysis in CO₂ saturated PB electrolyte solution using a CF electrode with all three enzymes immobilized compared to reference measurements without CO₂ (black symbols), without enzyme (grey line) or without potential applied (blue and light blue lines). At the retention time of around 1.9 min a peak is rising after electrolysis, indicating methanol generation.

A significant peak at the retention time at around 1.85 min is only observed for the enzyme containing electrode after electrolysis in CO₂ saturated PB electrolyte solution (red line). From standard calibration an amount of around 0.15 ppm corresponding to $1.2 \cdot 10^{-7}$ mol of methanol produced. Calculation according to charges consumed during electrolysis delivered 10% of faradaic efficiency.

Results shows that for both systems, using TRIS-HCl buffer as well as PB, methanol generation was only generated when an alginate modified CF electrode with enzymes

immobilized was used and after the system was saturated with CO₂. Exchanging buffer solutions supports reproducibility of the direct electron injection into enzymes immobilized on an electrode and therefore proves the bio-electrocatalytic reduction of CO₂ to methanol without any co-enzyme or mediator required.

Further, for experiments in PB also headspace analysis in gas chromatography was performed to determine assumed water splitting as competing reaction. Figure 58 shows the headspace constitution of the cathode compartment after saturating the system with N₂ or CO₂ respectively as well as after electrolysis in the saturated systems. An oxygen peak at 0.31 min can be observed for all samples taken. At the retention time of H₂ at 0.14 min a peak is only observed for samples taken after electrolysis, which indicates hydrogen evolution due to water splitting reaction. However, for electrolysis in CO₂ saturated buffer solution an even higher concentration is observed than for electrolysis in N₂ saturated buffer solution. This is due to high volatility of the gas sample during transfer to the measurement device.

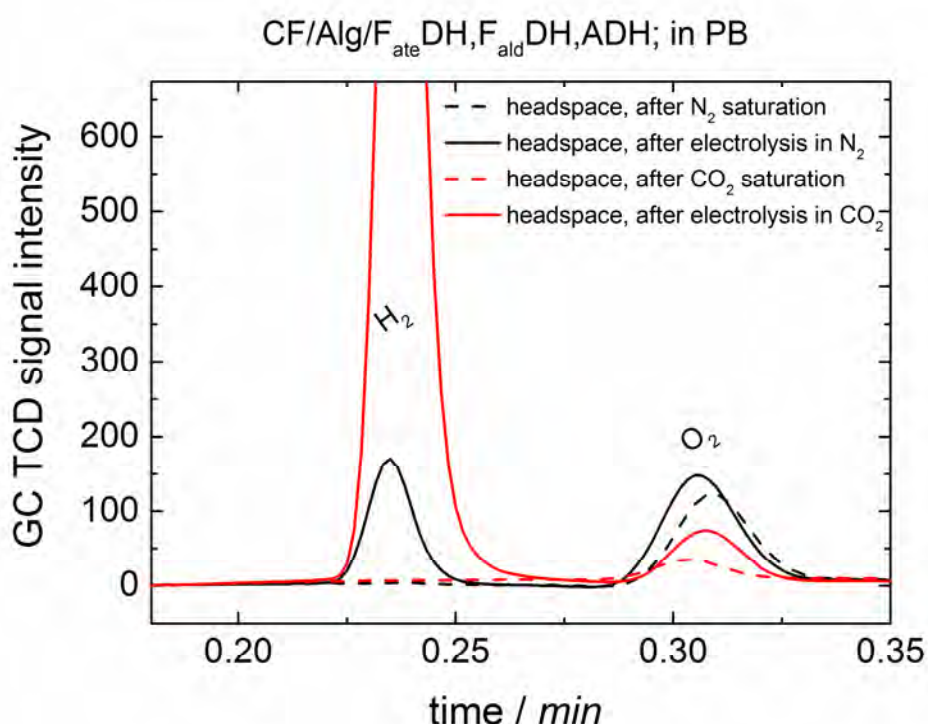


Figure 58 Gas chromatograms of the headspace from before and after electrolysis using an enzyme modified electrode in N₂ as well as CO₂ saturated buffer solution.

Direct electrochemical CO₂ reduction with a significant amount of charge consumed for the reduction of CO₂ to methanol using these enzyme modified electrodes offers a selective, reproducible and mild method for the production of artificial fuels and opens the way to biodegradable and sustainable energy conversion.

3.2.5. Alcohol Dehydrogenase for Butyraldehyde Reduction to Butanol

As a further step of the study, non-electrochemical control experiments using alcohol dehydrogenase containing alginate gel-beads and the co-enzyme NADH were performed for proving the activity of the enzyme for reduction reactions towards higher alcohols as well. In this experiment samples were taken immediately after adding NADH and butyraldehyde, as well as after 8 hours of reaction time. Analysis of those samples was done in liquid injection gas chromatography.

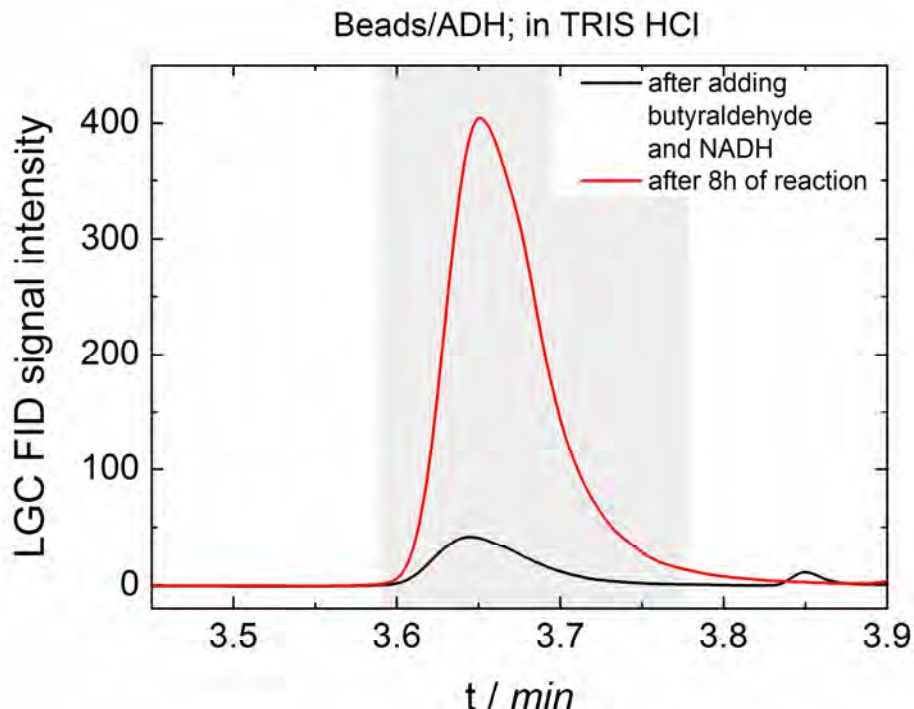


Figure 59 Liquid injection gas chromatograms of a non-electrochemical control experiment using enzyme containing alginate gel-beads and NADH as co-enzyme. An intensive peak is observed at the retention time of butanol (3.64 min) after 8 h of reaction time.

Figure 59 shows the chromatogram after adding butyraldehyde as educt and the co-enzyme NADH at the beginning of the reaction and after 8 h of reaction time. The retention time and amount of butanol were identified by liquid injection gas chromatography using external and internal standards. For butanol 3.64 min was determined as retention time. The small peak that can be observed in the chromatogram already at the very beginning after adding co-enzyme and butyraldehyde, indicates a fast reduction reaction to butanol with NADH as electron and proton donor.

These results show the successful employment of alcohol dehydrogenase immobilized in alginate gel-beads for the reduction of butyraldehyde to butanol with high efficiencies.

The amount of NADH added was 7.5 mg which corresponds to $1.127 \cdot 10^{-5}$ mol. From liquid injection gas chromatography about 200 ppm of butanol were determined which corresponds to a concentration of $1.067 \cdot 10^{-5}$ mol of butanol in 4 mL buffer solution.

Per molecule NADH one molecule of butyraldehyde is reduced to one molecule butanol which gives an efficiency of 96% for the production of butanol with NADH as electron and hydrogen donor. This indicates high activity of the ADH as expected since ADH is known as the most stable enzyme of the dehydrogenase cascade.

3.2.6. Enzymatic Electrochemical Reduction of Butyraldehyde Using ADH

Electrochemistry

For the substitution of NADH as electron and proton donor investigations to address alcohol dehydrogenase electrochemically were done. Therefore alginate-silicate hybrid gel, containing the enzyme, identically prepared as for previous experiments and the bead experiment discussed in 3.2.5, was applied to a carbon felt electrode. Characterization of the electrode was done by performing cyclic voltammetry in a N_2 saturated system and after adding 0.1 mL of butyraldehyde liquid. Figure 60 displays the electrochemical characterization by cyclic voltammetry within one cycle each scanned at 5 mV s^{-1} . For the

electrochemical cell containing butyraldehyde, a remarkable increase was observed in comparison to the N_2 saturated system.

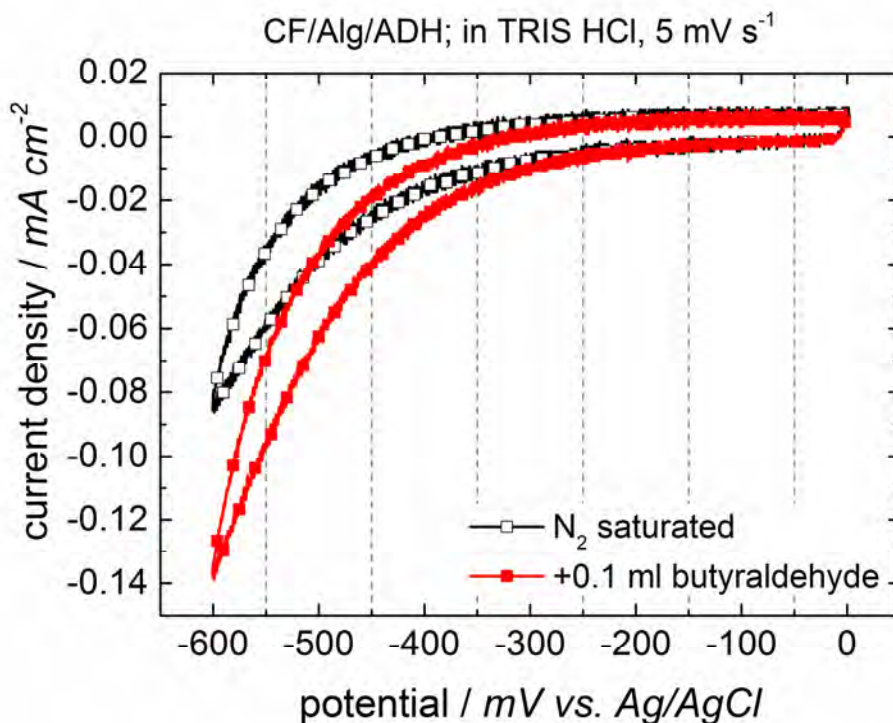


Figure 60 Cyclic voltammograms of an alginate modified carbon felt electrode containing alcohol dehydrogenase at a scan rate of 5 mV s⁻¹. CV's were recorded after saturating the electrochemical cell with N₂ and after adding 0.1 mL butyraldehyde. An increase in current density is observed after adding butyraldehyde.

The same effect was observed after scanning with a 10 times higher scan rate as demonstrated in Figure 61. However, recording more than one cycle shows a decrease in current densities with increasing number of cycles. This happens even after adding butyraldehyde although in general current densities increased in comparison to records of the N_2 saturated electrochemical system.

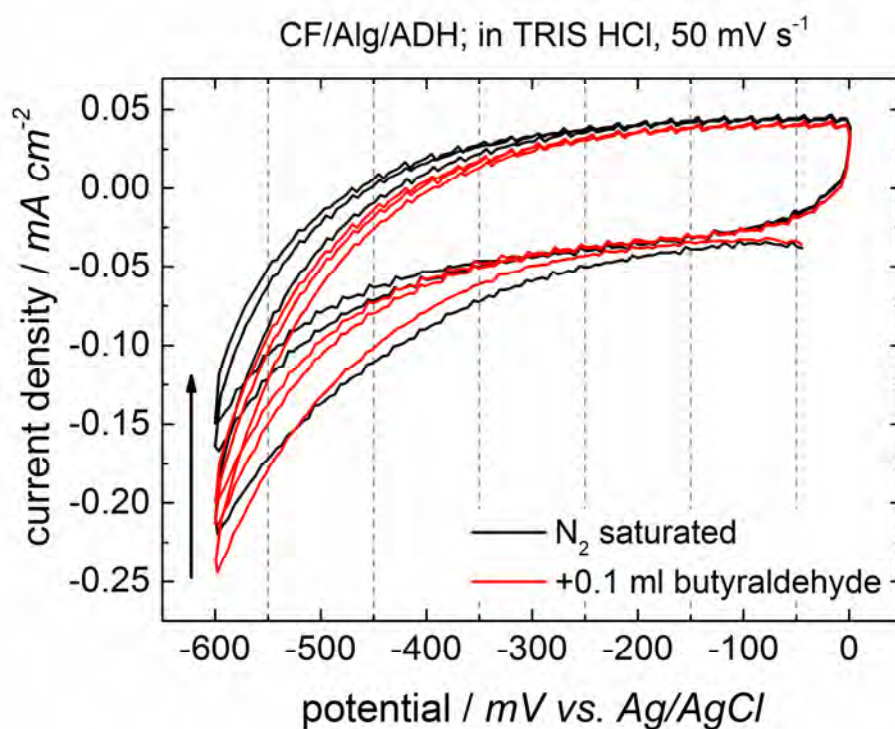


Figure 61 Cyclic voltammograms of an alginate modified carbon felt electrode containing alcohol dehydrogenase at a scan rate of 50 mV s⁻¹. CV's were recorded after saturating the electrochemical cell with N₂ and after adding 0.1 mL butyraldehyde. A decrease in current densities is observed with increasing number of cycles.

For comparison the same experiments were performed with an electrode prepared identically but without adding alcohol dehydrogenase. For this blank electrode cyclic voltammograms did not depict an increase after butyraldehyde was added (Figure 62). A decrease in current density was also observed in Figure 63 for increasing number of cycles for the blank electrode. From these results one can conclude that there are degradation effects occurring related to the alginate-silicate gel on the electrode, since this behavior is also observed for the alginate electrode without enzyme immobilized (Figure 63) and has also been reported for results with F_{ate}DH previously in this chapter.

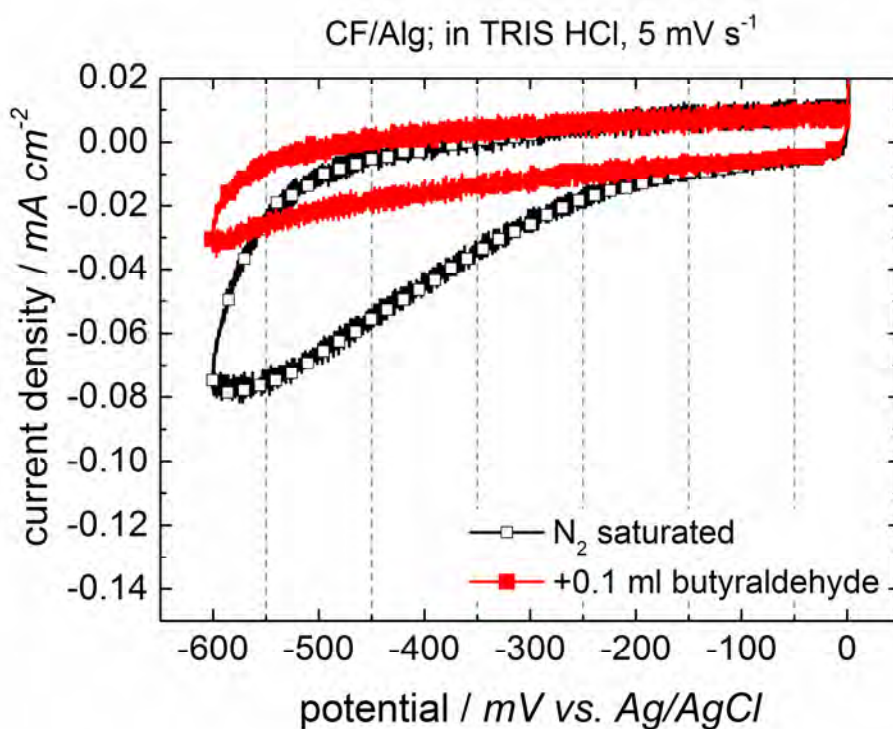


Figure 62 Cyclic voltammogram of an alginate modified carbon felt electrode at a scan rate of 5 mV s⁻¹ and cycling between 0 mV and -600 mV vs. Ag/AgCl after saturation with N₂ and after adding butyraldehyde. There is no increase shown indicating a reduction of butyraldehyde.

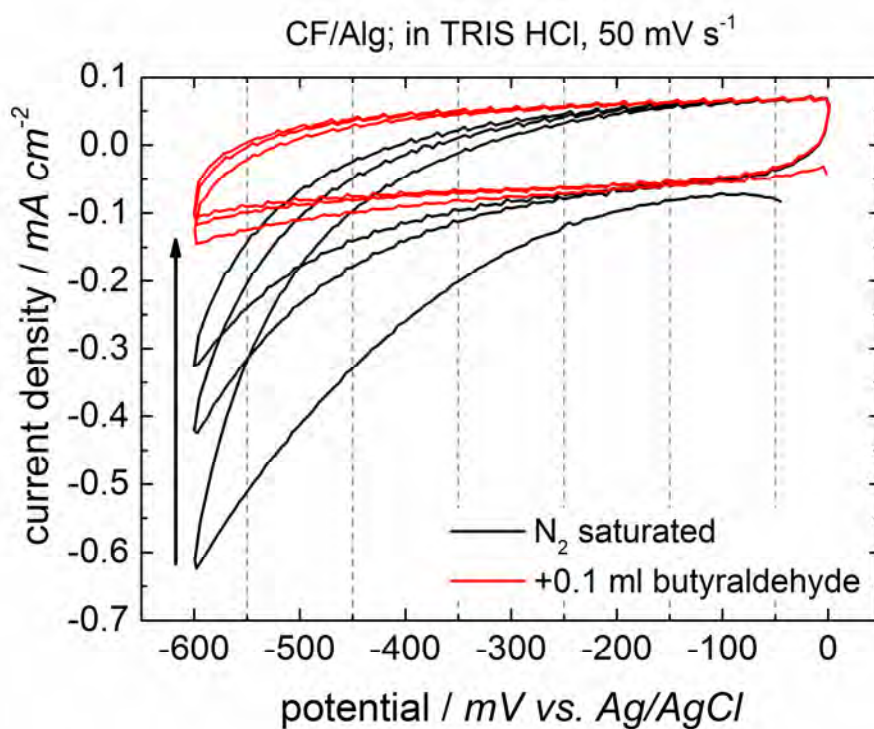


Figure 63 Cyclic voltammograms of an alginate modified carbon felt electrode at a scan rate of 50 mV s⁻¹ and cycling 3 times between 0 mV and -600 mV vs. Ag/AgCl after saturation with N₂ and after adding butyraldehyde. The arrow indicates decrease in current density with increasing number of cycles.

Figure 64 shows the comparison of cyclic voltammograms (CV) of an alginate-modified carbon felt electrode with immobilized alcohol dehydrogenase and an equally prepared alginate gel- modified carbon felt electrode without enzyme at a scan rate of 5 mV s^{-1} . The CV's were recorded after adding 0.1 mL of butyraldehyde. Only for the electrode containing the enzyme a reductive current can be observed starting at $-400 \text{ mV vs. Ag/AgCl}$. Comparing those cyclic voltammograms emphasizes once more that a reductive current is only observed when enzyme and butyraldehyde are apparent both at the same time. These results indicate that electrons can be injected directly into the immobilized alcohol dehydrogenase to catalyze the reduction of butyraldehyde to butanol.

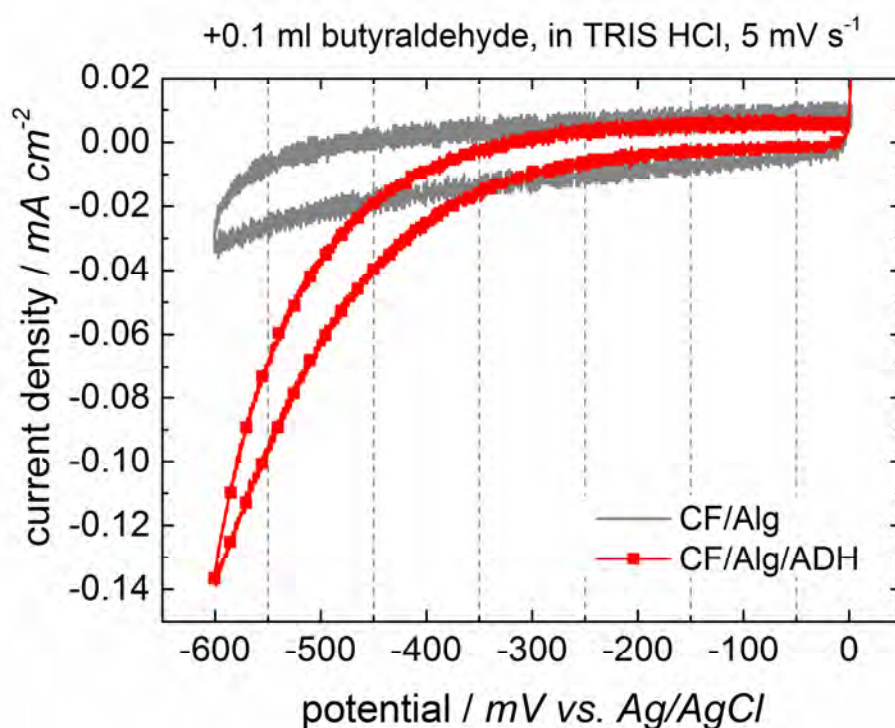


Figure 64 Cyclic voltammograms (CV) after adding butyraldehyde to the electrolyte solution, using an alginate-enzyme modified carbon felt (CF) electrode (red, dotted) and an equally modified electrode without enzyme (black) at a scan rate of 5 mV s^{-1} .

To prove the formation of butanol by the reduction process, electrolysis experiments for 8 h at $-600 \text{ mV vs. Ag/AgCl}$ have been performed. Figure 65 depicts the current over time behavior for the potentiostatic experiment using the enzyme electrode and adding

butyraldehyde to the electrolyte solution. Samples of the electrolyte solution before and after electrolysis were analyzed using liquid injection gas chromatography.

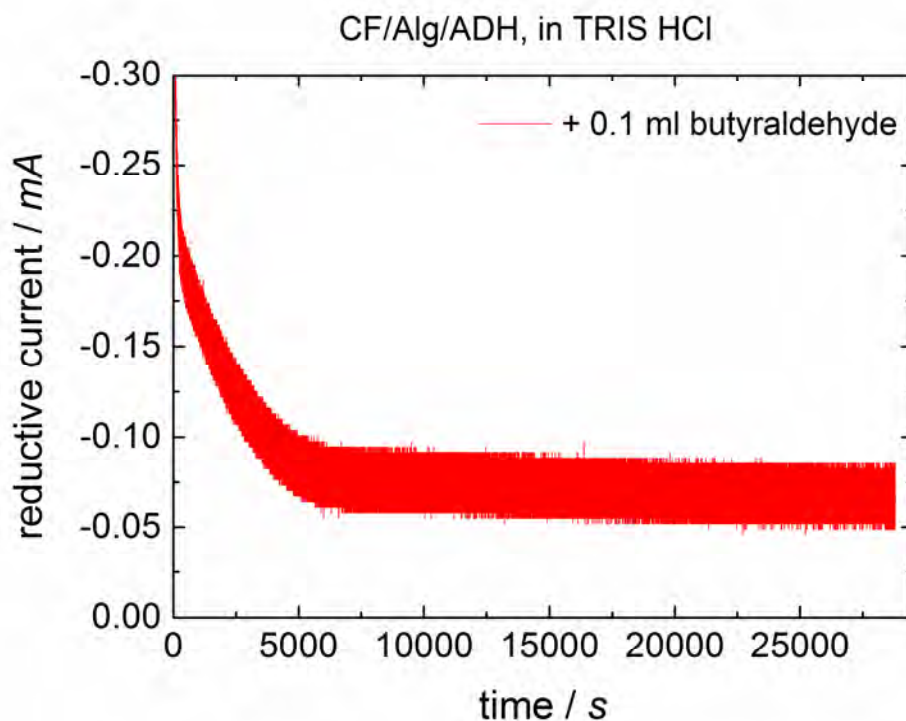


Figure 65 Current-time plot of the electrolysis experiment using an alcohol dehydrogenase containing, gel modified CF electrode and electrolyte solution containing butyraldehyde.

Analyzing the current vs. time curve (Figure 65), 2400 mA s were calculated from the area enclosed by the curve which corresponds to 2.4 C (Q) that were consumed during electrolysis over 8 h at -600 mV vs. Ag/AgCl. With the number of moles n

$$n = \frac{Q}{zF}$$

and using Faraday constant $F=96485.33 \text{ C mol}^{-1}$ and number of charges required for the reduction as $z=2$, the theoretical number of mol of butanol was calculated as $1.244 \cdot 10^{-5}$.

Analytics

Analysis of liquid samples in liquid injection gas chromatography from before and after electrolysis compared to reference measurements is shown in Figure 66. Reference experiments have been performed both with enzyme free electrodes in butyraldehyde containing electrolyte solutions, as well as with the opposite combination, enzyme containing electrodes in butyraldehyde free solutions. Comparison of chromatograms depicts a rising peak at the retention time of butanol (3.64 min) for the sample after electrolysis in butyraldehyde containing electrolyte solution where the enzyme modified electrode was used. The small vanishing peak, which was there for the sample before electrolysis, at 3.59 min is related to GC sample handling and has no significance for butanol detection. Formation of butanol during the reduction process due to potentiostatic electrolysis was further only observed when the experiment was performed when both, the enzyme modified electrode and butyraldehyde, were apparent. The same experiment conducted with a blank electrode without ADH immobilized shows a small peak at the retention time of butanol, which is also there before electrolysis and therefore is regarded as artefact of the chromatography technique. From quantitative analysis of the GC measurements an amount of 20 ppm butanol in 20 mL electrolyte solution was detected for the electrolysis experiment with the alginate modified CF electrode with ADH immobilized, which is calculated as $5.4 \cdot 10^{-6}$ mol.

Comparing experimentally determined and theoretically calculated amount of butanol (from Figure 65) a corresponding Faradaic efficiency of around 40% was found. These results support a reaction mechanism with direct electrochemical access of the dehydrogenase enzyme and subsequent reduction of butyraldehyde to butanol.

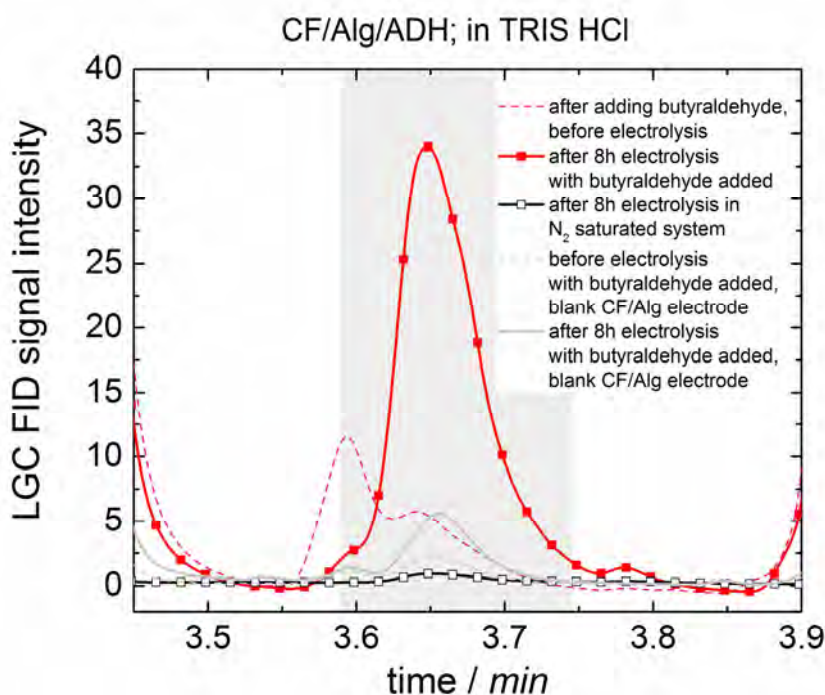


Figure 66 Liquid injection gas chromatograms before and after electrolysis with butyraldehyde using a gel-modified electrode with immobilized alcohol dehydrogenase compared to reference measurements without butyraldehyde or without enzyme. At the retention time of 3.64 min a peak is rising after electrolysis, indicating butanol generation.

Further, comparison of results using only ADH with previously reported enzymatic reduction reactions, indicates the highest efficiencies for non-electrochemical as well as electrochemical approaches. ADH is known as a very stable enzyme with high activity. This supports the observed results and additionally clarifies possible electrochemical characterization, which was not reasonable for previous approaches.

3.3. Microscopic Characterization of Carbon Felt

Characterization of carbon felt substrate, which was used for both electrochemical approaches using microorganism or enzymes respectively, was done using incident light microscopy and scanning electron microscopy (SEM). Figure 67 displays SEM images of pristine carbon felt. Right-hand side picture shows the resulting image at 84 fold

magnification. The complex network and sponge-like constitution of carbon fibers is clearly depicted by this image and high surface area is obvious. Further left-hand side image depicts one of the fibers at higher magnification at 3000 fold with a diameter of 10 μm for the fiber. For a cutout of a 1 cm^2 area therefore a fiber-surface area is estimated at 2 cm^2 .

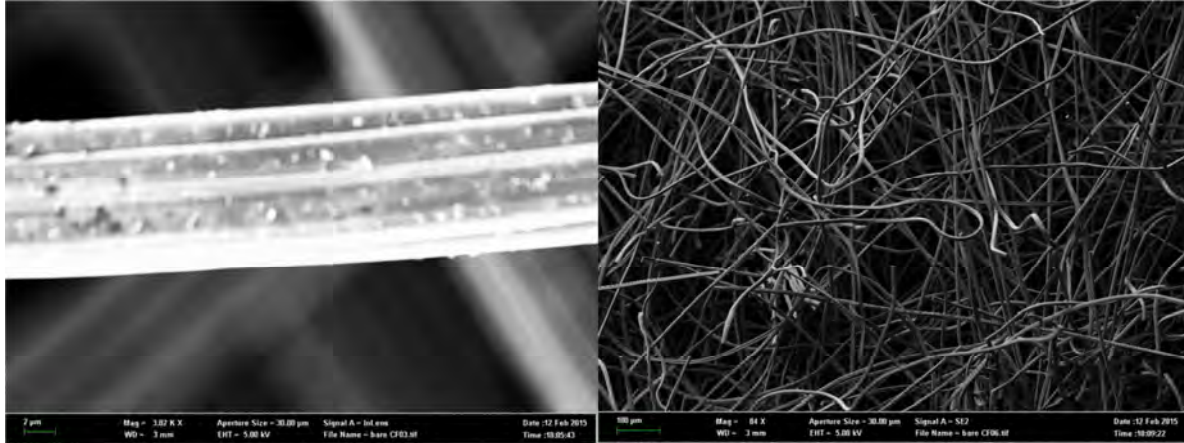


Figure 67 Scanning Electron Microscopy images showing a pristine carbon felt substrate at 3000 fold (left) and 84 fold (right) magnification.

Microscopy images demonstrated in Figure 68 show a pristine carbon felt and carbon felt covered with alginate-silicate hybrid gel, as it was used for enzymatic electrochemistry approaches. Sufficient coverage of the carbon felt with alginate based gel is observed, however holes in the alginate displayed on the right-hand side image indicates that coverage is discontinuous and makes therefore charge and substance diffusion from and to alginate as well as carbon felt itself possible.

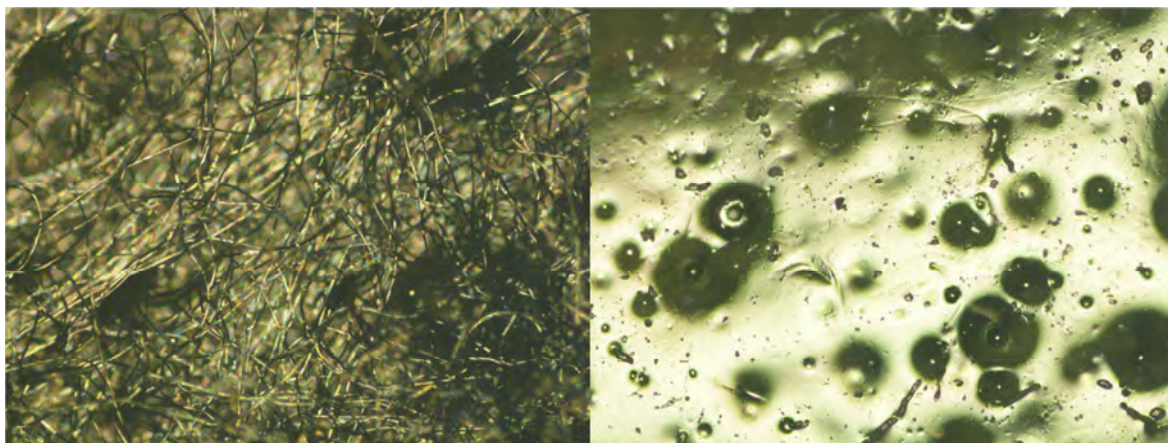


Figure 68 Microscopy images taken at 5 fold magnification for pristine carbon felt (left) and alginate-silicate modified carbon felt (right).

Alginate coverage of the carbon felt was further investigated in SEM. Wide-range but discontinuous coverage is again observed as depicted in the left-hand side picture of Figure 69. The right-hand side image shows the alginate covered carbon felt at higher magnification (2000 fold). White islands are expected to indicate residues of salts from precipitation in 0.2 M CaCl_2 solution. SEM imaging was done in courtesy of JEOL.

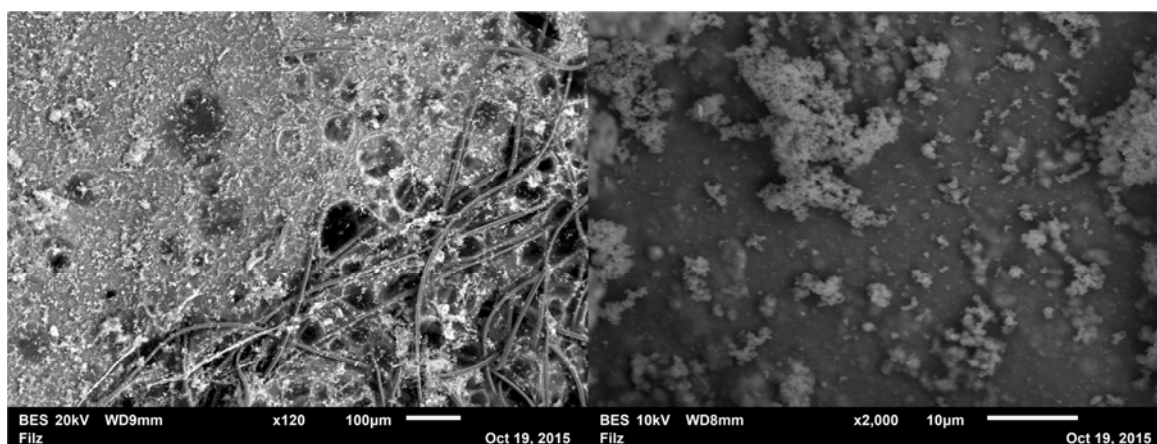


Figure 69 SEM imaging done at 20 kV with 120 fold magnification (left) and at 10 kV with 2000 fold magnification (right) showing alginate-silicate gel coverage of a carbon felt electrode, in courtesy of JEOL.

4. Summary and Conclusion

In this work an approach towards combination of renewable energy storage with CO₂ reduction at the same time is presented. Carbon dioxide therefore served as carbon source and carbon feedstock for the generation of artificial fuels. Renewable energies represent possible energy source for providing electrons required for electrochemical reduction of CO₂. In the last decades there have been several works presented on such approaches. However, most of them report on the utilization of organic, metallic or organo-metallic compounds applied as catalysts to lower the activation barrier of the required energy for the reduction. Those compounds often do not yield high efficiencies and depict no high selectivity according to the product obtained from the reduction.

In other approaches the use of biocatalyst such as enzymes and microorganisms has been shown. This sort of catalysts is known from natural processes where they yield high efficiencies and selectivity towards product generation. Nevertheless such processes require electron and proton donors or co-factors respectively, which are provided without limited supply. In natural processes such substances are regenerated, since they are oxidized during reduction reactions. For the purpose of CO₂ reduction in experiments for possible large-scale application, however, such co-factors and equivalents are neither feasible nor practical because of high costs for supply and regeneration.

In this work the application of such biocatalysts are investigated by mimicking natural processes and providing required co-factors. Those results are compared to systems where the biocatalysts are adapted to electrochemical processes with no electron or proton donors required. In order to substitute co-factors, enzymes are applied to electrochemical systems. In such electrochemical reduction reaction electron supply occurs due to direct electron injection into the biocatalysts from an electrode.

Two different approaches are demonstrated, showing results using living biocatalysts, namely methanogenic microorganisms and non-living biocatalysts, namely dehydrogenase enzymes.

Methanogenic microorganisms are shown for their electrotrophic behavior and application on electrodes for catalyzing the reduction of CO₂ to CH₄. Techniques to tune those microorganisms to an electron only process without requiring any H₂ added artificially are presented. Faradaic efficiencies (according to the charges consumed during potentiostatic electrolysis) from 3.4 to 22% are observed. Further stabilized long-term performance with constant methane output is depicted.

Direct electron injection into immobilized dehydrogenase enzymes was proven in three different investigations. Results on using single enzymes for one-step reduction reactions as well as the combination of three enzymes to a cascade for the reduction of CO₂ all the way to methanol are presented. Potentiostatic electrolysis without any sacrificial co-enzyme delivered for the electrochemical CO₂ reduction to methanol about 0.15 ppm. Faradaic efficiencies of around 10% were obtained. Further even higher faradaic efficiencies (40%) were obtained using only alcohol dehydrogenase for the generation of higher alcohols, particularly butanol from butyraldehyde reduction. These results show for the first time that all three dehydrogenase enzymes can directly be addressed with electrochemistry without any sacrificial mediator or electron donor needed. Those results were proven by electrochemical as well as analytical investigations. Electrochemical characterization often delivered only little information of the performed reductions. This is assumed to be due to elaborated electrode constitution (enzymes immobilized in alginate matrix applied to carbon felt), that makes imaging reduction processes less significant. However, analytical measurements in addition to electrochemical experiments delivered convincing results correlated to the reduction reactions.

Utilization of biocatalysts is advantageous due to reactions occurring at ambient conditions delivering high yields and high selectivity according to the products generated. Direct electrochemical CO₂ reduction with a significant amount of charge consumed for the reduction of CO₂ using biocatalyst modified electrodes offers a selective, reproducible and mild method for the production of artificial fuels and opens the way to biodegradable and sustainable energy conversion. This substitutes expensive co-factors and synthetic catalysts with low selectivity and yield and therefore opens the way for possible application also at industrial scales for artificial fuel production.

5. Appendix

Symbols and Abbreviations

CF	carbon felt
CO ₂	carbon dioxide
H ₂	hydrogen
CH ₃ OH	methanol
N ₂	nitrogen
CH ₄	methane
CO	carbon monoxide
CO ₃ ²⁻	carbonate
KCl	potassium chloride
Ag	silver
AgCl	silver chloride
HCl	hydrochloric acid
KCl	potassium chloride
KH ₂ PO ₄	potassium dihydrogen phosphate monobasic
K ₂ HPO ₄	dipotassium hydrogen phosphate
NADH	nicotinamide adenine dinucleotide
TEOS	tetraethylorthosilicate
TRIS	tris(hydroxymethyl)-aminomethane
PB	phosphate buffer
CaCl ₂	calcium chloride
KOH	Potassium hydroxide
MgSO ₄ · 7 H ₂ O	Magnesium sulfate
MnSO ₄ · 7 H ₂ O	Manganese sulfate
NaCl	Sodium chloride

$\text{FeSO}_4 \cdot 7 \text{H}_2\text{O}$	Iron sulfate
$\text{CoSO}_4 \cdot 7 \text{H}_2\text{O}$	Cobalt sulfate
$\text{ZnSO}_4 \cdot 7 \text{H}_2\text{O}$	Zinc sulfate
$\text{CuSO}_4 \cdot 7 \text{H}_2\text{O}$	Copper sulfate
$\text{KAl}(\text{SO}_4)_2 \cdot 12 \text{H}_2\text{O}$	Potassium aluminium sulfate
H_3BO_3	Boric acid
$\text{Na}_2\text{MoO}_4 \cdot 2 \text{H}_2\text{O}$	Sodium molybdate
$\text{NiCl}_2 \cdot 6 \text{H}_2\text{O}$	Nickel chloride
$\text{Na}_2\text{SeO}_3 \cdot 5 \text{H}_2\text{O}$	Sodium selenate
NH_4Cl	Ammonium chloride
CCU	Carbon capture and utilization
CCS	Carbon capture and sequestration
NHE	normal hydrogen electrode
CAP-IC	capillary ion chromatography
LGC	liquid injection gas chromatography
CV	cyclic voltammogram
F	Faraday constant
Q	charge
z	number of electrons flowing
n	amount of substance [mol]
FID	flame ionization detector
C	coulomb
As	Ampere seconds
ATR-FTIR	Attenuated total reflection- Fourier transform infra-red
MEC	Microbial Electrolysis Cell
F_{ateDH}	Formate dehydrogenase
F_{aldDH}	Formaldehyde dehydrogenase
ADH	Alcohol dehydrogenase

List of Figures

<i>Figure 1</i> Records of the atmospheric CO ₂ content at Mauna Loa from 1958 by the Scripps Institution of Oceanography show a steady increase. Fluctuating behavior of the curve indicates the variation of the CO ₂ content within a year depending on the time of year and season respectively. ^[3]	2
<i>Figure 2</i> Record of the development of CO ₂ concentration in the atmosphere dated back to 800 000 years from present, recorded from ice core data. From 1958 data are obtained from records from Mauna Loa observatory. ^[3]	3
<i>Figure 3</i> Correlation of atmospheric CO ₂ content and earth's temperature back to 800k years before present from records of ice core measurements. ^[1]	3
<i>Figure 4</i> Correlation of time and space according to utilization and transport for renewable energies.	4
<i>Figure 5</i> Possible storage options for CO ₂ in underground storage options like under ocean and in deep rocks. ^[1]	5
<i>Figure 6</i> Possible reaction routes and materials from CO ₂ as feedstock in the CCU approach. ^[11]	6
<i>Figure 7</i> Metabolic pathway of clostridia towards various products depending on the source of substrate to be metabolized, presented by Tracy et al. ^[40]	11
<i>Figure 8</i> Reduction mechanisms of CO ₂ catalyzed by dehydrogenase enzymes. 3-step reduction of CO ₂ to methanol with NADH as sacrificial co-enzyme (A) and via a direct electron transfer to the enzyme without any co-enzyme (B).	16
<i>Figure 9</i> Proposed electron transfer from an electrode to formate dehydrogenase during reduction of CO ₂ to formate, reported by Reda et al. ^[77]	17
<i>Figure 10</i> Microbial electrolysis cell. Photograph on the left hand side and schematic of the cell on the right hand side display the setup used. Setup shows anode compartment (right) and cathode compartment (left) separated by membrane which was fixed between the compartments using a clamp. Electrical contacts for the electrodes as well as gas in- and outlets were implemented via septa.	20
<i>Figure 11</i> Microbial electrolysis cell after inoculation of sewage suspension containing microorganism to the cathode compartment (right-hand side).	23
<i>Figure 12</i> Molecular structures of alginic acid sodium salt (left hand side) and tetraethylorthosilicate (right hand sides).	29
<i>Figure 13</i> Molecular structure of tris(hydroxymethyl)-aminomethane-HCl (TRIS-HCl).	30
<i>Figure 14</i> Preparation of alginate based beads. Solution of alginate-silicate hybrid sol-gel (A) was dropped into 0.2 M CaCl ₂ solution for precipitation (B). After 20 min of precipitation, obtained beads (C and D) were rinsed and used directly for experiments.	31
<i>Figure 15</i> Preparation of a carbon felt electrode modified with alginate-silicate hybrid sol-gel. The carbon felt electrode (B) was soaked with the prepared matrix gel (A) and precipitated in	

<i>0.2 M CaCl₂ solution for 20 min (C). The obtained gel covered electrode (D) was used as working electrode in electrochemical measurements.</i>	32
<i>Figure 16 Setup for reduction reaction using alginate-silicate gel beads and NADH as electron and proton donor.</i>	33
<i>Figure 17 Two-compartment-cells for enzymatic electrochemistry measurements. The left-hand side schematic depicts the setup for purging and saturating with gases. The right-hand side setup shows a schematic for the addition of liquid components like butyraldehyde to the setup.</i>	34
<i>Figure 18 Schematic of the electrochemical CO₂ reduction using enzymes. Electrons are injected directly into the enzymes, which are immobilized in alginate-silicate hybrid gel (green) on a carbon felt working electrode. CO₂ is reduced at the working electrode. Oxidation reactions take place at the counter electrode.</i>	36
<i>Figure 19 Gas chromatograms of the headspace constitution of the cathode compartment in MEC1. Chromatograms show the development of amount of reduction product during the growing process. An increase of methane concentration is observed within four days of growing of microorganisms on the carbon felt electrode.</i>	42
<i>Figure 20 Biofilm formed after proceeding growing of the microorganisms on the electrode for 3 days. The red circle displays the microorganisms grown on the electrode.</i>	43
<i>Figure 21 Cyclic voltammograms of the biocathode in the non-adapted state. The biocathode was electrochemically characterized after purging and saturating the system with N₂ or CO₂/H₂ respectively. Further for comparison the same measurements were performed for a pristine carbon felt electrode without biofilm.</i>	44
<i>Figure 22 Gas chromatograms featuring the development of the headspace gas constitution during adaption with CO₂ and H₂. Concentration of H₂ added was reduced subsequently with every cycle. Adaption was performed within 3 cycles and 3 weeks respectively.</i>	45
<i>Figure 23 Gas chromatograms showing long-term performance of MEC1 after completed adaption with CO₂ and H₂. Methane production in general decreased, in comparison to performance immediately after adaption. However, methane generation was rather constant within 22 weeks of performance despite of lower concentration, as seen for the methane peaks at 0.48 min of several records in gas chromatography.</i>	46
<i>Figure 24 Gas chromatograms showing the development of methane generation within adaption of the microorganisms using glucose.</i>	47
<i>Figure 25 Gas chromatography records for the long-term performance of MEC1 after repeated adaption with glucose. Production of methane from CO₂ reduction shows a remarkable increase in comparison to results from long-term performance before adaption with glucose.</i>	48
<i>Figure 26 Correlation of amounts of H₂ and CH₄ in the headspace of the cathode compartment of MEC1 during long-term performance after the second adaption.</i>	49
<i>Figure 27 Cyclic voltammograms of the adapted biocathode in MEC1 in N₂ and CO₂ saturated system. An increase in reductive current is only observed after the system was purged with</i>	

<i>CO₂. Further comparison with a pristine carbon felt electrode without any biofilm supports that CO₂ reduction only occurs when there are microorganisms apparent.</i>	50
<i>Figure 28 Gas chromatograms of the cathode compartment when there was no potential applied. Chromatograms were recorded after saturating the system with CO₂ and after 20 h when there was no potential applied. There is no methane formation observed.</i>	51
<i>Figure 29 Gas chromatograms of headspace gas samples after growth of microorganisms on the carbon felt electrode and during enrichment of the biofilm. Analysis shows a slow and small increase of methane concentration after 4 weeks of enhancing the biofilm.</i>	52
<i>Figure 30 Gas chromatograms of headspace gas samples from MEC2 during adaption with glucose and CO₂/H₂. Methane formation was observed already during adaption as can be seen for the peak at 0.48 min corresponding to the retention time of methane.</i>	53
<i>Figure 31 Gas chromatograms of headspace gas samples of MEC2 during long-term performance with CO₂ only after adaption. A periodic increase- and decrease-behavior is observed for the methane peak intensity and concentration respectively at 0.48 min.</i>	54
<i>Figure 32 Correlation of concentration values of H₂ and CH₄ during long-term performance over several weeks.</i>	55
<i>Figure 33 Cyclic voltammograms of a biocathode and a pristine carbon felt electrode.</i>	56
<i>Figure 34 Electropolymerization of the Co²⁺ Nocera catalyst on Pt. Increasing number of cycles results in an increase of current densities due to changed resistivity of the electrode due to film formation on the electrode.</i>	58
<i>Figure 35 Potentiostatic electropolymerization subsequent to potentiodynamic film formation. Application of +1100 mV vs. Ag/AgCl for about 1 h features a constant current flowing.</i>	59
<i>Figure 36 Photograph of the obtained Pt electrode covered with Nocera catalyst after electropolymerization procedure.</i>	59
<i>Figure 37 SEM surface image depicting island-like constitution of the Co-based Nocera catalyst. Besides islands white spots are observed that are expected due to salt residues from electropolymerization procedure.</i>	60
<i>Figure 38 Elementary constitution of the islands and white spots from SEM image. Constitution depicts high amounts of cobalt and platinum as expected for the catalyst film. Besides there are hardly any impurities detected. Small traces of potassium and phosphate were also expected due to the phosphate buffer electrolyte solution.</i>	61
<i>Figure 39 Gas chromatography of headspace gas samples from the anode compartment of MEC1. Chromatograms are shown for samples taken before and after 5 h of potentiostatic electrolysis.</i>	62
<i>Figure 40 Oxygen evolution on the surface of the Nocera catalyst electrode due to catalyzed oxidative water splitting reaction in the anode compartment of MEC1.</i>	63
<i>Figure 41 Chromatogram from CAP-IC comparing samples from directly after starting the reduction reaction and after completed reduction.</i>	66

Figure 42 Cyclic voltammogram of an alginate modified carbon felt electrode with $F_{ate}DH$ immobilized at a scan rate of 5 mV s^{-1} and cycling between 0 mV and -1200 mV vs. Ag/AgCl after saturation with N_2 as well as after saturation with CO_2 . CV for the N_2 saturated system depicts even higher current densities than CV after saturating with CO_2 . _____ 68

Figure 43 Cyclic voltammograms of an alginate modified carbon felt electrode containing $F_{ate}DH$ at a scan rate of 50 mV s^{-1} . CV's were recorded after saturating the electrochemical cell with N_2 and after saturation with CO_2 . A decrease in current densities is observed with increasing number of cycles. _____ 68

Figure 44 Current-time plot of the electrolysis experiment in a N_2 saturated system and the same experiment in CO_2 saturated system using a formate dehydrogenase containing, gel modified CF electrode. _____ 69

Figure 45 Capillary Ion chromatograms before and after electrolysis in a CO_2 saturated system using a gel- modified electrode with immobilized $F_{ate}DH$. At the retention time of around 5.75 min a peak is rising after electrolysis in comparison to a sample before electrolysis. This indicates formate generation from potentiostatic electrolysis. _____ 71

Figure 46 Liquid injection gas chromatograms of a non-electrochemical control experiment in TRIS-HCl buffer using enzyme containing alginate gel-beads and NADH as co-enzyme. A peak is observed to evolve and increase at the retention time of methanol at 1.87 min after addition of NADH indicating CO_2 reduction to be started (grey, red and dark red line). However, a peak at that retention time is also observed for the TRIS-HCl buffer solution itself (dashed line). _____ 73

Figure 47 Liquid injection gas chromatograms of a non-electrochemical control experiment using enzyme containing alginate gel-beads and NADH as co-enzyme in PB buffer solution. An increasing peak is obtained at the retention time of methanol at 1.86 min after addition of NADH indicating CO_2 reduction to methanol (grey, red and dark red line). There is no peak observed as long as NADH was not added as electron donor. _____ 74

Figure 48 Cyclic voltammograms at a scan rate of 10 mV s^{-1} of an alginate modified carbon felt electrode containing all three dehydrogenase. TRIS-HCl was used as buffer solution. CV's were recorded after saturating the electrochemical cell with N_2 as well as after saturation with CO_2 . There is no remarkable difference observed. _____ 76

Figure 49 Cyclic voltammograms at a scan rate of 50 mV s^{-1} of an alginate modified carbon felt electrode containing all three dehydrogenase. TRIS-HCl was used as buffer solution. CV's were recorded after saturating the electrochemical cell with N_2 as well as after saturation with CO_2 . There is no remarkable difference observed. _____ 77

Figure 50 Cyclic voltammograms of the carbon felt electrode modified with enzyme containing alginate at different scan rates between 5 and 100 mV s^{-1} using TRIS-HCl as buffer solution. Currents are increasing with increasing scan rates. This is assumed for diffusion controlled processes as it is also expected for processes occurring on such a gel modified electrode. _____ 78

Figure 51 Current-time curves from electrolysis of a carbon felt electrode, modified with enzyme containing alginate. Experiments were conducted potentiostatic at a constant potential of -1200 mV vs. Ag/AgCl in a N₂ or CO₂ saturated TRIS-HCl electrolyte solution. Current behavior over time for the N₂ saturated system shows a certain basic current due to competing reactions taking place independently from the CO₂ reduction for all electrochemical experiments. _____ 79

Figure 52 Liquid injection gas chromatograms before and after electrolysis in CO₂ saturated TRIS-HCl electrolyte solution using a CF electrode with all three enzymes immobilized compared to reference measurements without CO₂ (black symbols) or without enzyme (grey line). At the retention time of around 1.9 min a peak is rising after electrolysis, indicating methanol generation. _____ 80

Figure 53 Cyclic voltammograms at a scan rate of 10 mV s⁻¹ of an alginate modified carbon felt electrode containing all three dehydrogenase. PB was used as buffer solution. CV's were recorded after saturating the electrochemical cell with N₂ as well as after saturation with CO₂. There is no remarkable difference observed. _____ 82

Figure 54 Cyclic voltammograms at a scan rate of 50 mV s⁻¹ of an alginate modified carbon felt electrode containing all three dehydrogenase. PB was used as buffer solution. CV's were recorded after saturating the electrochemical cell with N₂ as well as after saturation with CO₂. There is no remarkable difference observed. _____ 83

Figure 55 Cyclic voltammograms of the carbon felt electrode modified with enzyme containing alginate at different scan rates between 5 and 100 mV s⁻¹ using PB as buffer solution. Currents increase with increasing scan rates. This is assumed for diffusion controlled processes as it is also expected for processes occurring on such a gel modified electrode. ___ 84

Figure 56 Current-time curves from electrolysis of a carbon felt electrode, modified with enzyme containing alginate. Experiments were conducted potentiostatic at a constant potential of -1200 mV vs. Ag/AgCl in a N₂ or CO₂ saturated TRIS-HCl electrolyte solution. Current behavior over time for the N₂ saturated system shows a certain basic current due to competing reactions taking place independently from the CO₂ reduction for all electrochemical experiments. _____ 85

Figure 57 Liquid injection gas chromatograms before and after electrolysis in CO₂ saturated PB electrolyte solution using a CF electrode with all three enzymes immobilized compared to reference measurements without CO₂ (black symbols), without enzyme (grey line) or without potential applied (blue and light blue lines). At the retention time of around 1.9 min a peak is rising after electrolysis, indicating methanol generation. _____ 86

Figure 58 Gas chromatograms of the headspace from before and after electrolysis using an enzyme modified electrode in N₂ as well as CO₂ saturated buffer solution. _____ 87

Figure 59 Liquid injection gas chromatograms of a non-electrochemical control experiment using enzyme containing alginate gel-beads and NADH as co-enzyme. An intensive peak is observed at the retention time of butanol (3.64 min) after 8 h of reaction time. _____ 88

<i>Figure 60 Cyclic voltammograms of an alginate modified carbon felt electrode containing alcohol dehydrogenase at a scan rate of 5 mV s⁻¹. CV's were recorded after saturating the electrochemical cell with N₂ and after adding 0.1 mL butyraldehyde. An increase in current density is observed after adding butyraldehyde.</i>	90
<i>Figure 61 Cyclic voltammograms of an alginate modified carbon felt electrode containing alcohol dehydrogenase at a scan rate of 50 mV s⁻¹. CV's were recorded after saturating the electrochemical cell with N₂ and after adding 0.1 mL butyraldehyde. A decrease in current densities is observed with increasing number of cycles.</i>	91
<i>Figure 62 Cyclic voltammogram of an alginate modified carbon felt electrode at a scan rate of 5 mV s⁻¹ and cycling between 0 mV and -600 mV vs. Ag/AgCl after saturation with N₂ and after adding butyraldehyde. There is no increase shown indicating a reduction of butyraldehyde.</i>	92
<i>Figure 63 Cyclic voltammograms of an alginate modified carbon felt electrode at a scan rate of 50 mV s⁻¹ and cycling 3 times between 0 mV and -600 mV vs. Ag/AgCl after saturation with N₂ and after adding butyraldehyde. The arrow indicates decrease in current density with increasing number of cycles.</i>	92
<i>Figure 64 Cyclic voltammograms (CV) after adding butyraldehyde to the electrolyte solution, using an alginate-enzyme modified carbon felt (CF) electrode (red, dotted) and an equally modified electrode without enzyme (black) at a scan rate of 5 mV s⁻¹.</i>	93
<i>Figure 65 Current-time plot of the electrolysis experiment using an alcohol dehydrogenase containing, gel modified CF electrode and electrolyte solution containing butyraldehyde.</i>	94
<i>Figure 66 Liquid injection gas chromatograms before and after electrolysis with butyraldehyde using a gel- modified electrode with immobilized alcohol dehydrogenase compared to reference measurements without butyraldehyde or without enzyme. At the retention time of 3.64 min a peak is rising after electrolysis, indicating butanol generation.</i>	96
<i>Figure 67 Scanning Electron Microscopy Image showing a pristine carbon felt substrate at 3000 fold (left) and 84 fold (right) magnification.</i>	97
<i>Figure 68 Microscopy images taken at 5 fold magnification for pristine carbon felt (left) and alginate-silicate modified carbon felt (right).</i>	98
<i>Figure 69 SEM imaging done at 20 kV with 120 fold magnification (left) and at 10 kV with 2000 fold magnification (right) showing alginate-silicate gel coverage of a carbon felt electrode, in courtesy of JEOL.</i>	98

List of Tables

<i>Table 1 Compounds and corresponding concentrations in trace element solution required for medium and electrolyte solution of the MEC respectively, provided by PROFACTOR GmbH. .</i>	<i>21</i>
<i>Table 2 Compounds and corresponding concentrations in vitamin solution required for medium and electrolyte solution of the MEC respectively, provided by PROFACTOR GmbH. .</i>	<i>22</i>
<i>Table 3 Concentrations of components added to 20 mM phosphate buffer for obtaining a medium according to Cheng.</i>	<i>22</i>
<i>Table 4 Method for analysis of headspace gas samples in gas chromatography.</i>	<i>27</i>
<i>Table 5 Corresponding values in percentage for the elementary constitution determined from SEM-EDX analysis.</i>	<i>61</i>

List of Equations

<i>Equation 1 Reaction for the mineralization of CO₂.^[6]</i>	6
<i>Equation 2 Theoretical standard redox potentials for the reduction of CO₂ vs. NHE in aqueous solution at pH 7.</i>	7
<i>Equation 3 Reaction pathway for the reduction of CO₂ with H₂ added artificially, catalyzed by anaerobic microorganisms.</i>	12
<i>Equation 4 Reaction pathway for the reduction of CO₂ within microbial electrolysis, without H₂ added artificially.</i>	13
<i>Equation 5 Reaction pathway based on Michaelis-Menten equation for enzyme kinetics.</i>	15

Bibliography

- [1] S. Arrhenius, "On the influence of Carbonic Acid in the Air upon the Temperature of the Ground." *Phil. Mag.*, vol. 41, pp. 237-276, 1896.
- [2] C. D. Keeling, "The concentration and isotopic abundances of atmospheric carbon dioxide in rural areas.", *Geochim. Cosmochim. Acta*, vol. 13, pp. 322-334, 1958.
- [3] Scripps Institution of Oceanography, UC San Diego, 2015, <https://scripps.ucsd.edu/programs/keelingcurve/>, November 22nd, 2015.
- [4] United States Environment Protection Agency, Causes of Climate Change, 2015, <http://www3.epa.gov/climatechange/science/causes.html>, October 21st, 2015.
- [5] S. J. Friedmann, *Carbon capture and storage*. UCRL Book, 2007.
- [6] M. Aresta, *Carbon Dioxide as Chemical Feedstock*, Wiley-VCH, Weinheim, 2010.
- [7] M. Aresta, G. Fortz, *Carbon Dioxide as a Source of Carbon: Biochemical and Chemical Uses*, D. Reidel Publishing Company, Dordrecht, 1987.
- [8] G. A. Olah, A. Goepfert, G. K. Surya Prakash, *Beyond Oil and Gas: The Methanol Economy*, Wiley-VCH, Weinheim, ed. 2, 2009.
- [9] C.-J. Liu, R. G. Mallinson, M. Aresta, *Utilization of Greenhouse Gases*, American Chemical Society, 1. ed., 2003.
- [10] M. Aresta, *Carbon Dioxide Recovery and Utilization*, Kluwer Academic Publishers, Dordrecht, 2003.
- [11] S. N. Riduan, Y. Zhang, "Recent developments in carbon dioxide utilization under mild conditions", *Dalton Trans.*, vol. 39, pp. 3347-3357, 2010.
- [12] M. North, R. Pasquale, "Mechanism of Cyclic Carbonate Synthesis from Epoxides and CO₂", *Angew. Chemie*, vol. 121, pp. 2990-2992, 2009.
- [13] P. Styring, K. Armstrong, "Catalytic carbon dioxide conversions to value-added chemicals", *Catal. Appl.*, vol. 29, pp. 28-31, 2011.
- [14] G. A. Olah, G. K. S. Prakash, "Recycling of Carbon Dioxide into Methyl Alcohol and Related Oxygenates for Hydrocarbons", US Patent 5928806 A, 1999.
- [15] B.S. Rajanikanth, K. Shimizu, M. Okumoto, S. Kastura and A. Mizuno, "Application of Pulsed Discharge Plasma for Methanol Synthesis", *IEEE IAS Annu.Meet.*, pp. 1459, 1995.
- [16] J. Qiao, Y. Liu, F. Hong, J. Zhang, "A review of catalysts for the electroreduction of carbon dioxide to produce low-carbon fuels", *Chem. Soc. Rev.*, vol. 43, pp. 631-675, 2013.
- [17] A. Bandi, M. Specht, T. Weimer, K. Schaubert, "CO₂ recycling for hydrogen storage and transportation-electrochemical CO₂ removal and fixation", *Energy Convers. Mgmt.*, vol. 36, pp. 899-902, 1995.
- [18] T. Mizuno, A. Naitoh, K. Ohta, "Electrochemical reduction of CO₂ in methanol at - 30°C", *J. Electroanal. Chem.*, vol. 391, pp. 199-201, 1995.
- [19] Y. Surendranath, D. Kwabena Bediako, D. G. Nocera, "Interplay of oxygen-evolution kinetics and photovoltaic power curves on the construction of artificial leaves.", *PNAS*, vol. 109, pp. 15617-15621, 2012.

- [20] M. Kaneko, I. Ochura, *Photocatalysis: Science and Technology*, Springer, Heidelberg, 2002.
- [21] K. Kalyanasundaram, M. Graetzel, "Artificial photosynthesis : biomimetic approaches to solar energy conversion and storage", *Curr. Opin. Biotechnol.*, vol. 21, pp. 298-310, 2010.
- [22] D. Nocera, "The artificial leaf", *Acc. Chem. Res.*, vol. 45, pp. 767-776, 2012.
- [23] M. Schreier, L. Curvat, F. Giordano, L. Steier, A. Abate, S. M. Zakeeruddin, J. Luo, M. T. Mayer, M. Graetzel, " Efficient photosynthesis of carbon monoxide from CO₂ using perovskite photovoltaics", *Nat. Commun.*, vol. 6, pp. 1-6, 2015.
- [24] S. Cosnier, A. Deronzier, J.-C. Moutet "Electrocatalytic reduction of CO₂ on electrodes modified by fac-Re(2,2'-bipyridine)(CO)₃Cl complexes bonded to polypyrrole films", *J. Mol. Catal.*, vol. 45, pp. 381-391, 1988.
- [25] S. Cosnier, A. Deronzier, J.-C. Moutet, "Electrochemical coating of a platinum electrode by a polypyrrole film containing the fac-Re(2,2'-bipyridine)(CO)₃Cl system", *J. Electroanal. Chem.*, vol. 207, pp. 315-321, 1986.
- [26] S. Cosnier, A. Deronzier, J.-C. Moutet, J. F. Roland, "Alkylammonium and pyridinium group-containing polypyrroles, a new class of electronically conducting anion-exchange polymers", *J. Electroanal. Chem.*, vol. 271, pp. 69-81, 1989.
- [27] J. M. Smieja, C. P. Kubiak, "Re(bipy-tBu)(CO)₃Cl-improved catalytic activity for reduction of carbon dioxide: IR-spectroelectrochemical and mechanistic studies", *Inorg. Chem.*, vol. 49, pp. 9283-9289, 2010.
- [28] B. Kumar, J. M. Smieja, C. P. Kubiak, "Photoreduction of CO₂ on p-type Silicon Using Re(bipy-Bu^t)(CO)₃Cl: Photovoltages Exceeding 600 mV for the Selective Reduction of CO₂ to CO", *J. Phys. Chem.*, vol. 114, pp. 14220-14223, 2010.
- [29] E. E. Benson, C. P. Kubiak, A. J. Sathrum, J. M Smieja, "Electrocatalytic and homogeneous approaches to conversion of CO₂ to liquid fuels", *Chem. Soc. Rev.*, vol. 38, pp. 89-99, 2008.
- [30] B. Kumar, M. Llorente, J. Froehlich, T. Dang, A. Sathrum, C. P. Kubiak, "Photochemical and Photoelectrochemical Reduction of CO₂", *Annu. Rev. Phys. Chem.*, pp. 541-569, 2012.
- [31] E. Portenkirchner, J. Gasiorowski, K. Oppelt, S. Schlager, C. Schwarzinger, H. Neugebauer, G. Knör, N. S. Sariciftic, "Electrocatalytic Reduction of Carbon Dioxide to Carbon Monoxide by a Polymerized Film of an Alkynyl Substituted Rhenium(I)-Complex", *ChemCatChem*, vol. 5, pp 1790-1796, 2013.
- [32] E. Portenkirchner, S. Schlager, D. Apaydin, K. Oppelt, M. Himmelsbach, D. A. M. Egbe, H. Neugebauer, G. Knör, T. Yoshida, N. S. Sariciftci, "Using the Alkynyl-Substituted Rhenium(I) Complex (4,4'- Bisphenyl -Ethyne- 2,2' Bipyridyl) Re (CO)₃Cl as Catalyst for CO₂ Reduction-Synthesis, Characterisation and Application", *Electrocatal.*, vol. 6, pp 185-197, 2015.
- [33] E. B. Cole, P. S. Lakkaraju, D. M. Rampulla, A. J. Morris, E. Abelev, A. B. Bocarsly, "Using a one-electron shuttle for the multielectron reduction of CO₂ to methanol: kinetic, mechanistic, and structural insights", *J. Am. Chem. Soc.*, vol. 132, pp. 11539-11551, 2010.

- [34] E. Portenkichner, C. Enengl, S. Enengl, G. Hinterberger, S. Schlager, D. Apaydin, H. Neugebauer, G. Knör, N. S. Sariciftci, "A Comparison of Pyridazine and Pyridine as Electrocatalysts for the Reduction of Carbon Dioxide to Methanol", *ChemElectroChem*, vol. 1, pp. 1543-1548, 2014.
- [35] M. F. Baruch, J. E. Pander III, J. L. White, A. B. Bocarsly, "Mechanistic Insights into the Reduction of CO₂ on Tin Electrodes using in Situ ATR-IR Spectroscopy", *ACS Catal.*, vol. 5, pp. 3148-3156, 2015.
- [36] K. P. Kuhl, T. Hatsukade, E. R. Cave, D. N. Abram, J. Kibsgaard, T. F. Jaramillo, "Electrocatalytic Conversion of Carbon Dioxide to Methane and Methanol on Transition Metal Surfaces", *J. Am. Chem. Soc.*, vol. 136, pp. 14107-14113, 2014.
- [37] A. Bachmeier, V. C. C. Wang, T. W. Woolerton, S. Bell, J. C. Fontecilla-Camps, M. Can, S. W. Ragsdale, Y. S. Chaudhary, F. Armstrong, "How Light-Harvesting Semiconductors Can Alter the Bias of Reversible Electrocatalysts in Favor of H₂ Production and CO₂ Reduction", *J. Am. Chem. Soc.*, vol. 135, pp. 15026-15032, 2013.
- [38] Y. S. Chaudhary, T. W. Woolerton, C. S. Allen, J. H. Warner, E. Pierce, S. W. Ragsdale, F. Armstrong, "How Light-Harvesting Semiconductors Can Alter the Bias of Reversible Electrocatalysts in Favor of H₂ Production and CO₂ Reduction", *Chem. Commun.*, vol. 48, pp. 58-60, 2012.
- [39] S. Patil, K. Hasan, D. Leech, C. Hägerhäll, L. Gorton, "Improved microbial electrocatalysis with osmium polymer modified electrodes", *Chem. Commun.*, vol. 48, pp. 10183-10185, 2012.
- [40] B. E. Logan, *Microbial Fuel Cells*, Wiley, New Jersey, 2008.
- [41] H. L. Ehrlich, "Are gram-positive bacteria capable of electron transfer across their cell wall without an externally available electron shuttle?", *Geobiology*, vol. 6, pp. 220-224, 2008.
- [42] M. Rosenbaum, F. Aulenta, M. Villano, L. T. Angenent, "Cathodes as electron donors for microbial metabolism: which extracellular electron transfer mechanisms are involved?", *Bioresour. Technol.*, vol. 102, pp. 324-333, 2011.
- [43] G. Bokinsky, P. P. Peralta-Yahya, A. George, B. M. Holmes, E. J. Steen, J. Dietrich, T. S. Lee, D. Tullman-Ercek, C. Voigt, B. Simmons, J. D. Keasling, "Synthesis of three advanced biofuels from ionic liquid-pretreated switchgrass using engineered *Escherichia coli*", *PNAS*, vol. 108, pp. 19949-19954, 2011.
- [44] J.-y. Xin, Y.-x. Zhang, S. Zhang, C.-g. Xia, S.-b. Li, "Methanol production from CO₂ by resting cells of the methanotrophic bacterium *Methylosinus trichosporium* IMV 3011", *J. Basic Microbiol.*, vol. 47, pp. 426-435, 2007.
- [45] B. P. Tracy, S. W. Jones, A. G. Fast, D. C. Indurthi, E. T. Papoutsakis, "Clostridia: the importance of their exceptional substrate and metabolite diversity for biofuel and biorefinery applications", *Curr. Opin. Biotechnol.*, vol. 23, pp. 364-381, 2012.
- [46] J. G. Ferry, "Enzymology of one-carbon metabolism in methanogenic pathways.", *FEMS Microbiol. Rev.*, vol. 23, pp. 13-38, 1999.

- [47] U. Deppenmeier, V. Müller, G. Gottschalk, "Pathways of energy conservation in methanogenic archaea." *Arch. Microbiol.*, vol. 165, pp. 149–163, 1996.
- [48] J. G. Ferry, "Fundamentals of methanogenic pathways that are key to the biomethanation of complex biomass", *Curr. Opin. Biotechnol.*, vol. 22, pp. 351-357, 2011.
- [49] S. Shima, E. Warkentin, R. K. Thauer, U. Ermler, "Structure and function of enzymes involved in the methanogenic pathway utilizing carbon dioxide and molecular hydrogen", *J. Biosci. Bioeng.*, vol. 93, pp. 519-530, 2002.
- [50] H. Wang, Z. Ren, "A comprehensive review of microbial electrochemical systems as a platform technology.", *Biotechnol. Adv.*, vol. 31, pp. 1796-1807, 2013.
- [51] S. A. Cheng, D. F. Xing, D. F. Call, B. E. Logan, "Direct biological conversion of electrical current into methane by electromethanogenesis." *Environ. Sci. Technol.*, vol. 43, pp. 3953-3958, 2009.
- [52] M. C. A. A Van Eerten-Jansen, A. T. Heijne, C. J. N. Buisman, H. V. M. Hamelers, "Microbial electrolysis cells for production of methane from CO₂: Long-term performance and perspectives." *Int. J. Energy Res.*, vol. 36, pp. 809-819, 2012.
- [53] M. Villano, F. Aulenta, C. Ciucci, T. Ferri, A. Giuliano, M. Majone, "Bioelectrochemical reduction of CO₂ to CH₄ via direct and indirect extracellular electron transfer by a hydrogenophilic methanogenic culture.", *Bioresour. Technol.*, vol. 101, pp. 3085-3090, 2010.
- [54] K. Sato, H. Kawaguchi, H. Kobayashi, "Bio-electrochemical conversion of carbon dioxide to methane in geological storage reservoirs", *Energy Conversion an Management*, vol. 66, pp. 343-350, 2013.
- [55] M. Hara, Y. Onaka, H. Kobayashi, Q. Fu, H. Kawaguchi, J. Vilcaez, K. Sato, Mechanism of "Electromethanogenic Reduction of CO₂ by a Thermophilic Methanogen", *Energy Procedia*, vol. 37, pp. 7021-7028, 2013.
- [56] Y. Kuramochi, Q. Fu, H. Kobayashi, M. Ikarashi, T. Wakayama, H. Kawaguchi, J. Vilcaez, H. Maeda, K. Sato, "Electromethanogenic CO₂ Conversion by Subsurface-reservoir Microorganisms", *Energy Procedia*, vol. 37, pp. 7014-7020, 2013.
- [57] H. Kobayashi, N. Saito, Q. Fu, H. Kawaguchi, J. Vilcaez, T. Wakayama, H. Maeda, K. Sato, "Bio-electrochemical property and phylogenetic diversity of microbial communities associated with bioelectrodes of an electromethanogenic reactor", *J. Biosci. Bioeng.*, vol. 116, pp. 114-117, 2013.
- [58] H. Li, P. H. Opgenorth, D. G. Wernick, S. Rogers, T.-y. Wu, W. Higashide, P. Malati, Y.-x. Huo, K.-M. Cho, J. C. Liao, "Integrated Electromicrobial Conversion of CO₂ to Higher Alcohols", *Science*, vol. 335, pp. 1596, 2012.
- [59] S. A. Patil, K. Hasan, D. Leech, C. Hägerhäll, L. Gorton, "Improved microbial electrocatalysis with osmium polymer modified electrodes.", *Chem. Commun.*, vol. 48, pp. 10183-10185, 2012.
- [60] L. Jourdin, S. Freguia, B. C. Donose, J. Chen, G. C. Wallace, J. Keller, V. Flexer, "A novel carbon nanotube modified scaffold as an efficient biocathode material for improved microbial electrosynthesis", *J. Mater. Chem.*, vol. 2, pp. 13093-13102, 2014.

- [61] Y. Jiang, M. Su, Y. Zhang, G. Zhan, Y. Tao, D. Li, "Bioelectrochemical systems for simultaneous production of methane and acetate from carbon dioxide at relatively high rate." *Int. J. Hydrogen Energy*, vol. 38, pp. 3497-3502, 2013.
- [62] S. Freguia, B. Viridis, F. Harnisch, J. Keller, "Bioelectrochemical systems: Microbial versus enzymatic catalysis", *Electrochim. Acta*, vol. 82, pp. 165-174, 2012.
- [63] M. Aresta, A. Dibenedetto, "Development of environmental friendly syntheses: use of enzymes and biomimetic systems for the direct carboxylation of organic substrates", *Rev. Mol. Biotechnol.*, vol. 90, pp. 113-128, 2002.
- [64] M. Aresta, A. Dibenedetto, "Utilisation of CO₂ as chemical feedstock: opportunities and challenges", *Dalton Trans.*, pp. 2975-2092, 2007.
- [65] V. C.-C. Wang, S. W. Ragsdale, F. A. Armstrong, "Investigations of two bidirectional carbon monoxide dehydrogenases from *Carboxydotherrmus hydrogenoformans* by protein film electrochemistry", *ChemBioChem*, vol. 14, pp. 1845-1851, 2013.
- [66] U. Ruschig, U. Müller, P. Willnow, T. Höpner, "CO₂ reduction to formate by NADH catalysed by formate dehydrogenase from *Pseudomonas oxalaticus*." *Eur. J. Biochem.*, vol. 70, pp. 325-330, 1976.
- [67] O. Heichal-Segal, S. Rappoport, S. Braun, "Immobilization in Alginate-Silicate Sol-Gel-Matrix Protects β -Glucosidase Against Thermal and Chemical Denaturation", *Biotechnol.*, vol. 13, pp. 798-800, 1995.
- [68] M. Aresta, E. Quaranta, R. Liberio, C. Dileo, I. Tommasi, "Enzymatic Synthesis of 4-OH-Benzoic Acid from Phenol and CO₂: the First Example of Biotechnological Application of a Carboxylase Enzyme.", *Tetrahedron*, vol. 54, pp. 8841-8846, 1998.
- [69] R. Obert, B.C. Dave, "Enzymatic Conversion of Carbon Dioxide to Methanol : Enhanced Methanol Production in Silica Sol-Gel Matrices", *J. Am. Chem. Soc.*, vol. 121, pp. 12192-12193, 1999.
- [70] S.-W. Xu, Y. Lu, J. Li, Z.-y. Jiang, H. Wu, "Efficient Conversion of CO₂ to Methanol Catalyzed by Three Dehydrogenases Co-encapsulated in an Alginate-Silica (ALG-SiO₂) Hybrid Gel", *Ind. Eng. Chem. Res.*, vol. 45, pp. 4567-4573, 2006.
- [71] Y. Lu, Z.-Y. Jiang, S.-W. Xu, H. Wu, "Efficient conversion of CO₂ to formic acid by formate dehydrogenase immobilized in a novel alginate-silica hybrid gel", *Catal. Today*, vol. 115, pp. 263-268.
- [72] A. Dibenedetto, P. Stufano, W. Macyk, T. Baran, C. Fragale, M. Costa, M. Aresta, "Hybrid technologies for an enhanced carbon recycling based on the enzymatic reduction of CO₂ to methanol in water: chemical and photochemical NADH regeneration.", *ChemSusChem*, vol. 5, pp. 373-378, 2012.
- [73] L. Michaelis, M. L. Menten, "Die Kinetik der Invertinwirkung", *Biochem. Z.*, vol. 49, pp. 333-369, 1913.
- [74] P. K. Addo, R. L. Arechederra, A. Waheed, J. D. Shoemaker, W. S. Sly, S. D. Minter, "Methanol Production via Bioelectrocatalytic Reduction of Carbon Dioxide: Role of Carbonic

Anhydrase in Improving Electrode Performance”, *Electrochem. Solid-State Lett.*, vol. 14, pp. E9-E13, 2011.

[75] Y. Amao, N. Shuto, “Formate dehydrogenase–viologen-immobilized electrode for CO₂ conversion, for development of an artificial photosynthesis system”, *Res. Chem. Intermed.*, vol. 40, pp. 3267-3276, 2013.

[76] S. Kuwabata, R. Tsuda, H. Yoneyama, “Electrochemical Conversion of Carbon Dioxide to Methanol with the Assistance of Formate Dehydrogenase and Methanol Dehydrogenase as Biocatalysts”, *J. Chem. Soc.*, vol. 116, pp. 5437-5443, 1994.

[77] T. Reda, C. M. Plugge, N. J. Abram, J. Hirst, “Reversible interconversion of carbon dioxide and formate by an electroactive enzyme”, *PNAS*, vol. 105, pp. 10654-10658, 2008.

[78] M. Kanan, D. G. Nocera, “In situ formation of an oxygen-evolving catalyst in neutral water containing phosphate and Co²⁺”, *Science*, vol. 321, pp. 1072-1075, 2008.

[79] A. Fuchsbaauer, *Electrochemical Processes for CO₂ Recycling*, PhD Thesis, Linz, 2010.

[80] E. Millner, K. Scott, I. Head, T. Curtis, E. Yu, “Electrochemical Investigation of Aerobic Biocathodes at Different Poised Potentials: Evidence for Mediated Extracellular Electron Transfer”, *Chem. Eng. Trans.*, vol. 41, pp. 355-360, 2014.

Statement of Authorship

I hereby confirm that this PhD thesis was written autonomously by me and without foreign help. No other than the cited references were used. The present thesis is identical to the electronic submitted text document.

Eidesstattliche Erklärung

Ich erkläre an Eides statt, dass ich die vorliegende Dissertation selbstständig und ohne fremde Hilfe verfasst, andere als die angegebenen Quellen und Hilfsmittel nicht benutzt bzw. die wörtlich oder sinngemäß entnommenen Stellen als solche kenntlich gemacht habe. Die vorliegende Dissertation ist mit dem elektronisch übermittelten Textdokument identisch.

Linz,

.....

Funding

This work was accomplished with the financial support of the European Union and the county of Upper Austria for funding the Regio 13 project “REG-STORE”, the Austrian Science Foundation FWF within the Wittgenstein Prize (Z222-N19) and the Austrian research funding association (FFG) under the scope of the “Energieforschung” program within the CO2TRANSFER project (848862).

Curriculum Vitae



Name: Stefanie Schlager
Title: DI DI Dr.
Adress: Aubrunnerweg 13/02
4040 Linz/ Austria
Phone: 00 43 732 2468 8854
Private: 0043 664 5317538
E-mail: stefanie.schlager@jku.at

Personal Data

Date/Place of Birth: March, 26th 1988 in Vöcklabruck, Austria
Nationality: Austrian
Marital Status: Unmarried

Education

1/2012-2/2016 PhD at the Linz Institute for Organic Solar Cells (LIOS)
Title: Biocatalytic and Bio-electrocatalytic Reduction of CO₂ Using Enzymes and M
1/2015-1/2016 Second Diploma Thesis at the Linz Institute for Organic Solar Cells (LIOS)
Title: Semiconductor-Electrolyte Interfaces for CO₂ Reduction
9/2010 - 11/2011 Diploma Thesis at the Linz Institute for Organic Solar Cells (LIOS)
Title: Organic Schottky Diodes, Final exam with distinction
10/2006 - 7/2010 Johannes Kepler University Linz, Austria
Two studies: Economics/Chemical Engineering and Technical Chemistry
9/1998 - 6/2006 Bundesgymnasium Vöcklabruck
School Leaving Exam passed with Distinction

Language and Computer Skills

Language: German (mother tongue), English (fluent), French (advanced), Latin (advanced)
Computer: Microsoft Office (Word, Excel, Power Point), InkScape, ChemSketch, LaTeX/LyX, Origin

Special Training and Relevant Occupational Experience

8/2008 - 9/2008 Internship at VOEST alpine, Institute for Research and Development, Project: "Elimination of boron and nickel from FeO_x"
7/2009 - 9/2009 Internship at the Linz Institute for Organic Solar Cells (LIOS), Project: "Transistors using AlO_x"
8/2010 - 9/2010 Internship at VOEST alpine, Institute for Research and Development, Project: "New Biofuels"
May 2011 EMRS, Nice: Poster presentation
"Organic Schottky diodes with induced charge carriers"
September 2011 NIMS-MFA-LIOS Workshop Budapest
Talk: "Diodes with organic Schottky junctions"
November 2012 Poster presentation, Second Biennial CO₂ Workshop, Princeton/NJ
April 2013 Poster presentation, MRS Meeting, San Francisco
May 2013 Scholarship for Research, JKU (VRⁱⁿ Univ.Prof.ⁱⁿ Dr.ⁱⁿ Gabriele Kotsis)
August 2013 Talk and poster presentation, Solar Energy For World Peace Conference, Istanbul
September 2013 Conducting student seminar, Internationale Akademie Traunkirchen, "Solar energy"
December 2013 Poster presentation, MRS Meeting, Boston
February 2014 Talk, BIOEL Workshop, Kirchberg in Tirol
December 2014 Talk, MRS Meeting, Boston
July 2014 Conducting student seminar, Internationale Akademie Traunkirchen, "CO₂ Recycling"
March 2015 Poster presentation, BIOEL Workshop, Kirchberg in Tirol
March 2015 Invited talk, Chromtour Thermo Scientific, Graz
April 2015 Project leader for granted project CO₂TRANSFER (FFG, 848862)
September 2015 Invited talk, Chemistry and Life 2015, Conference, Brno
September 2015 Invited talk, 4th Conference on CO₂, Conference, Essen
December 2015 Talk, MRS Meeting, Boston
December 2015 Talk, AMEBA Symposium, University of Vermont, Burlington

Interests

Sports: Snowboarding, Skiing, Wakeboarding, Jogging, Yoga, Taebo
Traveling: London, Brasov, Barcelona, Kopenhagen, Essen, Genf, Budapest, Nice, Oslo, Amsterdam, Berlin, Frankfurt am Main, Kassel, New York, San Francisco, Boston, ...
Creativity: Fabrication and research in natural, biodegradable Cosmetics, crafting, sewing, painting, playing piano, ...

Conferences

- EMRS Spring Meeting 2011, Nice, May 2011 S.Schlager, P.Stadler, H.Neugebauer, N. S. Sariciftci: Photo-induced charge carriers in intrinsic P3HT diodes, Poster
- MOPNA Workshop 2011, Budapest, September 2011 S. Schlager, P. Stadler, Matthew S. White, H. Neugebauer, N. S. Sariciftci, Diodes with Bulk Schottky Junctions, Talk
- Second Biennial CO₂ Workshop, Princeton/NJ, November 2012 S. Schlager, E. Portenkirchner, J. Gasiorowski, M. C. Scharber, R. Menon, N. S. Sariciftci, Polypyrrole Electrodes for CO₂ Reduction; Poster
- MRS Spring Meeting 2013, San Francisco, April 2013 S. Schlager, E. Portenkirchner, J. Gasiorowski, M. C. Scharber, R. Menon, N. S. Sariciftci, Polypyrrole Electrodes for CO₂ Reduction; Poster
- Solar Energy for World Peace Conference, Istanbul, August 2013 S. Schlager, D. Hiemetsberger, D. H. Apaydin, E. Portenkirchner, D. Voglhuber, N. S. Sariciftci, Electrochemical Reduction of CO₂ with immobilized Dehydrogenase Enzymes, Talk
- MRS Fall Meeting 2013, Boston, December 2013 S. Schlager, D. Hiemetsberger, A. Wagner, D. H. Apaydin, E. Portenkirchner, N. S. Sariciftci, Electrochemical Reduction of CO₂ with immobilized Dehydrogenase Enzymes, Poster
- BIOEL 2014, Kirchberg in Tirol, February 2014 S. Schlager, L. Puttinger, A. Fuchsbauer, M. Haberbauer, D. H. Apaydin, H. Neugebauer, N. S. Sariciftci, CO₂ Reduction in Microbial Electrolysis Cells (MEC), Talk
- MRS Fall Meeting 2014, Boston, December 2014 S. Schlager, A. Fuchsbauer, M. Haberbauer, G. Hinterberger, D. H. Apaydin, M. Weichselbaumer, H. Neugebauer, G. N. S. Sariciftci, Electrochemical Reduction of CO₂ Using Biological Catalysts, Talk
- BIOEL 2015, Kirchberg in Tirol, March 2015 S. Schlager, H. Neugebauer, M. Haberbauer, G. Hinterberger, N. S. Sariciftci, Bio-electrocatalytic reduction of butyraldehyd to butanol with direct electron injection into alcohol dehydrogenase immobilized on an electrode, Poster
- Chromtour Thermo Scientific, Graz, March 2015, Bio-elektrokatalytische Reduktion von CO₂ zu Methan und Alkoholen unter Verwendung von Enzymen und Mikroorganismen, Invited Talk.
- Chemistry and Life 2015, Brno, September 2015, Bio-electrocatalytic CO₂ Reduction using Enzymes and Microorganisms, Invited Talk.

- 4th Conference on Carbon Dioxide as Feedstock for Fuels, Chemistry and Polymers, Essen, September 2015, S. Schlager, M. Haberbauer, A. Fuchsbauer, G. Hinterberger, L. M. Dumitru, H. Neugebauer, N. S. Sariciftci Bio-electrocatalytic CO₂ Reduction using Enzymes and Microorganisms, Invited Talk.
- MRS Fall Meeting 2015, Boston, December 2015 S. Schlager, M. Haberbauer, A. Fuchsbauer, G. Hinterberger, L. M. Dumitru, H. Neugebauer, W. Schnitzhofer, N. S. Sariciftci, Bio-electrochemical reduction of CO₂ using methanogenic microorganisms, Talk
- AMEBO Symposium 2015, University of Vermont, Burlington, December 2015, S. Schlager, M. Haberbauer, A. Fuchsbauer, G. Hinterberger, L. M. Dumitru, H. Neugebauer, W. Schnitzhofer, N. S. Sariciftci, Bio-electrocatalytic CO₂ Reduction using Enzymes and Microorganisms, Talk

Publications, Projects and Prizes

- S. Schlager, A. Fuchsbauer, M. Haberbauer, G. Hinterberger, H. Neugebauer, N. S. Sariciftci, Microbial Electrolysis Cell for CO₂ reduction to CH₄ using adapted methanogenic mixed cultures, in preparation.
- S. Schlager, H. Neugebauer, M. Haberbauer, G. Hinterberger, N. S. Sariciftci, Direct electrochemical addressing of immobilized alcohol dehydrogenase for the heterogeneous bio-electrocatalytic reduction of butyraldehyde to butanol, *ChemCatChem* (2015), 7, 967-971.
- E. Portenkirchner, J. Gasiorowski, K. Oppelt, S. Schlager, C. Schwarzinger, H. Neugebauer, G. Knör, N. S. Sariciftci, Electrocatalytic Reduction of Carbon Dioxide to Carbon Monoxide by a Polymerized Film of an Alkynyl-Substituted Rhenium (I) Complex, *ChemCatChem* 5 (2013), 1790.
- E. Portenkirchner, C. Enengl, S. Enengl, G. Hinterberger, S. Schlager, D. Apaydin, H. Neugebauer, G. Knör, N. S. Sariciftci, A comparison of Pyridazine and Pyridine as Electrocatalysts for the Reduction of Carbon Dioxide to Methanol, *ChemSusChem* 1 (2014), 1543.
- E. Portenkirchner, S. Schlager, D. Apaydin, K. Oppelt, D. A. M. Egbe, H. Neugebauer, G. Knör, T. Yoshida, N. S. Sariciftci, Using the alkynyl-substituted rhenium (I) complex (4,4'-bisphenyl-ethynyl-2,2'-bipyridyl)Re(CO)₃Cl as catalyst for CO₂ reduction- Synthesis, Characterization and Application, *Electrocatal.* DOI 10.1007/s12678-014-0230-1.
- J. Gasiorowski, S. Boudiba, K. Hingerl, C. Ulbricht, V. Fattori, F. Tinti, N. Camaioni, R. Menon, S. Schlager, L. Boudida, N. S. Sariciftci, D. Egbe, Anthracene-Containing Conjugated Polymer Showing Four Optical Transitions Upon Doping: A Spectroscopic Study, *Journal of Polymer Science, Part B: Polymer Physics* 52 (2014), 338.

- REGSTORE, Regio 13 with PROFACTOR GmbH, FH Wels, FH Linz, Energieinstitut JKU, accomplished April 2014.
- CO2TRANSFER, FFG Energieforschung 1. Ausschreibung, with acib GmbH, Institut für Technologie Anorganischer Stoffe ICTAS/ JKU, starting April 1st 2015
- S. Schlager, L. Dumitru, M. Haberbauer, A. Fuchsbauer, H. Neugebauer, D. Hiemetsberger, A. Wagner, E. Portenkirchner, N. S. Sariciftci, Electrochemical reduction of carbon dioxide to methanol by direct electron injection into immobilized enzymes on a modified electrode, ChemSusChem (2016).
- MRS Fall Meeting 2015, Presentation Award.